UNIVERSITEIT VAN PRETORIA
UNIVERSITY OF PRETORIA
YUNIBESITHI YA PRETORIA

# Groundwater Resource Directed Measures in karst terrain with emphasis on aquifer characterisation in the Cradle of Humankind near Krugersdorp, South Africa

by

Martin Holland

Submitted in partial fulfilment of the requirements for the degree Master of Science in the Faculty Natural and Agricultural Sciences, University of Pretoria.

August 2007

## *Acknowledgements*

The following people were of great help and guidance during this thesis:

- First, I would like to express my thanks to my supervisor, Dr. Kai Witthüser, for offering me the opportunity to carry out my research, for his continuous support and his amicable mentorship.
- I also want to express my gratitude to Mr. Marius van Biljon and Mr. Garfield Krige for providing invaluable hydrogeological base data and information of recent studies in the Zwartkrans dolomitic compartment.
- My grateful thanks go to Mr. Mike Butler and Dr. Uwe Horstmann from Ithemba LABS for the environmental isotope analysis.
- I would also like to thank my loving wife and daughter for their belief in me and the sacrifices made during the time it took to complete this research.
- I am grateful to my parents for supporting my academic education through all these years.

UNIVERSITEIT VAN PRETORIA
UNIVERSITY OF PRETORIA
YUNIBESITHI YA PRETORIA

# Groundwater Resource Directed Measures in karst terrain with emphasis on aquifer characterisation in the Cradle of Humankind near Krugersdorp, South Africa

by

Martin Holland

Supervisor: Dr. K.T. Witthüser
Co-supervisor: Prof. J.L. Van Rooy
Department: Geology
Degree: M.Sc Engineering and Environmental Geology

## Summary

Karst terrain present a highly heterogeneous aquifer system created and organised by groundwater flow which make them very different from other aquifers. Consequently karst aquifers are highly vulnerable to contamination due to the rapid transport of pollutants in conduit systems. The karst of the Cradle of Humankind World Heritage Site, play a major role in assimilation or carrying of acid mine drainage, sewage effluent return flow and agricultural fertilisers, emphasising the need for a sustainable balance between utilisation and protection.

Groundwater Resource Directed Measures (GRDM) recognises the need for groundwater to be included in the integrated management of water resources and is regarded as a strategy and approach to implement the National Water Act (Act 36 of 1998). However, the application of Resource Directed Measures in highly utilised karst terrain remains a challenging task. The level of confidence of GRDM assessments in karst depends on our ability to adequately characterise the dual- recharge, flow and storage processes. In this context, karst terrains do present some common characteristics in their groundwater flow conditions, which allow us to use common exploration and exploitation methods to study its structure and functioning.

Despite the World Heritage status and ongoing exploitation, the karst of the Cradle of Humankind was not yet systematically investigated nor is it understood. This study has been undertaken to determine the current hydrogeological status of the karst aquifer and to investigate methodologies for GRDM assessments in karst terrain. As infiltration of contaminated water has altered the chemical composition of the natural waters of the karst system it was important to determine pollution indicators and to assess whether the pollution could be attributed to distinct anthropogenic sources. Cluster analysis, in conjunction with conventional graphical displays and distribution maps provide a consistent and reliable method for delineating sources that influence groundwater chemistry.

It has been proven from the hydrograph response graphs and isotope investigation that the karst aquifer represents both slow diffuse and rapid concentrated allogenic and autogenic recharge mechanisms. The groundwater flow has been influenced by dykes creating compartments isolated hydrogeologically from each other, suggesting a highly complex karst system. Based on the conceptual findings it is obvious that GRDM assessments in karst aquifers need a much more comprehensive understanding of the underlying groundwater system compared to homogenous aquifers. Reserve determination in karst is further influenced by the uncertainties concerning inflows (sinking streams), outflows (abstraction) and baseflow where springs comprise the source of numerous streams.

The investigation revealed the potential shortcomings inherent from the lack of site-specific data and recommended a better understanding of the interaction between ground- and surface water while identifying the most vulnerable areas to exploitation. In return this will greatly improve the significance of the GRDM assessments and account for better decision making of the development of karst groundwater resources in the Cradle of Humankind and other karst terrain.

# Table of Contents

**1. Introduction ..... 1**
**1.1 Background ..... 1**
**1.2 Site selection ..... 2**
**1.3 Objectives and Aims ..... 4**

**2. Conceptual Framework ..... 6**
**2.1 Karst Hydrology ..... 6**
2.1.1 Karst Development Process ..... 6
2.1.2 Conceptual Model of Karst ..... 7
2.1.3 Methodological Approaches ..... 9
**2.2 Groundwater Management in Karst ..... 15**
2.2.1 Historical Background ..... 15
2.2.2 Legislative Framework ..... 15
**2.3 Groundwater Resource Directed Measures (GRDM) ..... 16**
2.3.1 GRDM Implementing Phases ..... 17
2.3.2 Resource Classification ..... 18
2.3.3 Quantification of the Reserve ..... 20
2.3.4 Resource Quality Objectives (RQO's) ..... 21

**3. Hydrogeological Investigation Methods ..... 23**
**3.1 Characterisation of Karst Aquifers ..... 23**
**3.2 Groundwater Recharge Estimation ..... 24**
3.2.1 Chloride Mass-Balance Method ..... 24
3.2.2 Cumulative Rainfall Departure Method ..... 26
3.2.3 Qualified Guess ..... 27
**3.3 Hydrograph Analysis ..... 27**
3.3.1 Spring Discharge Hydrograph Analysis ..... 27
3.3.2 Borehole Hydrograph Recession Analysis ..... 30
**3.4 Hydraulic Tests ..... 33**
3.4.1 Slug Tests ..... 33
**3.5 Hydrochemical Characterisation ..... 36**
3.5.1 Geochemical Investigation ..... 36
3.5.2 Environmental Isotopes ..... 37
**3.6 Conceptual Model ..... 39**

**4. Description of the COHWHS karst Aquifer ..... 41**
**4.1 Physiography ..... 41**
4.1.1 Surface Water Drainage ..... 43
4.1.2 Climate ..... 45
4.1.3 Geomorphology ..... 48
**4.2 Geology ..... 49**
4.2.1 Basement Complex ..... 52
4.2.2 Witwatersrand Super-Group ..... 52
4.2.3 Black Reef Formation ..... 52
4.2.4 Chuniespoort Group ..... 52
4.2.5 Pretoria Group ..... 54
4.2.6 Mafic Dykes ..... 54

4.2.7 Regional Structure ..... 56
**4.3 Hydrogeology ..... 57**
4.3.1 Groundwater Level ..... 57
4.3.2 Groundwater Recharge ..... 61
4.3.3 Hydrograph Analysis ..... 66
4.3.4 Aquifer Parameters ..... 74
**4.4 Chemical Hydrogeology ..... 76**
4.4.1 Geochemical Description ..... 76
4.4.2 Isotope Hydrogeology ..... 86
**4.5 Conceptual Model ..... 89**

**5. Groundwater Resource Directed Measures (GRDM) Assessment 95**
**5.1. Preparatory Phase ..... 95**
**5.2. Description of Study Area ..... 95**
**5.3. Delineation of Resource Units ..... 95**
**5.4. Resource Classification ..... 96**
**5.5. Reserve Quantification ..... 97**
**5.6. Resource Quality Objectives ..... 100**

**6. Conclusion and Recommendations ..... 103**
**6.1. General ..... 103**
**6.2. GRDM Assessment ..... 104**
**6.3. Recommendations ..... 104**

**6. References ..... 106**

## List of Figures

Figure 1.1. Locality of study area. ..... 3
Figure 2.1. Illustration of the various modes of recharge, flow and discharge in a karst system (Gunn, 1986 in Drew and Hötzl, 1999). ..... 8
Figure 2.2. Karst assemblage variation in terms of time (Cvijic, 1893). ..... 10
Figure 2.3. A systems model for karst (Marker, 1980). ..... 11
Figure 2.4. Morphological Types: I Mature types (not present today), II Plateau type, III Escarpment type, IV Bushveld type (Adapted from Martini and Kavalieris, 1976). ..... 12
Figure 2.5. Sequential process of GRDM Studies (Parsons and Wentzel, 2007). ..... 17
Figure 2.6. Relationship between various interim classification systems (Xu et al., 2003). .. 18
Figure 3.1. Overview of the applied hydrogeological methods and their applicability. ..... 23
Figure 3.2. Components of catchment runoff contributing to stream flow (Hiscock, 2005). . 28
Figure 3.3. The flood hydrograph from a rainfall event (Musy, 2001). ..... 29
Figure 3.4. Schematic presentation of recession with three micro-regimes of discharge, and the corresponding volumes of water discharged from the three different types of storage. ..... 30
Figure 3.5. Schmeatic representation of the recession with three micro-regimes of groundwater flow. ..... 31
Figure 3.6. Geometry and symbols for slug test developed by H. Bouwer (Fetter, 2001). .... 34
Figure 4.1. Current topography and surface water catchments of the main study area with springs indicating possible groundwater contribution to river flow. ..... 42

Figure 4.2. Location of rainfall stations together with the spatial distribution of the mean annual precipitation of the quaternary catchments as depicted by DWAF, 2005.46
Figure 4.3. Long-term annual rainfall comparison between meteorological stations in the vicinity of the study area. ..... 47
Figure 4.4. Monthly correlation between Krugersdorp and Pelindaba rainfall stations. ..... 47
Figure 4.5. Geology of the Cradle of Humankind World Heritage Site. ..... 50
Figure 4.6. Faults/Dykes from published geology maps together with the linear anomalies interpreted from high resolution aeromagnetic data. ..... 55
Figure 4.7. Locality of Caves in relation to major faults (data from Jamison et al., 2004). ... 56
Figure 4.8. Map with monitoring boreholes where continuous water level loggers were installed. ..... 58
Figure 4.9. Correlation between surface topography and groundwater levels. ..... 59
Figure 4.10. Groundwater level elevation contours of boreholes measured during Dec/Jan 2006/2007 (Inverse Distance Weighting - Interpolation). ..... 60
Figure 4.11. Chloride sample locations for determining recharge. ..... 63
Figure 4.12. Hydrogeological isolated compartments created by vertical cross-cutting dykes with representing water levels. ..... 64
Figure 4.13. CRD simulation of sub-unit E of the Zwartkrans compartment. ..... 66
Figure 4.14. Monitoring locations for hydrograph analysis. ..... 67
Figure 4.15. Long-term hydrograph for Nouklip flow gauge station. ..... 68
Figure 4.16. Response curve of the discharge over time for the 1999 hydrological year for the Nouklip gauging station according to the Maillet equation. ..... 68
Figure 4.17. Sterkfontein 1 hydrograph with recession segment captured. ..... 71
Figure 4.18. Sterkfontein 2 hydrograph with recession segment captured. ..... 71
Figure 4.19. Sterkfontein 3 hydrograph with recession segment captured. ..... 72
Figure 4.20. Kromdraai hydrograph with recession segment captured. ..... 72
Figure 4.21. Location of boreholes which was subjected to slug testing (photos indicating slugs). ..... 75
Figure 4.22. Sampling location in relation to geology. ..... 78
Figure 4.23. Spatial Distribution of the hydrochemical groups identified by the HCA. ..... 81
Figure 4.24. Piper diagram presenting the composition of 148 groundwater and surface water samples collected from 1996 to 2007. ..... 82
Figure 4.25. Hydrochemical section sampling points. ..... 83
Figure 4.26. Schoeller plot of hydrochemical section A to B. ..... 84
Figure 4.27. Schoeller plot of hydrochemical section C to D. ..... 85
Figure 4.28. Isotope sample location with photos. ..... 86
Figure 4.29. δ18O vs. δD of sample set relative to global meteoric water line (GMWL) (Craig, 1961) and long term Pretoria meteoric water line (PMWL). ..... 88
Figure 4.30. Tritium content of dataset in tritium units (TU). ..... 89
Figure 4.31. 3D surface terrain model of Zwartkrans compartment (vertical exaggeration x 2). ..... 90
Figure 4.32. Cross section along the Tweelopiespruit as illustrated in Figure 4.31 indicating the major aquifer properties. ..... 92
Figure 4.33. Gravity survey at the mine water decanting area on the dolomitic outlier (Data obtained from Van Biljon, 2006). ..... 94

## List of Tables

Table 2.1. Guide for setting the present status category of a groundwater unit based on observed environmental impact indicators (Parsons and Wentzel, 2007). ..... 19
Table 2.2. Guide for determining the level of stress of a groundwater unit (Parsons and Wentzel, 2007). ..... 20

Table 2.3. Present status category assessment based on groundwater contamination (Parsons and Wentzel, 2007). ..... 20
Table 4.1. Meteorological stations in the study area. ..... 47
Table 4.2. Lithostratigraphy of the geology of the region; area of investigation highlighted. (SACS, 1980:205; Foster, 1984; Obbes, 2001). ..... 51
Table 4.3. CMB results for the Zwartkrans compartment. ..... 62
Table 4.4. CMB results for the Tweefontein compartment. ..... 63
Table 4.5. Abstraction for irrigation in Sub-Unit E. ..... 65
Table 4.6. Recharge estimations based on qualified guesses and previous reports. ..... 66
Table 4.7. Parameters characterizing the recession analysis based on the Mailet equation. .. 69
Table 4.8. Hydrogeologic parameters calculated from monitoring borehole hydrograph data. ..... 73
Table 4.9. Summary of Aquifer parameters, K and T from slug test interpretations. ..... 74
Table 4.10. Mean values for the groups distinguished by the hierarchical cluster analysis. .. 79
Table 4.11. Analytical results of 21 isotope samples taken from the karst aquifer. ..... 87
Table 5.1. Categorisation of resource units in the Cradle of Humankind World Heritage Site. ..... 96
Table 5.2. Population Data. ..... 98
Table 5.3. GRDM assessment for both Zwartkrans and Tweefontein compartments. ..... 99
Table 5.4. General chemistry for Zwartkrans and Tweefontein compartment. ..... 100

## List of Photos

Photo 1. The dam constructed to intercept water decanting from the Black Reef incline shaft (left) and pumping stations to divert mine drainage water back to the treatment dam (right). ..... 44
Photo 2. Percy Stewart Sewage Works facility with its effluent return flow outlet (left), and the Blougatspruit downstream of the Percy Stewart facility before its confluence with Blaauwbankspruit (right). ..... 44
Photo 3. A view of the undulating topography of the Cradle of humankind (left) and sinkhole formation near Sterkfontein caves (right). ..... 49
Photo 4. Typical chert rich dolomite associated with the Monte Christo Formation, outcrop near Sterkfontein quarry ..... 53
Photo 5. Sunken stream near sample SS-01(left) and iron precipitation near sample GP-0227 (right). ..... 84

## List of Appendices

Appendix A. Monitoring Boreholes. ..... A-1
Appendix B. Results of Hydrograph Analysis. ..... B-1
Appendix C. Results of Slug Test Analysis. ..... C-1
Appendix D. Results of Cluster Analysis. ..... D-1

# 1. Introduction

## 1.1 Background

*"The term karst is used to describe an area of limestone or other highly soluble rock, in which the landforms are of dominantly solutional origin and in which the drainage is underground in solutionally enlarged fissures and conduits (caves). Karst processes significantly change the flow, transport and storage behaviour of groundwater in such systems. Karst aquifers distinguish from non-karst systems by rapid infiltration, poor filtration and purification, high flow velocities, partly turbulent flow conditions, low retention capacity and partly short residence time in the underground. All these properties make karst groundwater particularly vulnerable to pollution and therefore require special care and protection of karst systems (IAH Karst Commission, 2004)"*

Karst aquifers are difficult to characterise because of their inherent heterogeneity. Several major groundwater aquifers in South Africa are located within the Malmani dolomite (karst aquifers) of the Chuniespoort Group. Many towns, rural areas and farming practices are largely or entirely dependant upon karst aquifers for their drinking water, and water for agricultural and industrial use (Barnard, 2000). However, because of the origin of the karst features, they are not an exploitable aquifer everywhere, groundwater storage being in some cases negligible or impossible to liberate (Bakalowicz, 2005). Karst landscapes are particularly dynamic and subject to rapid change. The management of karst groundwater resources in South Africa is essential and in order to do this, a conceptual understanding of the aquifer structure, flow, boundary conditions and it's interaction with surface water is necessary.

The promulgation of the National Water Act (Act 36 of 1998) and the recognition of groundwater resources as public domain (*Government Gazette*, 1998), provide a legal framework for the effective and sustainable management of South Africa's groundwater resources. The National Water Act introduced resource based tools to protect and conserve water resources and is becoming increasingly important in the emerging Integrated Water Resource Management (IWRM) paradigm. Groundwater Resource Directed Measures (GRDM) is regarded as a strategy and approach developed to implement the Act (Parsons and Wentzel, 2007), with Resource Classification, Reserve Quantification and Resource Quality Objectives proposed as tools. The approaches proposed by DWAF (1999), Xu *et al*., (2003) and in the GRDM manual (Parsons and Wentzel, 2007) for assessing the groundwater component of Resource Directed Measures (RDM), are similar in their overall approach. All

require that a resource be classified, an allocatable volume of groundwater determined and RQO's set. Karst aquifers makes it difficult to quantify and predict the movement of groundwater and contaminants through and/or between different aquifer zones, in many instances it is difficult to quantify a sustainable water balance that would prevent over use of the groundwater resource. The application of Resource Directed Measures in karst terrain is a challenging task and becomes even more so when dealing with highly utilised aquifers. Despite its complexity, karst terrain can be characterised by its flow, structure and functioning, that allows us to assess and manage karst in a sustainable way.

## 1.2 Site Selection

The study area centres on the Cradle of Humankind World Heritage Site (COHWHS) which is underlain by karstified Malmani dolomite. It's vast treasure chest of fossilized remains of past life forms, particularly hominids (humans, their ancestors and relatives) found in the over 200 karst caves of the COHWHS ensured its Heritage status, and is therefore protected. The site consists of an ± 800 $km^2$ trapezoidal area some 40 km Northwest of Johannesburg in the province of Gauteng, South Africa. It extends from Krugersdorp in the Southwest to Hartebeespoort dam in the Northeast, a distance of 37 km with an average width Northwest to Southeast of 20 km (Figure 1.1).

The Malmani dolomites underlying the COHWHS were formed in a shallow early Proterozoic epeiric sea (Clendennin, 1989). The lithology in this area consists essentially of shallow marine stromatolitic dolostone and has been subdivided into five formations (geological units) of alternating chert poor and chert rich dolomite (Obbes, 2001). The dolomite is capped by a palaeo-karst of coarse grained chert made up of re-cemented broken clasts (breccia) beneath the overlying base of the Pretoria Group.

Compared with classic karst areas of Europe and America, the regional karst of the COHWHS is very different and perhaps unique. The karst of the Malmani dolomite is a world important example of a karst developed on a very old dolomite. Therefore, the lithologies have been subjected to deep burial, tectonization, folding, uplifting, and prolonged episodes of natural loss of soil and rock debris in the interior of the Kaapvaal Craton (Jamison *et al*., 2004). Another important and well documented characteristic of the regional karst of the Malmani dolomite is its subdivision into 'compartments' isolated hydrologically from each other by impervious near vertical dykes of dolerite and syenite, as well as by silicified faults. The major compartments of the COHWHS, according to the various geohydrological studies in the Krugersdorp area done by Fleisher (1981), Foster (1984), Bredenkamp *et al*.,

(1986) and Kuhn (1986) are the Zwartkrans and Tweefontein compartments. Recent work by Obbess (2001) and Jamison *et al*., (2004) established that many more fractures and dykes exist, and have also identified considerable deformation in the COHWHS, which suggests more complex karst systems are present.

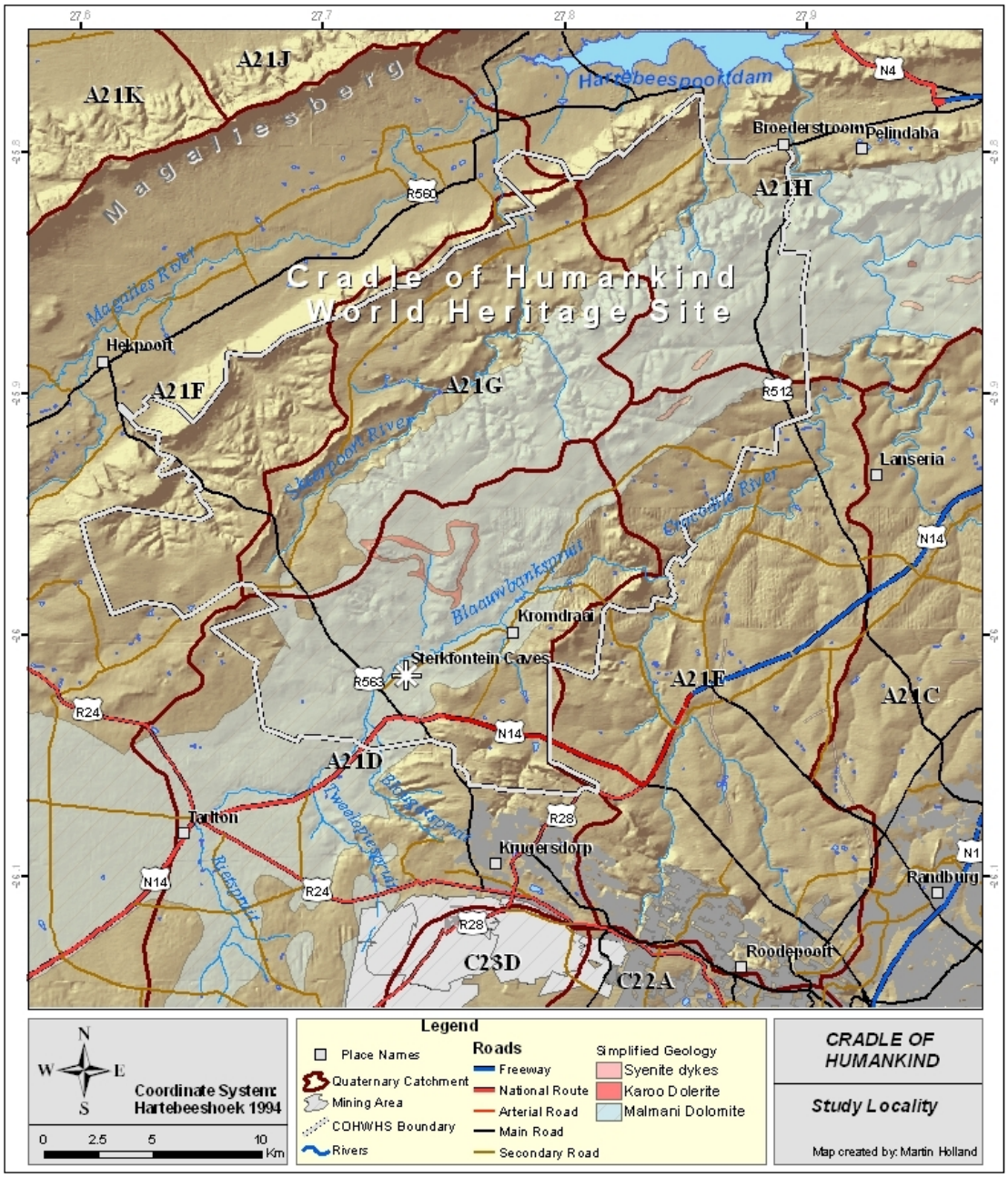


**Figure 1.1.** Locality of study area.

The investigation and understanding of this complex compartmentalised karst aquifer has become crucial since the first polluted mine water started to decant, south of the area near Krugersdorp, in August 2002. The gold-bearing reefs of the Witwatersrand Basin has been mined since 1887, during this period water was pumped from the mine workings to enable

deeper mining to take place. As the gold content in the reef declined more gold mines closed resulting in pumping operations being ceased. The rebounding water table has lead to significant pollution of groundwater in the abandoned mined areas. Acid Mine Drainage (AMD) caused by the oxidation and hydrolysis of metal sulphates, results in elevated heavy metal concentrations, a high sulphate content, an increased electrical conductivity and a lowering of the pH of the water in the mining area (Williams and Smith, 2000; Heikkinen *et al*., 2002). In addition to the mining activities, two municipal sewage treatment plants are located in the catchment, and intensive agricultural and industrial activities are carried out throughout the COHWHS. The tributaries of the catchment play a major role in assimilation or carrying off the mining, industrial and municipal wastewater together with run-off from agricultural land. These waters enter the underground network of the COHWHS through swallow holes, dolines and through the leakage of carbonate rock beneath the river bed. Such inflows are characteristic of karst terrain and pose a threat to existing surface and groundwater's in the area. Many human settlements in the area are dependant on these productive karst aquifers as their only water resource, emphasizing the need for aquifer management.

## 1.3 Objectives and Aims

The heritage status of the area, the importance of the Malmani dolomites and the ongoing exploitation of the karst aquifer provide an ideal scenario to implement and test methodologies for determining the groundwater component of RDM in karst terrain. The significance of GRDM assessments is largely dictated by data availability. Consequently, the most important requirement for this study is to consolidate all available information, evaluate the current status of the karst aquifer and refine and update the hydrogeological conceptual model. The significance of the groundwater recharge estimation in groundwater resources evaluation is highlighted and various hydrogeologic investigation methods to characterise karst aquifers are reflected.

As groundwater quality issues are not addressed under the Reserve, emphasis will be placed on this section to effectively classify the resource which will be linked to the Resource Quality Objectives. Despite extensive data collection and monitoring efforts from stakeholders no systematic interpretation of the regional groundwater chemistry have been made up to date. Investigations on the geochemistry of the area were limited to relatively small areas down gradient of the mining area and were part of larger environmental impact assessments. One of the aims of this study is to present a simple approach based on

multivariate statistical analysis, conventional graphical displays and spatial distribution maps, which could be useful in determining pollution indicators and to assess whether the pollution could be attributed to distinct anthropogenic sources. The primary purpose of the study is to characterise the karst aquifer based on groundwater -recharge, -quality and -flow, present the results of the Groundwater Resource Directed Measures (GRDM) assessment as a whole and provide an account of the application of procedures in karst terrain.

# 2. Conceptual Framework

## 2.1 Karst Hydrology

The word Karst originated from the German form of the Slavic word kras or krš, meaning a bleak waterless place, it is also the German name for a district east of Trieste having such terrain (EPA, 2002a). It was in this area in the middle 19$^{th}$ century that engineers observed solutionally enlarged flow paths, surface streams disappearing into holes and the presence of caves. The term *karst* unites specific morphological and hydrological features in soluble (mostly carbonate) rocks and is an internationally used term (Bögli, 1986).

### 2.1.1 Karst Development Process

Karst is commonly considered as the result of the solution process of carbonate rocks, named "karstification". The karstification process is driven by the amount of precipitation, eventually increased by the surface flow from swallow holes, the partial pressure of CO2 in soil and the hydraulic gradient given by the difference in elevation between the top of the karst recharge area and the spring level (Bakalowicz, 2005). Because the concentration of dissolved $CO_2$ is driven by both the temperature and the $CO_2$ partial pressure of the atmosphere related to (ground) water, climate is generally considered as the driving process in karstification (Dreybrodt, 1988).

As infiltrating rainwater is in equilibrium with the carbon dioxide in the atmosphere (~0.035%) and the soil zone (up to a few %), it forms carbonic acid ($H_2CO_3$). Water and carbonic acid readily produce reactive water that has a pH of 5.7 or lower, depending on other constituents in the atmosphere (EPA, 2006). As the rain and soil water react with the rock, the pH will rise, the water will become saturated with respect to dolomite, and the dissolution process will diminish or stop. The process can continue in areas where underground waters are mixed, if the resulting water mixture is again under-saturated with respect to dolomite. The weakly acidic groundwater circulating through the dolomitic succession causes dissolution of the carbonate minerals, resulting in the development of open cavities and caves. The process in dolomite may be represented as follows:

$$CaMg(CO_3)_2 + 2H_2O + 2CO_2 \rightarrow Ca^{2+} + Mg^{2+} + 4HCO_3^- \qquad (2\text{-}1)$$

A necessary condition for the process of karstification is the existence of places where water can export the products of dissolution (karst springs) and allow further inflow of aggressive solution. The flow through the initial fractures is typical laminar, because their aperture widths are in the range of several 100um (Romanov, 2003). Some of the fissures widen faster than others. Therefore the flow through them increases and consequently the rate of their widening increased also. This positive feedback loop is the reason for the development of secondary porosity and consequently for the development of a complex, extremely heterogeneous aquifer. Flow through some of the widened fractures finally becomes turbulent.

In most karst systems an initial active surface drainage by fluvial systems is replaced by subsurface circulation of water. In the mature state of karst all meteoric water disappear after very short travel distances into the ground and discharges at karst springs at the base level of erosion, leaving the elevated parts of the landscapes entirely dry without any surface water (Dreybrodt, 1988).

### 2.1.2 Conceptual Model of Karst

Karst specialists generally agree about the high degree heterogeneity and complexity of karst aquifers. The conceptual model representing the structure and hydraulic behaviour of karst can be drawn in various ways but the essential features are those shown in (Figure 2.1). This general model describes the various types of recharge and functions in karst system. Karst aquifers are often characterised by a dual or triple porosity, comprising of solutional voids, fractures and the rock matrix (intergranular pores). While the fractures and the rock matrix provides predominately storage potential (low permeability), the conduits act additionally as drains (high permeability). The main sources of recharge in karst aquifers include:

- Allogenic recharge: Surface water injected into the aquifer at the swallets of sinking streams. Both a diffuse and concentrated recharge component could be present (Figure 2.1).
- Autogenic recharge: Overland storm flow into closed depressions where it enters the aquifer through sinkhole drains (Figure 2.1).
    - Diffuse infiltration: In a simplified (vertical) conceptual model of the karst aquifer an epikarst zone might be present in the unsaturated zone (Trček, 2003). Precipitation run-off infiltrating through the soil may be held for days or weeks in the epikarst zone before it migrates downward through the rock matrix or along fractures to reach the water table.

- Recharge from perched catchments: Many geologic environments support locally perched groundwater systems above carbonate aquifers.

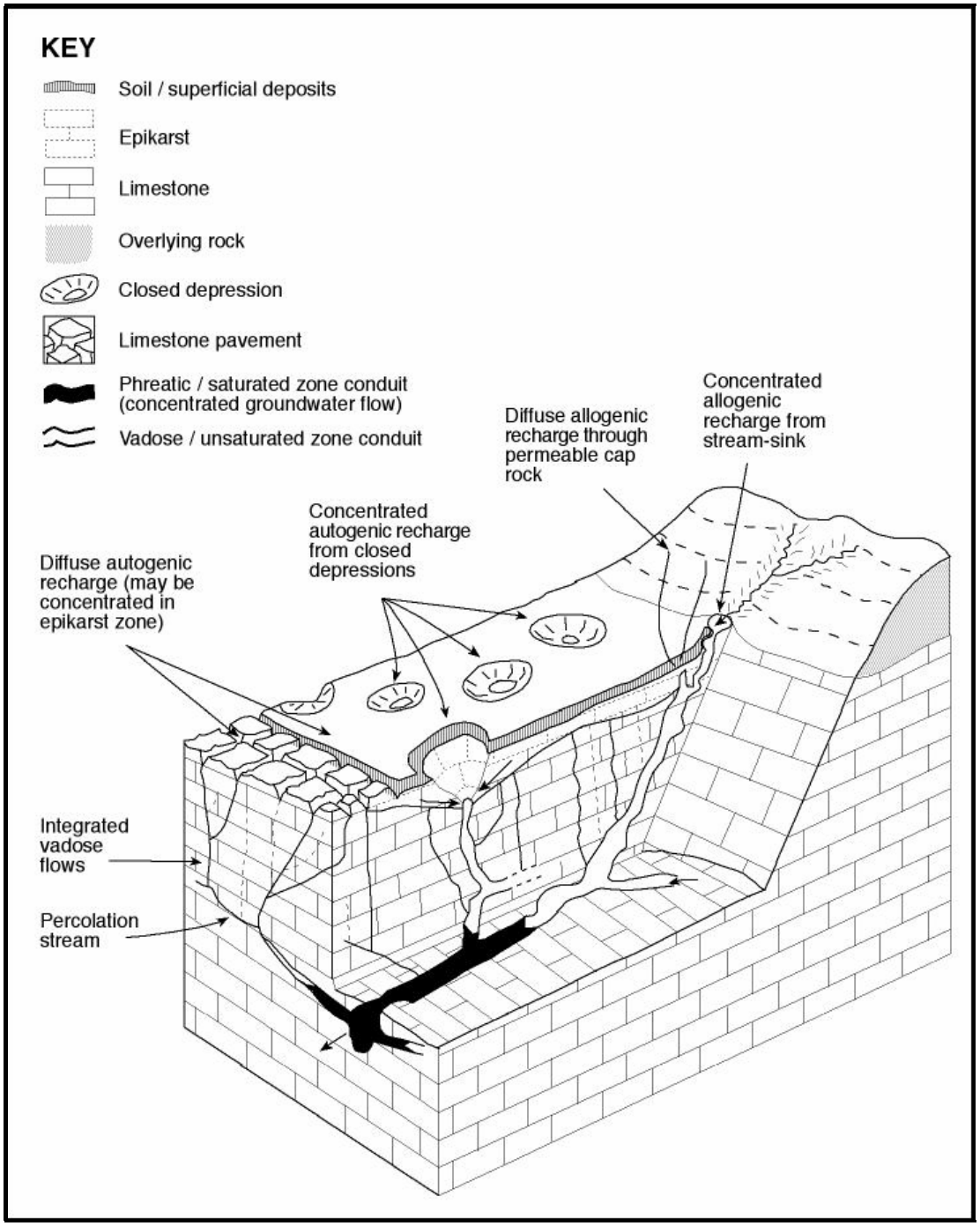


**Figure 2.1.** Illustration of the various modes of recharge, flow and discharge in a karst system (Gunn, 1986 in Drew and Hötzl, 1999).

Not all of these components are present in all aquifers, and their presence and relative importance are an important part of distinguishing one aquifer from another. Most theoretical and practical problems result from these dualities:

- duality of the infiltration processes ("diffuse" or slow infiltration into the low permeability volumes, "concentrated" or rapid infiltration into the channel network);
- duality of the groundwater flow field (low flow velocities in the fractured volumes, high flow velocities in the channel network);
- duality of the discharge conditions (diffuse seepage from the low permeability volumes, concentrated discharge from the channel network at the karst springs (Kiraly, 2003).

### 2.1.3 Methodological Approaches

Scientific investigations of the karst regions in South Africa have been carried out by geologists, hydrologists and geomorphologists since the early sixties (De Kock, 1964; Brink and Partridge, 1965). Therefore, different approaches prevailed in karst studies, each with their own concepts and methods. On the one hand, karst evolution and the cycle of karst development associated with the regional dolomite have long attracted attention from South African geomorphologists and geologists (Marker, 1971; Marker, 1972; Sweeting, 1973; Martini and Kavalieris, 1976; Marker, 1980; Wilkins *et al*., 1987). On the other hand, investigations on the groundwater potential of the regional dolomite emerged when more groundwater was needed for the growing population and the impact of the gold mining activities needed to be addressed. This led to numerous large-scale and widespread groundwater investigations in the Western-Transvaal carried out by Enslin and Kriel (1967), Fleisher (1981), Foster (1984); Bredenkamp *et al*., (1986), Kuhn (1986), Bredenkamp (1995), Bredenkamp *et al*. (1995) and Barnard (1997).

*Geomorphological approach*

Initial karst geomorphologists developed a model of karst development over time (Cvijic, 1893). Differences in assemblage were attributed to stage of development (Figure 2.2). This Classic karst cycle has received little modification through the ears, and has furnished an accepted framework within which to view the development of karst.

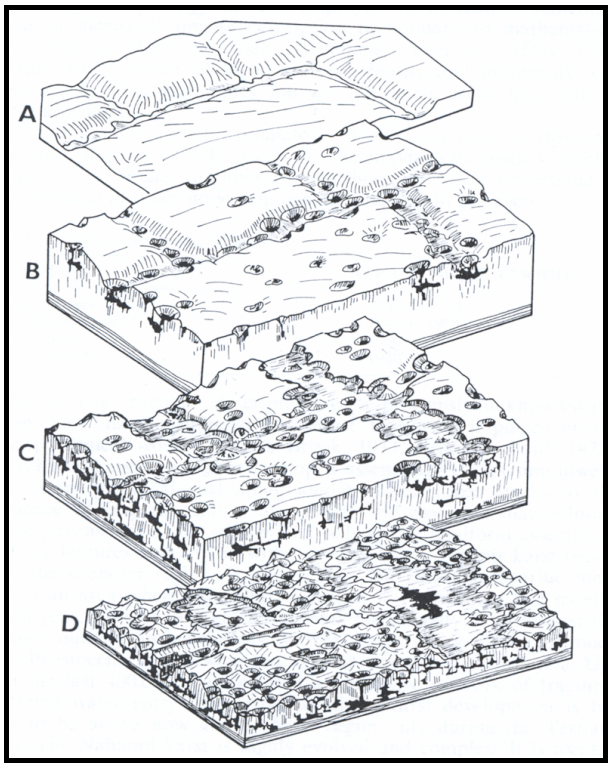


**Figure 2.2.** Karst assemblage variation in terms of time (Cvijic, 1893).

Brink and Partridge (1965) adapted the classical cycle of karst development in terms of subsurface cavern development and sinkhole formation in the karst of Transvaal. Cavern genesis was described to have undergone two-cycles of erosion relating ancient water table zones to major erosion surface, Post-Gondwana and Post-African cycles respectively. Their geomorphological approach displayed the connection between the development of subterranean caverns and the surface manifestations of subsidence and collapse. Their work also illustrated that accelerated development of sinkholes and compaction subsidence features on the far West Rand is the result of the lowering of the water table through pumping of the gold mines.

Perhaps the most influential contribution to the literature of South African karst geomorphology is the work done by Marker during the 1970's. Marker's doctorate in 1971 demonstrated without any doubt that the Transvaal karst was extremely old. Surface landforms and large caves could only be explained in terms of former much wetter conditions. Marker (1972) used karst as a climatic indicator, since karst landforms and landscapes

develop by solution and the solution process is governed by water availability and by vegetation growth through its control of available biotic carbon dioxide. During the early 1980's Marker (1980) introduced a SYSTEMS model approach which allows for the interplay of several variables acting on the central Karst system (Figure 2.3). The model was applied to selected Southern African karst regions including the Malmani Dolomite. Marker (1980) noted that even where the host rock is the same, tectonic, geologic and climatic variables mark the variation in South African karst assemblages.

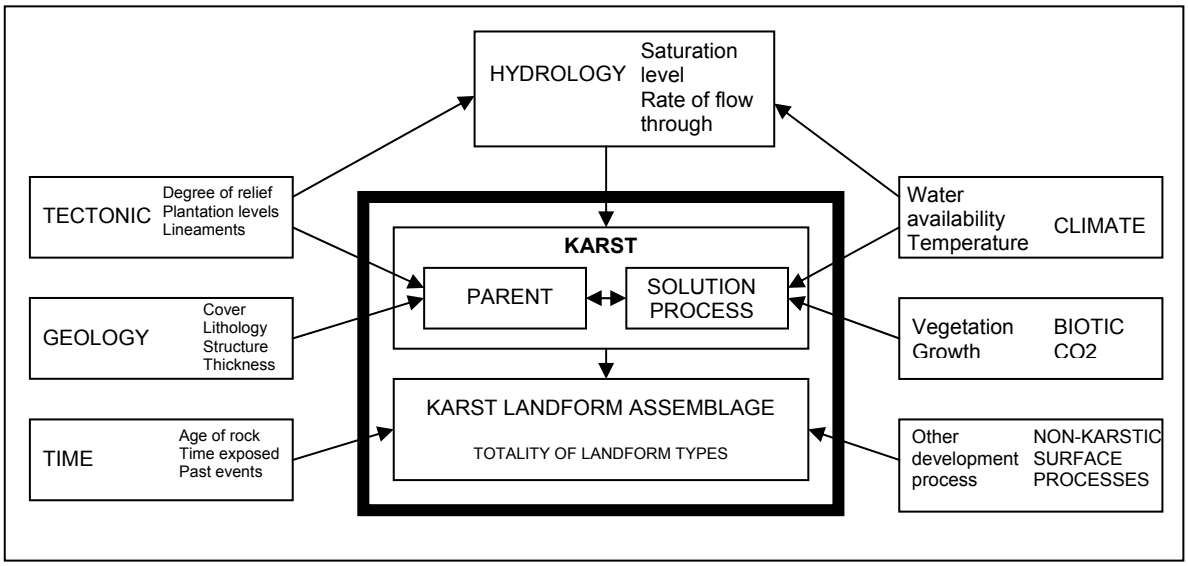


**Figure 2.3.** A systems model for karst (Marker, 1980).

Martini and Kavalieris (1976) indicated that South African karst differ in some aspects from classical karst as described for instance by Cvijic (1893). Their work distinguished four periods of karst formations, which correspond stratigraphically to major Post-dolomite breaks in deposition. The latest, Tertiary to Recent, has according to Martini and Kavalieris (1976), contributed most to present day permeability. In addition, the authors revealed four types of karst morphologies on South African dolomite (Figure 2.4).

- II – Plateau type: A thick blanket of residual material often conceals the dolomite. A few surface streams occur generated by springs and the area are characterised by swallow holes, sinkholes and depressions.
- III – Escarpment type: Karst morphology is not developed on a large scale although caves are abundant and often may belong to the system developed during the Plateau stage. A general character of the dolomite seems to be that karst topography can really develop only on a fairly flat surface. If the area is rugged with steeper gradients, physical erosion controls dominates the surface morphology. In this way the Transvaal karst contrasts strongly with other areas in the world where karst morphology can develop even on steep slopes.

- III – Bushveld type: Here again no major karst topography is developed. A few caves are known, some still active, but in general they are not common. A further evolution of this morphology should lead to a mature karst-stage landform: but in fact erosion cycles are succeeding so rapidly that the relief observed now will be rejuvenated before the completion of the cycles (Martini and Kavalieris, 1976).

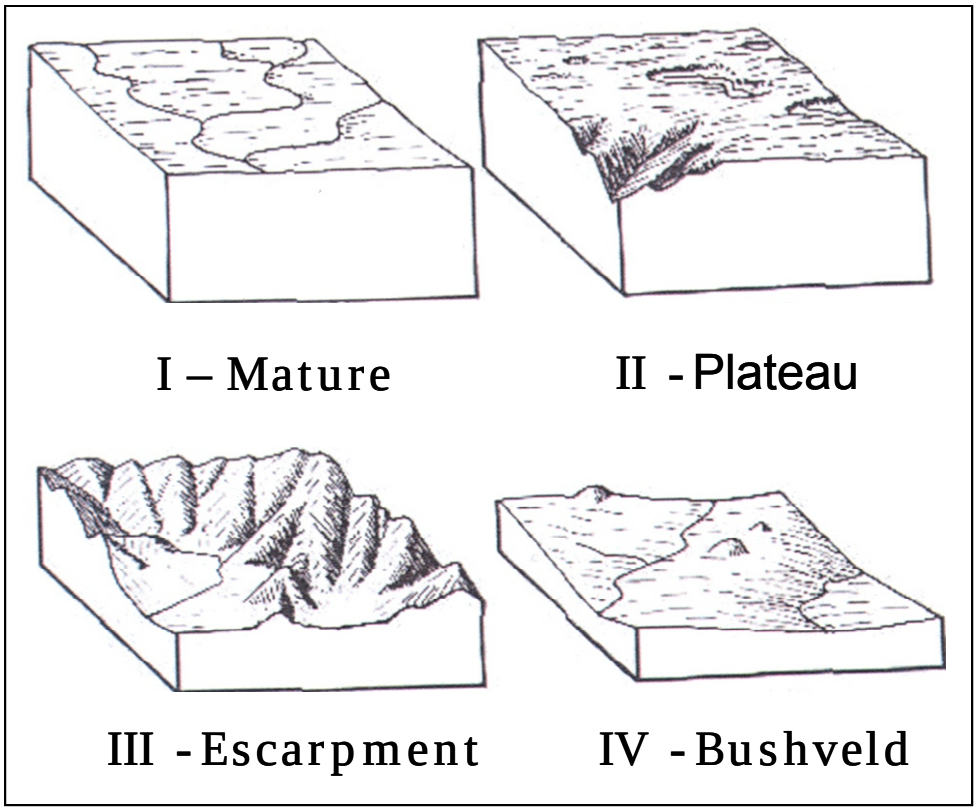


**Figure 2.4.** Morphological Types: I Mature types (not present today), II Plateau type, III Escarpment type, IV Bushveld type (Adapted from Martini and Kavalieris, 1976).

*Hydrological approach*

Hydrological investigations considered groundwater flow, recharge and storage as the major phenomena in karst. Mine dewatering to enable deeper mining to take place in the West Witwatersrand Goldfield has been continuing for almost 115 years. As a result of these large scale mine-pumping operations, the need for reliable recharge estimation was a desire for many authors and over the last three decades it remained the focus of many groundwater investigations in karst terrain. Perhaps the earliest hydrological study of the dolomitic terrain in the South-western Transvaal was conducted by Enslin and Kriel (1959). The authors calculated average transmissivity values of the dolomite as 3000 $m^2/d$ with specific yields (storativity) values ranging between 4.34% and 9.07%. The recharge of the dolomitic compartment was calculated at 10.57% of annual rainfall, with the best reliable dataset at the time. Further work on the Western Transvaal dolomites includes:

- Enslin (1971) stated that in dolomitic environments it is possible to abstract the total recharge percentage from rainfall due to the specific geological properties. This study highlighted the value of dolomitic terrain with regards to water provisioning, irrigation, industrial and mining supplies.
- Verhagen *et al*. (1979) carried out extensive studies on the application of natural isotopes to the Kalahari region and to some semi-arid dolomite areas.
- On recharge in the West Rand dolomites, Fleisher (1981) provided a major contribution to quantitative estimations, based on water balance studies.
    - The investigation on eight dolomitic compartments revealed a lowest recharge rate of 12.8% and a highest rate of 24% of the average rainfall. The high recharge rate was attributed to specifically favourable percolation conditions.
- Geohydrological studies on individual compartments within the Malmani dolomite include Foster (1984), Kuhn (1986), Bredenkamp *et al.* (1986) and Polivka (1987a and 1987b), Vegter and Foster (1990).
    - Polivka (1987a) differentiated average borehole yields in the Schoonspruit compartment for the different formations where the Eccles formation yielded 17.9 l/s, Lyttleton formation 3 l/s, Monte Christo 12 l/s and the Oaktree formation yielded 6 l/s. Chert-rich formations presenting the better aquifer.
    - Perhaps more significant to this study is the work done by Bredenkamp *et al.* (1986) on the Zwartkrans and Steenkoppies compartments. The investigation revealed recharge rates of between 15% and 21% of average annual rainfall with transmissivity vales varying between 1 $m^2$/d and 25000 $m^2$/d.
- Bredenkamp *et al*. (1991) has shown that for dolomitic aquifers, a linear rainfall/recharge relationship is obtained above an annual rainfall of 313 mm.
- Recharge has also been derived from the ratio of chloride concentrations of the rainfall to that of spring water (chloride method), or from average flow of a spring in relation to the recharge area (Bredenkamp *et al*., 1994).
- Bredenkamp *et al*. (1995) produced a manual on recharge and storativity estimation, using a variety of methods that have been developed as part of studies of the Grootfontein dolomitic aquifer.
- Appropriate institutional arrangements for groundwater management in dolomitic areas were conducted by Stephens and Bredenkamp (2002), which included a re-

examination of data, information and reports pertaining to delineating groundwater units in the North West Province.

- Xu and Beekman (2003) provided an overview of recharge methods and studies carried out in Southern Africa, particularly within arid and semi-arid environments. The authors also aimed to evaluate recharge methods in terms of limitations, applicability (range of fluxes, spatial and temporal scale) and ratings (accuracy, ease of application and cost).
    - The Chloride Mass Balance, Cumulative Rainfall Departure, Water Table Fluctuation, Hydrochemical and Isotope methods, are widely applied in dolomitic aquifers.

Some of the literature is very comprehensive and detailed, containing numerous case studies and detail. This detail is not repeated in this study, but will play a crucial role in characterising the karst aquifer under investigation.

*Proposed methodological approach*

From previous discussions it is clear that karst aquifers have complex and original characteristics, which make them very different from other aquifers. It is now accepted that no single approach can successfully determine the dynamics of karst (White, 2002; Bakalowicz, 2005). The commonly proposed methodology is an integrated approach where the karst hydrologists use a variety of methods to explore and study karst aquifers, in order to describe their functioning and their structure. These methods proposed by Bakalowicz, 2005 include;

- Characterisation of the structure by geological and morphological analyses (karstification) (Kiraly, 2003; Novel *et al*., 2006).
- Delineation of the karst system by means of geological and structural mapping (Kazemi, 2003; Shaban, 2004).
- Characterisation of their lump functioning
    - by using spring/borehole hydrographs and time series analyses (Kresic, 1997; Trček, 2003; Bäumle, 2003),
    - by using hydrogeochemical and isotope methods for analysing natural tracing (Kranjc, 1997; Wang *et al.*, 2001; Perrin, 2003; Perrin *et al*., 2003).
- Characterisation of their local functioning:
    - by artificial tracing tests (EPA, 2002b; Toran *et al*., 2007),
    - by slug and pumping tests (Rutler *et al*., 2003).

## 2.2 Groundwater Management in Karst

A large part of South Africa's population is entirely dependent on karst aquifers for drinking water, and water for agricultural and industrial use (Barnard, 2000). The sustainable management of karst water resources is absolutely essential considering that South Africa is among the 20 most water stressed countries in the world due to high rates of evaporation and limited surface water (Stephens and Bredenkamp, 2002). During the past decade there has been a major change in groundwater management thinking.

### 2.2.1 Historical Background

Prior to 1994, water law in South Africa was shaped by the Roman law, Roman Dutch law and later the English and American law. The results of these influences were the distinction made between public and private water (riparian principle). Through the introduction of the Water Act (Act 54, 1956) the concept of private water was entrenched and there was no obligation to share resources equitably (Stephens and Bredenkamp, 2002). This perception has created enormous problems for authorities charged with controlling the abstraction and the pollution of groundwater resources and led to a history of neglect and unsustainable groundwater utilisation in South Africa. The new National Water Act (Act 36 of 1998) (*Government Gazette*, 1998) attempts to redress the problem of past groundwater mismanagement by placing emphasis on the protection of groundwater resources for their sustainable development. This is reflected in the subsequent development of several policy documents and legislation to water.

### 2.2.2 Legislative Framework

Water resources in South Africa are managed according to the principles that underpin the National Water act of 1998. The water Act takes into account two main principles:

- Sustainability – has been proposed by some as a concept that will resolve water-use issues. However, the meaning of the word 'sustainability' is often contested and is operationally and conceptually one of the most complex that modern science has faced (Cabezas and Fath, 2002). When applied to groundwater usage, 'sustainability' implies use that does not cause long-term deterioration of the overall resource, in terms of any measurable criteria (e.g. quality and quantity) (Wright and Xu, 2000).

- Equity – Water resources should be developed, apportioned and managed in such a manner as to enable all user sectors to gain equitable access to the desired quantity, quality and reliability of water.

The goals of equity and sustainability are thus the guiding objectives of the National Water Act, but are accompanied by the following fundamental tenets of water management in this country (Xu and Beekman, 2003).

- Integrated Management – The emerging Integrated Water Resource Management (IWRM) paradigm aims to promote efficient management of all water resources and recognizes the unity of the water cycle and the interdependence of its elements (Beekman).
- The Reserve – The quantity, quality and reliability of water required to maintain the ecological functions on which humans depend should be reserved so that the human use of water does not individually or cumulatively compromise the long-term sustainability of aquatic and associated ecosystems (Parsons and Wentzel, 2007).
- National Water Resource Strategy (NWRS) –South Africa has been divided into 19 Water Management Area (WMA), which will be managed by catchment management agencies (CMA) and will be responsible for implementing the NWRS as well as catchment specific strategies.
- Public Interest – Public awareness is seen as the only permanent guard against degradation of groundwater (Veltman, 2003).

## 2.3 Groundwater Resource Directed Measures (GRDM)

Resource directed measures relating to groundwater is abbreviated as GRDM and takes into account the characteristically difference between surface and groundwater. Because GRDM is still in its infancy, and much of the strategy and tools for its implementation are new, it is necessary to apply and verify the groundwater component of Resource Directed Measures, especially in environmentally sensitive groundwater systems such as karst terrain. Adopting the principles of GRDM is regarded as a practical means of promoting sustainable development and reducing environmental degradation in groundwater resources (Parsons and Wentzel, 2007). The GRDM methodology comprises of six interrelated components illustrated in (Figure 2.5).

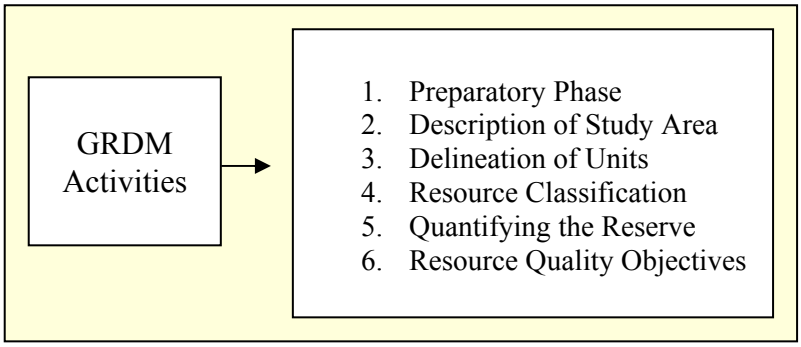


**Figure 2.5.** Sequential process of GRDM Studies (Parsons and Wentzel, 2007).

In addition to the six sequential phases of the GRDM assessment four levels of GRDM determination are recognized – desktop, rapid, intermediate and comprehensive. There is no strict linear relationship between the GRDM determination methods and the level of confidence, although it is commonly believed that the confidence level increases from desktop to comprehensive (Mavurayi, 2005). The choice of the confidence level of a study depends on, the commitment and resources available to undertake the GRDM assessment and, among others things, the magnitude of the impact of a proposed water use. The same level of assessment need not be applied across a study area and, a multi level GRDM assessments approach can be adopted (Parsons and Wentzel, 2007).

### 2.3.1 GRDM Implementing Phases

As a means of initiating the study and setting the level of GRDM assessment required, it is recommended that the following steps should be included in the GRDM process:

*Preparatory phase*

The preparation phase includes, identifying the area to be studied, identify and collect all data pertaining to the area and the extent of hydrogeological work required is to be assessed in terms of the availability of data and the required level of confidence of the GRDM assessment (Parsons and Wentzel, 2007).

*Description of Study Area*

The key outcome of this phase is a report describing the study area in general, the hydrogeological conditions and the conceptual model in particular (Parsons and Wentzel, 2007). This phase also entails data gathering and analysis typical of any groundwater resource assessment, but ensuring that the information is adequate to classify a resource, determining the reserve and set resource quality objectives.

*Delineation of Resource Units*

Resource units can comprise part of a quaternary catchment, or a group of quaternary catchments. However, dolomitic aquifers play a unique role in hydrological systems and needs to be delineated as a distinct water resource unit (Parsons and Wentzel, 2007). Therefore, quaternary boundaries are used to delineate groundwater units at a primary level, with aquifer type (dolomitic aquifers) being used as secondary level. When required and sufficient data exist, further delineation can be based on physical, management and/or functional criteria (Xu *et al*., 2003).

### 2.3.2 Resource Classification

The overall objective of classifying a water resource is to define its water resource (in terms of natural, good, fair and poor) and its management class (in terms of excellent, good and fair), as set out in Figure 2.6.

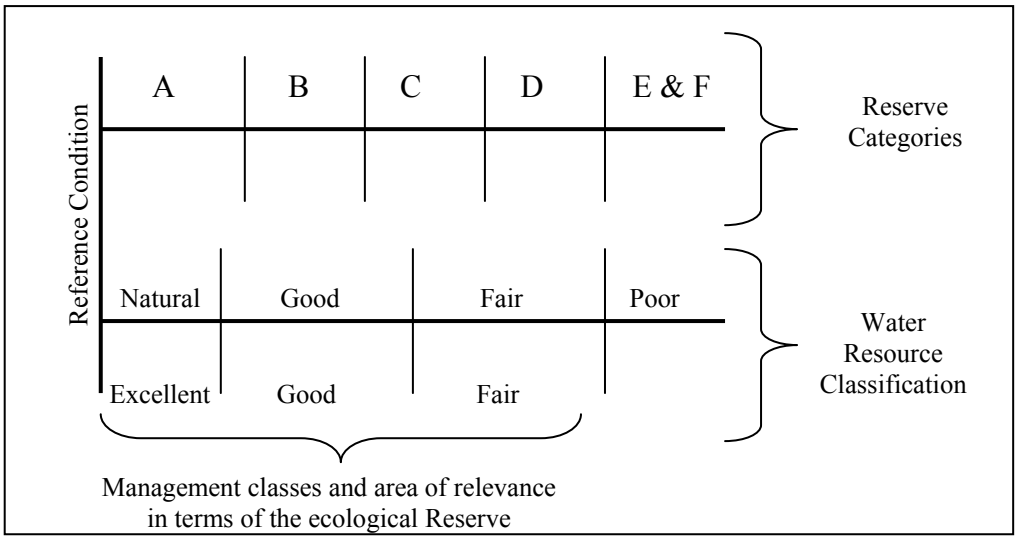


**Figure 2.6.** Relationship between various interim classification systems (Xu *et al*., 2003).

These four classes imply different levels of protection and impact acceptable to the stakeholders of the resource. They provide a frame of reference for the implementation of groundwater protection, use and management plans for that groundwater management unit. In considering appropriate classification procedures, it was assumed that the limits of sustainability would mark the difference between what would be considered acceptable and unacceptable use (Parsons and Wentzel, 2007). Defining the point at which a resource is no longer being used in a sustainable manner is generally very difficult. A guide for assessing the status of groundwater based on observed environmental impact indicators is presented in (Table 2.1).

**Table 2.1.** Guide for setting the present status category of a groundwater unit based on observed environmental impact indicators (Parsons and Wentzel, 2007).

| PRESENT STATUS CATEGORY | GENERIC DESCRIPTION | AFFECTED ENVIRONMENT |
|---|---|---|
| A | Unmodified, Pristine conditions | *No significant impacts observed* |
| B | Localized low level impacts, but no negative effects apparent | |
| C | Moderate levels of localized impacts – moderate or perceived impact on the environment | |
| D | Moderate levels of widespread impacts – limited but noticeable effect on the environment | *Moderate to crticial impacts to:*<br>- *spring flow*<br>- *river flow*<br>- *vegetation*<br>- *land subsidence*<br>- *sinkhole formation*<br>- *groundwater quality* |
| E | High levels of local impacts – serious effect on the environment | |
| F | High levels of widespread impacts – critical effect on the environment | |

Those resources categorized as being either ‘A’, ‘B’ or ‘C’ are considered as being utilised sustainable, while categorized as either ‘D’, ‘E’ or ‘F’ are being over-utilised, and some corrective management action is required. If no signs of unsustainable use are observed, then no category is assigned at this stage, and consideration is given to the level of stress. To provide a quantitative means of defining stress, a groundwater stress index was developed by dividing the volume of groundwater abstracted from a groundwater unit by the estimated recharge to that unit. After calculating the stress index, the guide presented in is used to set the present status category of each groundwater unit (Table 2.2).

**Table 2.2.** Guide for determining the level of stress of a groundwater unit (Parsons and Wentzel, 2007).

| PRESENT STATUS CATEGORY | DESCRIPTION | STRESS INDEX (abstraction/recharge) |
|---|---|---|
| A | Unstressed or slightly stressed | < 0.05 |
| B | | 0.05–0.20 |
| C | Moderately stressed | 0.20–0.40 |
| D | | 0.40–0.65 |
| E | Highly stressed | 0.65–0.95 |
| F | Critically stressed | > 0.95 |

Assessment of less impacted units can be more difficult as the signs of impact are less obvious. To assist in this assessment, a set of guiding tables has been prepared based on observed contamination (Table 2.3).

**Table 2.3.** Present status category assessment based on groundwater contamination (Parsons and Wentzel, 2007).

| PRESENT STATUS CATEGORY | GENERIC DESCRIPTION | AFFECTED ENVIRONMENT |
|---|---|---|
| A | Unmodified, pristine conditions | Natural groundwater quality conditions prevail |
| B | Localised, low levels of contamination, but no negative impacts apparent | Largely natural groundwater quality conditions prevail |
| C | Moderate levels of localised contamination, but little or no negative impacts apparent | Some localised contamination detected; may impact the purpose for which groundwater is used |
| D | Moderate levels of widespread contamination, which limit the use or potential use of the aquifer | Groundwater contamination is quite widespread but levels are relatively low; may impact the purpose for which groundwater is used |
| E | High levels of local contamination which render parts of the aquifer unusable | High levels of contamination detected in places; use of groundwater from impacted area to be restricted or prohibited |
| F | High levels of widespread contamination which render the aquifer unusable | Very high levels of contamination widespread throughout the aquifer. Groundwater use to be restricted or prohibited. |

### 2.3.3 Quantification of the Reserve

According to the National Water Act of 1998, "Reserve", means the quantity and quality of groundwater required 1) to supply the basic needs of the people who are now or who will, in the foreseeable future, be supplied by, the relevant water resource; and 2) to protect aquatic ecosystems, in order to secure ecologically sustainable development and use of the relevant water resource (DWAF, 1999). The former provides for the minimum living

requirements of individuals served by the water resource in question and includes water for essential uses, such as drinking, food preparation and personal hygiene (set at 25 l/d/person) (Water Services Act: Act No.108). The latter is largely reliant upon expert judgment and set at a value so as to ensure that the natural ecology of the identified area is maintained or improved, depending on the Management Class set. This study will assume that the maximum riparian ecological requirements are equal to the groundwater flow towards the river. To be able to quantify the groundwater component of the Reserve, the following relationship has to be solved:

$$GW_{allocate} = (Re + GW_{in} - GW_{out}) - BHN - GW_{Bf} \quad (2\text{-}2)$$

Where: $GW_{allocate}$ = groundwater allocation
Re = recharge
$GW_{in}$ = groundwater inflow
$GW_{out}$ = groundwater outflow
BHN = basic human needs
$GW_{Bf}$ = groundwater contribution to baseflow

### 2.3.4 Resource Quality Objectives (RQO's)

While the Reserve is a scientifically calculated volume of water kept apart from water that can be allocated for use, Resource Quality Objectives is a set of standards decided upon by water users of an area to protect their water resource for sustainable future use (Veltman, 2003). They provide goals and objectives that frame the vision for sustainable use of a water resource, and hence for the basis for catchment decision making. Typical RQO's could include:

- Groundwater levels;
- groundwater quality (presence and concentrations of particular substances in groundwater);
- groundwater abstraction volumes;
- the regulation or prohibition of instream or land-based activities which may affect the quantity of water in or the quality of the resource;
- aquifer structure and integrity.

While the concept of RQOs is conceptually easy to understand, the practical development and implementation thereof is not as easy. Because of natural variation of groundwater levels and quality across a resource unit, a few point measurements will probably be insufficient to set RQO's for a unit (Parsons and Wentzel, 2007). A new functional approach to setting resource quality objectives was introduced in a Water Research

Commission project by Colvin et al. (2004). Despite these new developments of guidelines relating to the setting of RQO's, the topic is still very recent and has not yet been fully updated into the GRDM manual. Because of the lack of guidance for setting RQO's for groundwater, work by Colvin *et al*. (2004), Parsons and Wentzel (2007) and the DWAF (2006) dolomitic guideline were used to consider RQO's in the study area.

# 3. Hydrogeological Investigation Methods

## 3.1 Characterisation of Karst Aquifers

To comprehend the dynamics of a karst aquifer, it is necessary to understand the recharge processes and the hydrodynamic flow systems that are controlled by the permeability of the aquifer and exchange of water between the different layers and compartments. The investigation of the karst system necessitates the following:

1) the accumulation of existing hydrogeological and related data for the study area,
2) a description of the study are in terms of its physical, climatic, geological and hydrological characteristics,
3) additional data through appropriate hydrogeologic investigations and,
4) the development of a conceptual understanding of hydrogeological conditions in the study area.

The hydrogeological methods used to explore and study the karst aquifer is presented in Figure 3.1. The methods proposed aim to improve the conceptual understanding of the karst aquifer.

**DATA ACCUMULATION**

↓

| Investigation Method | Application |
|---|---|
| Chloride mass balance<br>Cumulative rainfall departure | Estimation of recharge<br>Regional aquifer characterization |
| Hydrograph analysis | Estimation of Recharge<br>Regional aquifer characterization |
| Hydraulic tests (Slug tests) | Determination of hydraulic parameters (T, S)<br>Aquifer characterisation (e.g. conduits, barriers, leakage)<br>Assessment of well performance |
| Hydrochemical characterisation | Developing conceptual flow models<br>Assessment of groundwater quality and risks<br>Aquifer characterisation |
| Environmental isotopes | Estimation of recharge<br>Provide a signature of the origin of the groundwater type<br>Provide information on flow directions and recharge mechanisms |

↓

**CONCEPTUAL MODEL**

**Figure 3.1.** Overview of the applied hydrogeological methods and their applicability.

## 3.2 Groundwater Recharge Estimation

Groundwater recharge is defined as the portion of total rainfall falling into a drainage basin that ultimately reaches the water table in the phreatic zone of an aquifer (Jukić and Denić-Jukić, 2004). The recharge of an aquifer, over time, is governed by the intricate balance between several components of the hydrological cycle, each of which is a function of several controlling factors (Xu and Beekman, 2003):

- Rainfall (intensity, frequency, variability, spatial distribution);
- Evapotranspirative losses (temperature, wind, humidity and phreatophites);
- Discharge losses (interflow, springs, baseflow, lateral flow and artificial discharge);
- Catchment (soil type, thickness, spatial distribution, topographical feature, vegetation);
- Geology (rock types, characteristics of fracture networks, occurrence of dykes).

As groundwater recharge cannot be measured directly, it is estimated by using the results of hydrogeologic and geologic investigations, meteorological data, observed discharges or groundwater levels. Depending on the available data and information about internal structure of aquifers, various methods are used for the estimations.

### 3.2.1 Chloride Mass-Balance Method

Eriksson and Khunakasem (1969) first proposed that chloride concentration in ground water could be used to estimate a recharge flux in a semiarid, regional aquifer. Chloride can be considered a conservative tracer as it is generally not adsorbed or desorbed during transport through soil (Subyani and Sen, 2006). Chloride enters the soil as part of infiltrating rainfall and is subsequently concentrated by evaporation and transpiration (Wood and Sanford, 1995). Solutes will be deposited and transported through the upper soil during the rainy season at rates depending on the rainfall intensity. As water moves downward through the soil profile, some of it is removed by evapotranspiration, reducing the water flux and causing the remaining pore water chloride to become increasingly concentrated. Solutes may be removed from solution by plant uptake, by mineral precipitation, or by adsorption. Similarly solutes may be released by the decay of dead plant material, by mineral dissolution, or by desorption. In the absence of knowledge of these ancillary fluxes, only those constituents for which there are no net release or storage by the soil or rock matrix may be used. Chloride is the solute that most frequently and most conveniently meets these requirements (Kinzelbach *et al*., 2002). The solute concentrations in the soils or in the upper

unsaturated zone will vary seasonally or annually depending upon the intensity of the moisture flux due to the incident rainfall and evapotranspiration (Kinzelbach *et al*., 2002).

The CMB method can be applied to the saturated zone to estimate a 'true' total recharge originating from both diffuse and preferential flow components through the unsaturated zone. The chloride-mass-balance (CMB) method in the saturated zone has been used to estimate recharge in the karst terrains of Southern Africa (Bredenkamp 1993; Bredenkamp *et al*., 1995 and Xu & Beekman, 2003). This method entails determining the recharge over an entire drainage area by integrating the ratio of average chloride content in rainfall (wet and dry deposition) to that of groundwater over the whole area (Xu & Beekman, 2003). The CMB method can be represented by the equation (Kinzelbach *et al*., 2002):

$$Rt = \frac{P * Cl_p + D}{Cl_{gw}} \qquad (3\text{-}1)$$

Where: P = precipitation (mm per time)

Rt = *Total recharge* (mm per time)

$D$ = dry deposition (in mg per $m^2$ and time)

$Cl_P$ = concentration in precipitation (mg/l)

$Cl_{gw}$ = concentration in recharging groundwater (e.g. average over profile) (mg/l)

The $Cl_{gw}$ originates from various flow components in the unsaturated zone. For a regional Rt, $Cl_{gw}$ represents the harmonic mean of chloride concentrations in groundwater:

$$Cl_{gw} = \frac{N}{\sum_{i=1}^{N} \frac{1}{Cl_{gw-1}}} \qquad (3\text{-}2)$$

Application of the method requires that the only source of chloride in ground water be from precipitation. That is, chloride concentrations in the aquifer reflect the degree to which the chloride in rain water has been concentrated by evaporation (Wood and Sanford, 1995). For this analysis it is assumed that the water-table aquifer is receiving recharge only by direct precipitation on the surface and subsequent recharge through the unsaturated zone. The chloride-mass balance method is extremely powerful and can provide an excellent time-integrated estimate of ground water recharge if the assumptions and boundary conditions are fully realized.

### 3.2.2 Cumulative Rainfall Departure Method

The Cumulative Rainfall Departure (CRD) method is a water balance approach and is based on the premise that equilibrium conditions develop in an aquifer over time, i.e. average rate of losses equating to average rate of recharge of the system. In other words groundwater level fluctuations are caused by rainfall events. Bredenkamp *et al.* (1995) applied the method successfully in dolomitic aquifers.

The method requires monthly rainfall and groundwater level data, as well as information pertaining to aquifer properties (storativity), abstraction and the size of the recharge area. The CRD method allow aquifer characteristics and components such as i) recharge or storativity, and ii) the impact of abstraction or iii) the natural response of rainfall to be determined. The CRD series is represented by the mathematical relationship (Eq.3) (Bredenkamp, *et al*., 1995):

$$_{av}^{1}CRD_i = \sum_{n=1}^{i} R_n - k\sum_{n=1}^{i} R_{av} \quad (i = 0,1,2,3.....N) \qquad (3\text{-}3)$$

Where R is rainfall values with subscript "$_i$" indicating i-th month and "$_{av}$" the average. $k = 1+(Q_p+Q_{out})/(AR_{av})$. If, according to the regression $k > 1$, which indicates that pumping or an external impact has affected the water level, the natural water levels could be simulated from equation (3-3) by setting $k = 1$.

It is assumed that a CRD has a linear regression with a monthly water level change. Bredenkamp et al. (1995) derived:

$$\Delta h_i = (r/S).(_{av}^{1}CRD_i) \quad (i = 0,1,2,3.....N) \qquad (3\text{-}4)$$

Where r is recharge percentage of rainfall. A regression between $CRD_i$ and $\Delta h_i$ may be used to estimate the ratio of recharge to aquifer storativity (Xu and Van Tonder, 2001). Xu and Van Toner (2001) revised this method to accommodate for trends in rainfall time series. Recharge is calculated as (Xu and Beekman, 2003):

$$rCRD_i = S_y[\Delta h_i + (Q_{pi} + Q_{out})/(AS)] \quad with$$

$$CRD_i = \sum_{i=1}^{N} P_i - \left(2 - \frac{1}{P_{av} i}\sum_{i=1}^{N} P_i\right) iP_t \qquad (3\text{-}5)$$

Where r is that fraction of a CRD which contributes to recharge, $S_y$ is specific yield, $\Delta h_i$ is water level change during month i (L), $Q_{pi}$ is groundwater abstraction ($L^3/T$), $Q_{out}$ is natural outflow, A is recharge area ($L^2$), $P_i$ is rainfall for month *i* (L/T) and $P_t$ is a threshold value representing aquifer boundary conditions. $P_t$ may range from 0 to $P_{av}$, with 0

representing a closed aquifer (no outflow), and $P_{av}$ representing an open aquifer system (for instance controlled by spring flow). The ratio r/Sy can be estimated based on equation (3-5) through an optimisation process, which minimises the difference between calculated and observed water level fluctuations over a specific time interval. The storativity and recharge values, attributed to the specific borehole's reaction to averaged rainfall over an area, are obtained. The recharge excel spreadsheet (developed by Xu and Van Tonder, 2000) is used to simulate recharge for the karst aquifer.

### 3.2.3 Qualified Guess

Various maps exist which can be useful for obtaining a quick indication of recharge in a particular area. Examples include Vegter's recharge map, Groundwater component of River Base Flow and Harvest potential maps (Van Tonder and Xu, 2001). The qualified guesses for recharge from soil/vegetation and Geology are from expert opinion and general equations proposed by Xu and Van Tonder (2000). This approach provides only an indication of average recharge over an area, and cannot be used to determine recharge on a local scale (Parsons and Wentzel, 2007).

## 3.3 Hydrograph Analysis

Hydrograph analysis of water levels and spring discharge in karst areas can reflect overall response of the aquifer and help in evaluating its recharge, storage, transmissivity, degree of karstification and hydrogeologic boundaries (Shevenell, 1996; Powers and Shevenell, 2000; Samani, 2001; Kiraly, 2003; Kovács *et al*., 2005).

### 3.3.1 Spring Discharge Hydrograph Analysis

The hydrograph analysis was originally developed for surface runoff from rivers or springs. It is generally recognised that there are four different components of runoff, each of which reaches the stream by a different path (Figure 3.2) (Xu and Beekman, 2003):

- Surface runoff is the residual after interception; surface ponding and infiltration have been extracted from precipitation.
- Interflow is the water that infiltrates the soils surface and moves latterly through the soil horizons.
- Groundwater flow originates from water that percolates down to the groundwater table.

- Groundwater flow follows a more devious route to the stream than any other component. Water represented by the groundwater accretion from a particular storm is discharged into the stream over a long period of time.
- Channel precipitation is that precipitation which falls directly on the stream surface.

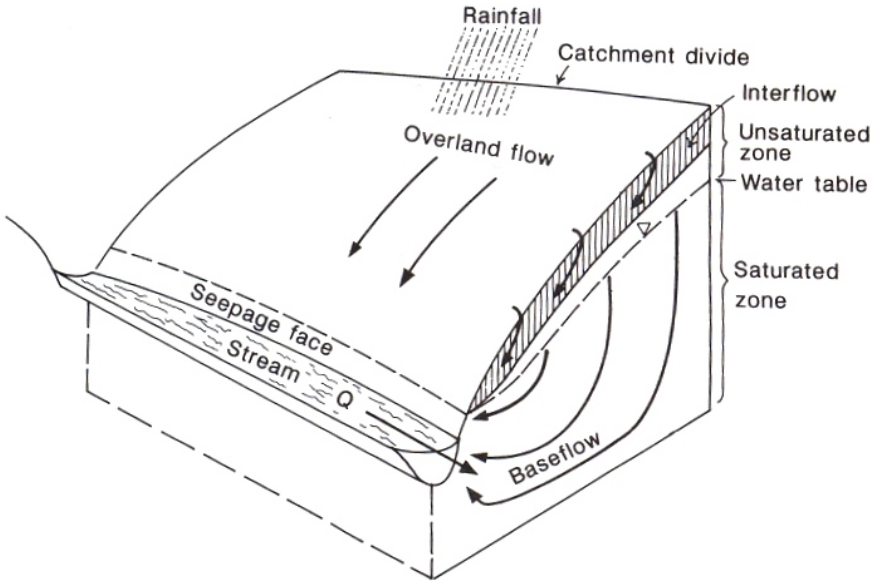


**Figure 3.2.** Components of catchment runoff contributing to stream flow (Hiscock, 2005).

After a storm event, infiltration and percolation of water continue, resulting in an elevated groundwater table which enhances the rate of baseflow. Hydrographs consist of a succession of individual peaks, each of which represents the global response of the aquifer given to a precipitation event (Kovács *et al*., 2005). The rising limb comprises of a concave segment and represents the flood curve (Figure 3.3). The peak represents the maximum infiltration state. The steep falling limb is called the flood recession curve and the slightly sloped segment is referred to as baseflow recession, which is the most stable section of any hydrograph. The three segments are related to surface runoff, interflow from the upper soil layers and baseflow from aquifers. The baseflow recession analysis focuses on the evaluation of the baseflow segment. The fundamental principle describing the recession is the exponential equation provided by Maillet (1905):

$$Q(t) = Q_0 e^{-\alpha t} \qquad (3\text{-}6)$$

where $Q(t)$ is the discharge at time $t$, and $Q_0$ is the initial discharge, $\alpha$ is the recession coefficient. On a semi logarithmic graph, this function is represented as a straight line with the slope - $\alpha$. The Maillet equation when plotted on a semi-log diagram is a straight line with coefficient of discharge, $\alpha$, being its slope (Krešić, 1997):

$$\alpha = \frac{\log Q_0 - \log Q_1}{0.4343.(t - t_0)} \qquad (3\text{-}7)$$

Introduction of the conversion factor (0.4343) is a convenience for expressing discharge in equation (3-7) in cubic meters per second, and time in days. The Maillet interpretation is based on the drainage of a simple reservoir, and presumes that the spring discharge is a function of the volume of water held in storage. Though this expression was actually designed for recession curves of porous aquifers it is usually adequate for describing baseflow recession of karst systems reflecting low-permeability fissured matrix drainage (Kovács *et al*., 2005).

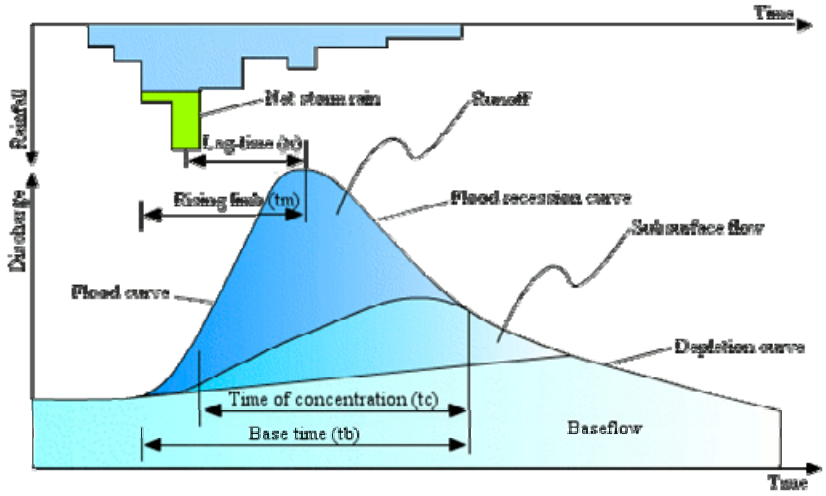


**Figure 3.3.** The flood hydrograph from a rainfall event (Musy, 2001).

The coefficient of discharge (α) and the volume of free gravitational groundwater stored in the aquifer above storing level (groundwater that contributes to spring discharge), are inversely proportional:

$$\alpha = \frac{Q_t}{V_t} \qquad (3\text{-}8)$$

Where $Q_t$ is the discharge rate at time $t$, and $V_t$ is the volume of water stored in the aquifer above the level of discharge.

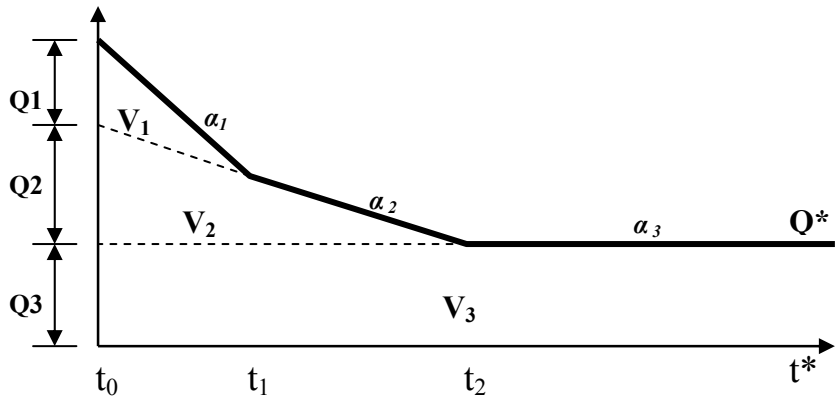


**Figure 3.4.** Schematic presentation of recession with three micro-regimes of discharge, and the corresponding volumes of water discharged from the three different types of storage.

The volume of groundwater remaining in the aquifer at the end of the third micro-regime is the function of discharge at time *t*, and the coefficient of discharge $\alpha_3$.

$$V^* = \frac{Q^*}{\alpha_3} \tag{3-9}$$

The volume of groundwater stored in the beginning of the recession is:

$$V_0 = [\frac{(Q_1 - Q_2)}{\alpha_1} + \frac{(Q_2 - Q_3)}{\alpha_2} + \frac{(Q_3)}{\alpha_3}].86400s \tag{3-10}$$

The difference between volumes $V_0$ and $V^*$ is the volume of all groundwater discharged during period $t$-$t_0$. Recession periods of large perennial karst springs, often have two or three micro-regimes of discharge as discussed above. However, the first micro-regime rarely corresponds to the simple exponential expression of Maillet (1905), and is better explained by the hyperbolic function of Boussinesq (1904):

$$Q_t = \frac{Q_0}{(1+\alpha t)^n} \tag{3-11}$$

A full description of the various steps to determine the discharge coefficient (α) and approximation of exponent *n*, is given in Krešić, 1997.

### 3.3.2 Borehole Hydrograph Recession Analysis

As with the streamflow recession, the three segments of the recession limbs from borehole hydrographs in a multiple porosity karst aquifer also represent three types of flow (storage): namely, diffuse or matrix flow (baseflow), flow through fractures, and flow through large conduits (quickflow) (Shevenell 1996; Kiraly, 2003; Raj, 2004; Hovorka *et al*., 2004). This technique was described and applied by Shevenell (1996) and then by Powers and Shevenell (2000) for a karst aquifer.

Shevenell (1996) and Powers & Shevenell (2000) investigated the recession limbs of hydrographs after storm events for wells in a karst aquifer. When recharge water abruptly enters an aquifer, it creates a pressure wave that propagates through the subsurface, creating a surge in water levels in boreholes and in spring discharge. As in stream flow, borehole hydrograph recession curve often appears to follow an exponential decay model ($Q(t) = Q_0 e^{-at}$). The rising limb is mainly a function of the precipitation event, whereas the recession limb is effectively independent of the nature of the rain event. The method of recession curve analysis for well hydrographs devised by Shevenell (1996) relies only on water level and not on discharge. The method generates ratios of flow between the different flow components, as well as ratios of the storativity, and, under some assumptions, the flow components themselves as well. Each of the three segments of the hydrograph (Figure 3.5) has a characteristic slope ($\alpha$) for any given storm event, and the slope is defined by the following equation:

$$\frac{\ln(Y_1/Y_2)}{t_2 - t_1} = \alpha_1 = \frac{\ln(Q_1/Q_2)}{t_2 - t_1} \qquad \frac{\ln(Y_2/Y_3)}{t_3 - t_2} = \alpha_2 = \frac{\ln(Q_2/Q_3)}{t_3 - t_2}$$

$$\frac{\ln(Y_3/Y_4)}{t_4 - t_3} = \alpha_3 = \frac{\ln(Q_3/Q_4)}{t_4 - t_3} \qquad \text{(3-12)}$$

Where, $Y_1$ and $Y_2$ are water levels corresponding to the water level and Q1 and Q2 are the associated flows (discharges) corresponding to the water levels at times $t_1$ and $t_2$.

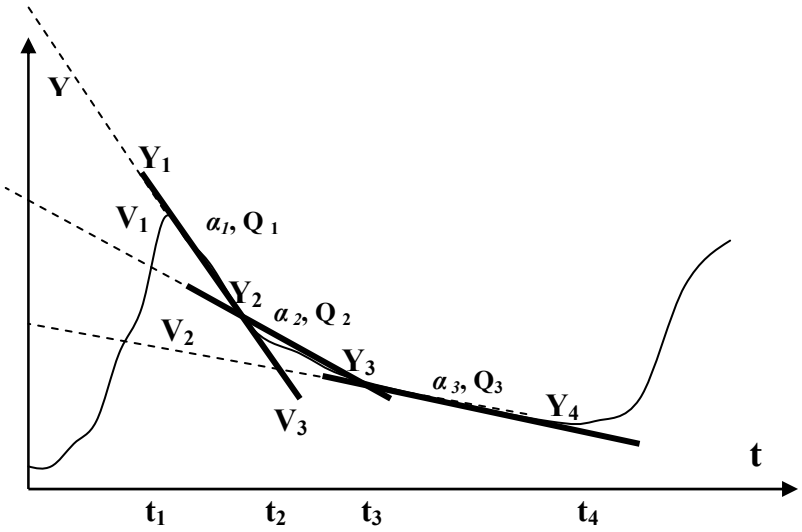


**Figure 3.5.** Schmeatic representation of the recession with three micro-regimes of groundwater flow.

Solving for $Q_1/Q_2$ in equation (3-12), the ratios of the theoretical flows can be calculated, where values of $Q_1$ to $Q_2$ represent conduit-dominated flow/drainage, values of $Q_2$ to $Q_3$ represent fracture-dominated flow, and values of $Q_3$ to $Q_4$ represent diffuse, matrix-dominated flow. The relationship of baseflow conditions to change in groundwater storage volume has been expressed by Fetter, 2001 as:

$$V_1 = Q_1(t_2 - t_1)/\ln(Q_1 - Q_2) \qquad (3\text{-}13)$$

Combining with equation (3-12) yields:

$$V_t = \frac{Q_t}{a_t} \qquad (3\text{-}14)$$

Where $V_t$ is the volume of water in dynamic storage at any time $t$, $Q_t$ the water representing the flow rate produced by stored water at any time $t$. It is assumed that the flow rate $Q_t$ from storage is reflected in the well hydrograph by the hydraulic head $Y_t$, and the two are related by equation (3-12), with both decreasing along each segment with time as a result of storage depletion. Using the discharge ($Q$) ratios above, the volumes ($V_t$) can be cast in terms of one $Q$ (e.g. $Q_0$). The volume of storage related to each segment on a well hydrograph can be expressed as a function of each of the individual Y values (Figure 3.5).

$$(V_1 - V_2) = \frac{(Q_1 - Q_2)}{a_1} \qquad (3\text{-}15) \text{ or}$$

equivalently as:

$$(V_1 - V_2) = AS_y(Y_1 - Y_2) \qquad (3\text{-}16)$$

Where $A$ is the drainage and $S_y$ is the specific yield. Using equation (3-15) to obtain ($V_1$-$V_2$) as a function of the $Q$ associated with the segment of the hydrograph being considered, and substituting this value as a function of $Q$ into equation (3-16) allows determination of a value for the ratio $AS_y/Q_1$ for each segment of the hydrograph. Using the ratios of $Q_1/Q_2$, obtained previously, the $S_y$ for each portion of the hydrograph (conduit, fracture, matrix regions) can be expressed as a function of one of the $Q$ values.

In estimating the average non-conduit $T$ of an unconfined aquifer from a baseflow recession curve, Rorabaugh 1960 developed an equation for estimating aquifer diffusivity (T/S) from the slope of the water level recession in a stream or observation well at critical time:

$$\frac{T}{S} = \frac{0.933L^2 \log(Y_1/Y_2)}{(t_2 - t_1)} \qquad (3\text{-}17)$$

Where $L$ is the distance from discharge to ground-water divide, and $S$ is the storage coefficient, which is equal to the $S_y$ for unconfined aquifers. Hydraulic diffusivity is defined as the ratio of transmissivity to storage coefficient (specific yield if unconfined) or equivalently of hydraulic conductivity to specific storage (Rutledge, 2006). Knowledge of either geometry of the drainage area or hydraulic diffusivity will allow calculation of the other.

## 3.4 Hydraulic Tests

Hydraulic test procedures are the classical approach to determine hydraulic aquifer parameters and to assess the borehole efficiency. Equally important, they can be interpreted in order to define the flow regime and to characterise the aquifer.

### 3.4.1 Slug Tests

A slug test involves the instantaneous injection or withdrawal of a volume or slug of water or solid cylinder of known volume. The cylinder replaces its own volume of water within the borehole, thus increasing the pressure in the borehole. As the equilibrium in the water level is changed, it will recover or stabilise to its initial level. If the rate of recovery or recession of the water level is measured, the transmissivity or hydraulic conductivity of the borehole can be determined (Bouwer and Rice, 1976; Van der Kamp, 1976).

The Bouwer and Rice (1976) method considers fully and partially penetrating wells in homogeneous, isotropic, incompressible, unconfined aquifers, although the method can be used under certain confined conditions (Mace, 1999). The geometry of the borehole for the Bouwer and Rice slug test is shown in (Figure 3.6).

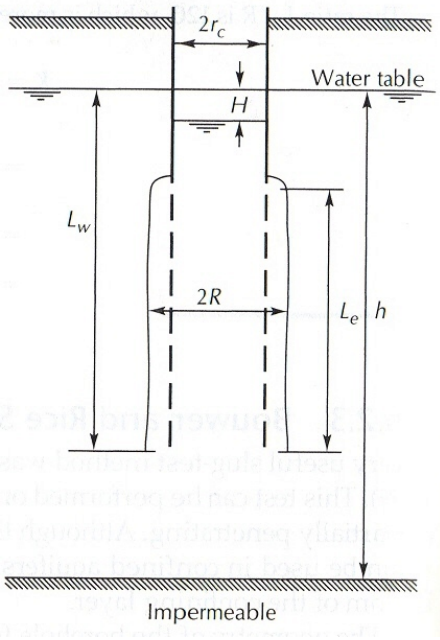


**Figure 3.6.** Geometry and symbols for slug test developed by H. Bouwer (Fetter, 2001).

The parameter $r_c$ is the radius of the well casing in which the water level is rising and $R$ is the radius of the gravel pack or developed area around the well screen. The Bouwer and Rice equation is (Fetter, 2001):

$$K = \frac{r_c^2 \ln(R_e / R)}{2L_e} \frac{1}{t} \ln\left(\frac{H_0}{H_t}\right) \qquad (3\text{-}18)$$

Where

$K$ is hydraulic conductivity

$R_c$ is the radius of the well casing

$R$ is the radius of the gravel envelope

$R_e$ is the effective radial distance over which head is dissipated

$L_e$ is the length of the screen or open section of the well

$H_0$ is the drawdown at time $t = 0$

$Ht$ is the drawdown at time $t = t$

$T$ is the time since $H = H_0$

A slug test performed in an aquifer of high hydraulic conductivity may produce an oscillatory water level change in the test well. This is referred to as an under damped response (Fetter, 2001). The amplitude of the oscillation decrease with time, but the damping (slope of line across top of peak of the absolute value of the displacement data) remains constant as well as the frequency. Van der Kamp (1976) presented the first significant paper leading to the analysis of oscillatory data using a sinusoidal approximation method.

$$H(t) = H_0 e^{-\gamma t} \cos \omega t \qquad (3\text{-}19)$$

Where

*H(t)* is hydraulic head at time

$H_0$ is the instantaneous change in hydraulic head

γ is a damping constant

ω is an angular frequency

The transmissivity is given by the expression

$$T = c + a \ln T \qquad (3\text{-}20)$$

And

$$c = -a \ln(0.79 r_s^2 S(g/L)^{1/2}$$

$$a = \frac{r_c^2 (g/L)^{1/2}}{8d}$$

$$d = \frac{\gamma}{(g/L)^{1/2}}$$

$$L = \frac{g}{\omega^2 + \gamma^2} \qquad (3\text{-}21)$$

Where

*T* is the aquifer transmissivity

$r_c$ is the radius of the well casing

$r_s$ is the radius of the well screen

*S* is the storage coeeficient

*L* is the effetve length of the water column

*g* is the gravitational constant

The solutions (slug tests) discussed above have relied upon the assumption of homogeneity in formation properties, even though it is widely recognized that hydraulic properties of fractures can vary significantly over the length of boreholes. Butler *et al*. (2003) presented a spreadsheet-based implementation for the analysis of slug tests performed in partially penetrating wells in formations of high hydraulic conductivity. In this procedure, theoretical type curves are graphically fit to normalized plots of slug-test response data to obtain estimates of the hydraulic conductivity of the near-well portions of the formation. The models are straightforward extensions of those of Bouwer and Rice (1976) and Hvorslev (1951) models and will be used in this study for slug test interpretations.

Slug tests are widely used and generally accepted (Shapiro and Hsieh, 1997; McElwee, 2002; Butler *et al*., 2003), it should be remembered that slug tests yield only local values of horizontal hydraulic conductivity (within a close proximity to the well). Even though slug testing may only qualitatively resemble the predicted responses of the model it remains a cost-effective, quick estimate of the hydraulic properties of aquifers.

## 3.5 Hydrochemical Characterisation

Advances in geochemical methods and approaches have aided our ability to interpret hydrochemical processes in groundwater systems, and improved understanding of how structural, geological, and hydrological features affect flow and chemistry in these systems (Glynn and Plummer, 2005). Hydrochemical and isotope studies are frequently included in karst groundwater investigations and give valuable additional information on the structure of the aquifer system (Perrin, *et al*., 2003; Mayer, 1999; Han and Liu, 2004; Bredenkamp *et al*., 2007). In regional studies, hydrochemical and isotope data can be used to distinguish different aquifers. They are also useful for the detection of zones of interaction (mixing) and groundwater contaminants.

### 3.5.1 Geochemical Investigation

Groundwater chemical interpretation is done with the help of graphical displays such as Piper diagrams, Stiff patterns and Schoeller diagrams, flow path observations or molar relationships. These graphical representations are very helpful in preliminary evaluation of groundwater types and the relation between groundwater and lithology (Mahlknecht *et al*., 2004). The problems, however, with these methods are that graphical displays include only a limited number of chemical elements and its interpretation is somehow subjective and difficult, especially with large sample sets (Güler *et al*., 2002).

Advances in graphical and multivariate statistical methods have aided our ability to interpret hydrochemical processes in groundwater systems (Guler, *et al*., 2002; Hussein, 2004; Singh *et al*., 2004; McNeil *et al*., 2005). Multivariate methods like cluster analysis classifies and compares different chemical parameters of the water analysis and determines the relationship between them. Generally, the approach is to divide the samples into hydrochemical signatures, which are groups of samples with similar chemical characteristics that can be spatially, correlated (Güler *et al*., 2002). These methods allow us to identify the possible sources of anthropogenic influences and determine their extent on the groundwater system of the COHWHS.

*Multivariate Statistical Analysis*

A Hierarchical Cluster Analysis (HCA) is commonly applied to classify observations so members of the resulting groups are similar to each other but distinct from other groups (Hussein, 2004, Guler *et al*., 2002; Thyne *et al*., 2003; Singh *et al*., 2003; Heikinien *et al*., 2002; Lamabrakis *et al*., 2004). The multivariate cluster analysis is used to identify structures in the geochemical dataset (chemical signatures), which are also spatially interpreted. The relationship of the statistically defined clusters of samples to geographic location illustrates the most important message that geochemical survey datasets contain i.e. the variation in regional distribution (Reimann *et al*. 2005).

A thorough evaluation of each element is needed, including assessment of the lower limits of detection, the range of values, and the nature (shape) of the data distribution. The data characterisation step is a prerequisite to successful data cleaning and transformation before multivariate statistical analysis is approached.

### 3.5.2 Environmental Isotopes

The environmental isotopes deuterium ($^{2}H$), oxygen-18 ($^{18}O$) and tritium ($^{3}H$) are suitable for tracing the origin of the water in the hydrological cycle because they are constituents of the water molecule (Kranjc, 1997). The, use of environmental isotope techniques may, in addition to conventional investigation methods, provide further insight into the storage properties of the natural hydrological system.

*Isotope Displacement - $^{2}\delta$ (ID)*

As it is not useful to present the absolute concentration of a single isotope, stable istotopic abundances are reported as a ratio to some abundant isotope of the same element or as positive or negative deviations of these isotope ratios ($R$) away from a standard (Weaver *et al*., 1999). If $R$ is the ratio of the heavy isotope to the light one, then relative fractionation is expressed in del notation as (Fetter, 2001):

$$\delta = \frac{R_{sample} - R_{s\tan dard}}{R_{s\tan dard}} \qquad (3\text{-}22)$$

Results are expressed as deviation in parts per thousand (‰). If value of $\delta$ is positive, then sample is enriched with the heavy isotope relative to the standard; a negative samples is isotopically light.

During phase changes of water between liquid and gas, the heavier water molecules tend to concentrate in the liquid phase, which fractionates the hydrogen and oxygen isotopes. Water that evaporates from the ocean is isotopically lighter than the water remaining behind and precipitation is isotopically heavier; that it contains more $^{2}H$ and $^{18}O$ than the vapour left behind in the atmosphere. These isotopic ratios from an environmental sample can be compared with the isotopic ratio of standard mean ocean water (SMOW) (Fetter, 2001).

When $\delta^{2}H$ is plotted as a function of $\delta^{18}O$ for water found in continental precipitation, an experimental linear relationship is found that can be described by the equation (Craig, 1961).

$$\delta^{2}H = 8\delta^{18}O + 10 \qquad (3\text{-}23)$$

This is known as the global meteoric water line (GMWL). The South African meteoric water line is represented by (Van Tonder and Xu, 2001):

$$\delta^{2}H = 8\delta^{18}O + 17 \qquad (3\text{-}24)$$

The position of any pair of $\delta^{2}H$ and $\delta^{18}O$ values on this line for rainwater worldwide will depend on local climatological conditions (temperature, latitude, altitude, and rainfall amount effects). After the infiltration of precipitation only physical processes such as diffusion, dispersion, mixing and evaporation alter the groundwater isotopic condition. Oxygen-18 ($^{18}O$) stable isotope is utilised to identify the recharge process and mixing of groundwater from different sources. Surface waters contain a distinct composition of stable isotopes due to enrichment caused by evaporation. Therefore, $^{18}O$ makes it possible to distinguish between evaporated waters and waters directly recharged from precipitation (Sukhija, *et al*., 2006).

*Tritium*

Tritium ($^{3}H$) is a radioactive isotope of hydrogen having mass 3 and half-life of 12.38 years (Hiscock, 2005). The unit of measurement is the tritium unit (TU) defined as 1 atom of tritium occurring in $10^{18}$ atoms of H and equal to 3.19 pCi $L^{-1}$. Tritium in the atmosphere is typically in the form of the molecule $H^{1}H^{3}O$ and enters the groundwater as recharging precipitation. When rainwater is isolated from the atmospheric source, i.e. during groundwater recharge, no new tritium is added and the tritium concentration will decrease with this characteristic half-life.

The changes in atmospheric $^{3}H$ are monitored by the IAEA through a global monitoring network (IAEA). In Southern Africa, tritium levels in rainfall rose from initial (natural) values of about 5 TU to 60 – 80 TU as a result of fall-out of nuclear weapon testing in the early 1960's. Due to this tritium is an ideal isotope to be used for age dating of groundwater that recharged after 1952 (Pannatier *et al*, 2000). According to Weaver *et al*., (1999) tritium studies can provide semi-quantitative age determinations of groundwater:

- Water with zero tritium (<0.5TU) has a pre-1952 age.
- Water with significant tritium concentrations (>5TU in the southern hemisphere) is of post-1952 age.
- Water with little, but measurable, tritium (between 0.5 and 5 TU) seems to be a mixture of pre- and post-1952 water.

Katz *et al*., (1997) used Tritium ($^{3}H$) to estimate the age of ground-water recharge in the Upper Floridan karst aquifer by comparing measured $^{3}H$ concentrations in ground water with the long-term $^{3}H$ input function of rainfall measured at the International Atomic Energy Agency (IAEA) precipitation monitoring station. The authors concluded that that recharge of rainfall to the Upper Floridan karst aquifer occurred during the past 30 to 40 years and most likely represents very recent recharge.

## 3.6 Conceptual Model

The development of a conceptual hydrogeological model is the single most important step in managing an aquifer. Many conceptual models have been created to represent groundwater flow through karst, constructed on the basis of observations in the field and subsequent interpretation of the data obtained (Perrin, 2003). The model should nevertheless adequately delineate the overall hydraulic characteristics of the investigation area. The process of developing a conceptual model of a karst aquifer system includes:

- Classification of geohydraulic units which combine rock formations with similar lithological and hydraulic properties,
- identifying features such as dominant faults, dykes and fracture zones,
- determining the hydraulic properties of such features and the assessment of their impact on the flow regime at the scale of interest,
- description of hydraulic characteristics such as porosity, permeability and storativity,
- describing the various types of recharge and functions,
- and a geochemical description of the aquifer.

With the information provided by the borehole inventory, the geological maps, spring hydrographs, slug tests, chemical and isotopic data, it is possible to generate a hydrogeological conceptual model describing in a quantitative/qualitative form the general behaviour of the aquifer.

# 4. Characterisation of the COHWHS Karst Aquifer

## 4.1 Physiography

The Cradle of Humankind World Heritage Site (COHWHS) comprises an area of approximately 47 000 Ha of which half of the surface area (approximately 22 890 Ha) is underlain by the dolomites of the Chuniespoort Group. It is within this Group that karst formation has occurred. Dykes that form boundaries to groundwater flow cross the dolomites, creating isolated hydrogeological compartments. The investigation focuses on the Zwartkrans compartment in the south and the Tweefontein compartment in the north and includes the dolomitic outlier (footprint shape) towards the south of the main dolomite limb (Figure 4.1). The Zwartkrans compartment covers an area of 15 398 Ha and contains the Sterkfontein and Wonder caves, and the major springs Danielrus, Kromdraai and Zwartkrans. The Zwartkrans compartment's hydrogeological boundaries are:

- the Pretoria group in the north,
- the Tweefontein compartment in the north-east with the Rietfontein dykes as boundary,
- the Basement complex and Witwatersrand Super-Group in the east and south, and
- the Steenkoppies compartment in the west with the Tarlton west dyke as boundary.

The Tweefontein compartment covers an area of 12 698 Ha and contains numerous caves with the major springs Nouklip and Broederstroom. The Tweefontein compartment is bounded by:

- the Pretoria group in the north,
- the Hennops compartment in the north-east (whether this dyke actually forms a hydrological barrier is uncertain),
- the Basement complex and Witwatersrand Super-Group in the south, and
- the Zwartkrans compartment in the south-west with the Rietfontein dykes as boundary.

Very little data exist for the Tweefontein compartment in comparison with the Zwartkrans compartment. This could be attributed to the compartment's sparse human activities and relative insignificance as aquifer compared to Zwartkrans compartment.

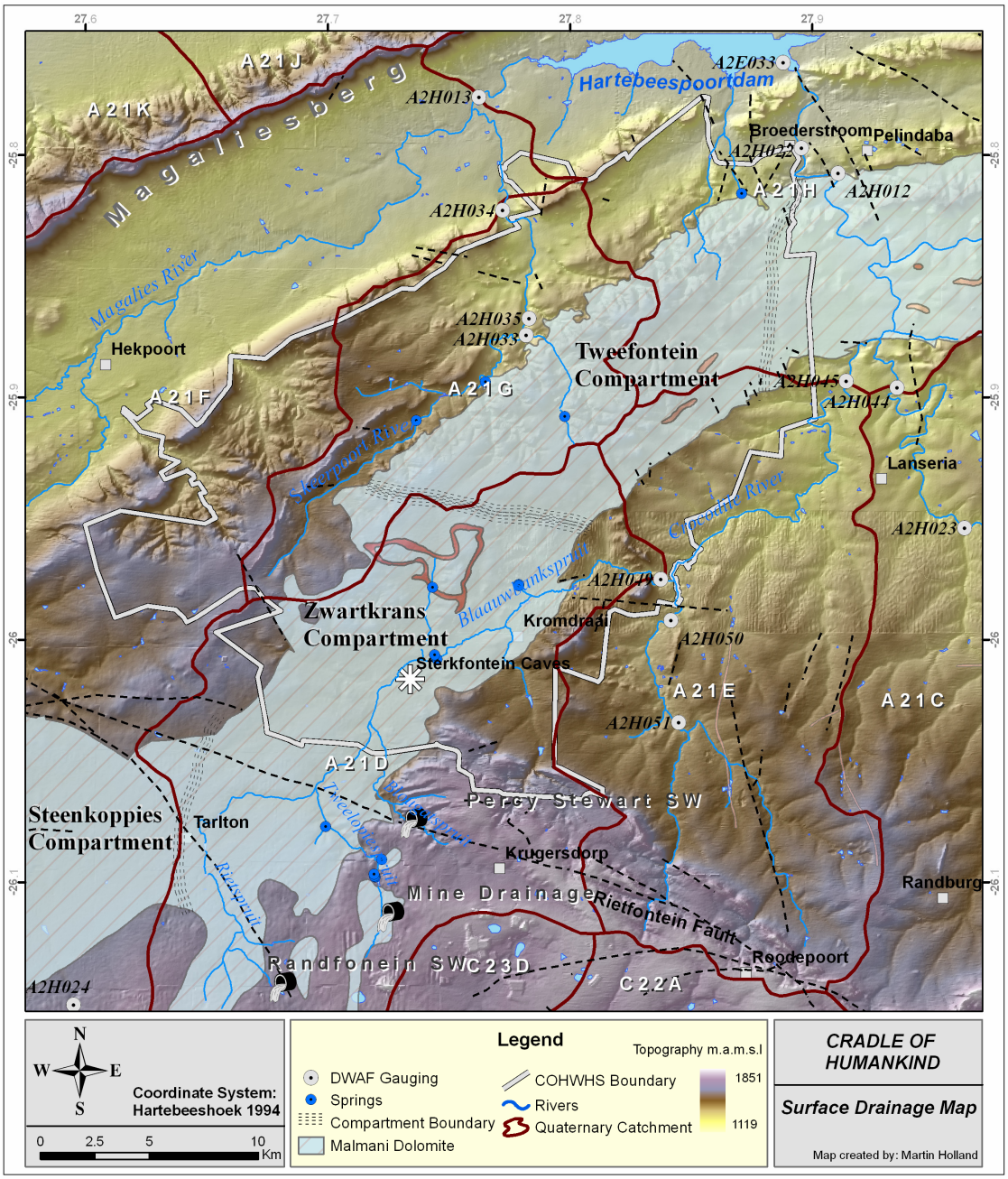


**Figure 4.1.** Current topography and surface water catchments of the main study area with springs indicating possible groundwater contribution to river flow.

The gently undulating landscape of the area is often interrupted with significant topographical differences which is attributed to different erosion and weathering characteristics of the band of dolomites and their associated breccias. The chert-poor units weather to a smooth topography covered by red silty type clayey soils devoid of chert. The chert-rich units weather to an uneven topography characterised by dissolution openings and a permeable chert residue with red silty and brown manganiferous soils (Obbes, 2001). The area is covered mainly by grass, with more dense vegetation along the rivers. The surface features of the COHWHS dolomites can often be related to the sub-surface bearing

characteristics e.g. valleys of surface drainage coincide with fractured zones in karstified dolomite. The low density of runoff drainage suggests high recharge and predominance of water flow underground, which eventually drains into surface streams at topographic lows or emanates as springs next to diabase dykes or formation contacts.

### 4.1.1 Surface Water Drainage

The compartments of the COHWHS forms part of the upper Crocodile River sub-system and is located within the Crocodile (West) and Marico Water Management Area as described by the Department of Water Affairs. The COHWHS forms part of the A21 tertiary drainage region and the quaternary drainage regions involved are A21D, A21E, A21G and A21H (Figure 4.1).

The Zwartkrans compartment is drained towards the north-east by the perennial Blaauwbankspruit Stream. The upper Blaauwbankspruit also termed Rietspruit, drains storm water and surface run-off from the town of Randfontein in addition to some 8.16 Ml/day of treated sewage effluent (Krige, 2006) from the Randfontein Sewage Works facility. For some distance, surface flow of the stream remains constant, but disperses into the underground network as soon as it crosses the Rietfontein Wrench fault system.

Probably the most important and influential tributary on the karst hydrology, is the Tweelopiespruit. This stream originates approximately 4.5 Km to the south of the Krugersdorp Game reserve and traverses a distinct dolomitic outlier. This dolomite outlier is associated with the decanting of 15 Ml/day of polluted mine water from the old Black Reef incline mine shaft (Van Biljon, 2006). At the time of the study the polluted mine water was treated through a process of lime addition and aeration as well as secondary treatment through a wetland system. This facility, which includes a HDPE-lined containment dam and pumping stations downstream, struggle to contain the flow from the decanting mine water during periods of high rainfall and significant amounts of mine water flows into the Tweelopiespruit (Photo 1). As the stream traverse towards the north it gains and loses significant amount of water along its flowpath as it moves from one geological section to the next. The flow in the stream increases, as it is fed from a number of springs along its course, but loses a significant amount of its flow as the stream crosses sections of the Rietfontein fault system (Figure 4.1). After its confluence with the Blaauwbankspruit it disappears almost completely through the leakage of carbonate rock beneath the riverbed.

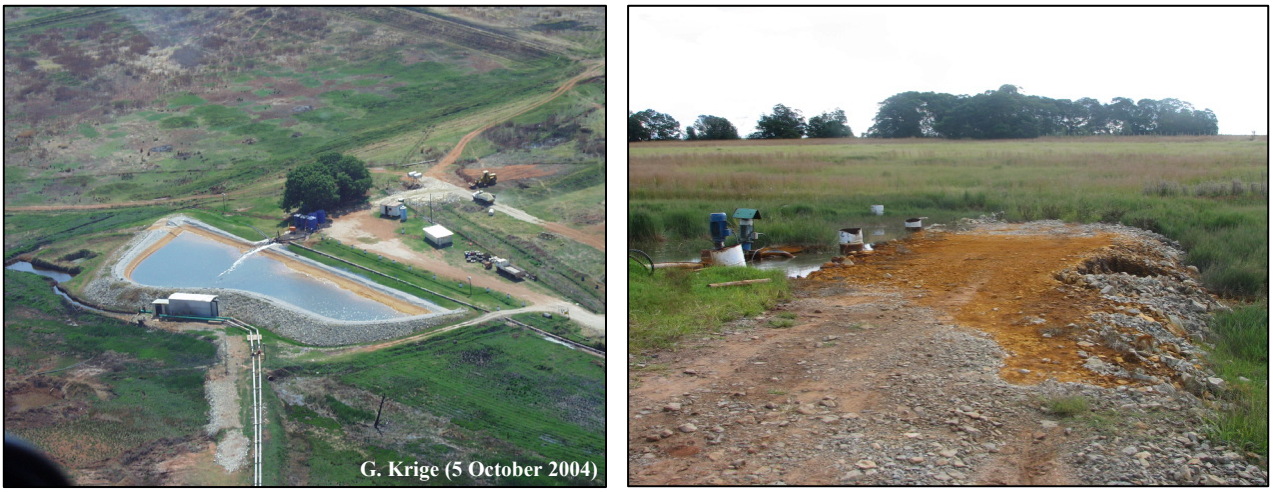


**Photo 1.** The dam constructed to intercept water decanting from the Black Reef incline shaft (left) and pumping stations to divert mine drainage water back to the treatment dam (right).

The second major tributary of the Blaauwbankspruit is the Blougatspruit which is responsible for the drainage of 19.3 Ml/day of treated sewage effluent in addition to surface run-off from the industrial area of Krugersdorp (Krige, 2006). The tributary flows through the quartzite hills, and after receiving the sewage effluent from the Percy Stewart Sewage Works facility (Photo 2), the stream flows further downstream onto the Dolomite.

**Photo 2.** Percy Stewart Sewage Works facility with its effluent returns flow outlet (left), and the Blougatspruit downstream of the Percy Stewart facility before its confluence with Blaauwbankspruit (right).

The Blaauwbankspruit catchment plays a major role in the carrying off mining, industrial and municipal wastewater together with run-off from agricultural land. The Blaauwbankspruit is fed by several perennial springs towards the centre of the Zwartkrans Compartment which increases the flow strength before its confluence with the Crocodile River in the east. Some drainage characteristics of the area include (Figure 4.1):

- A generally dendritic (branching form) drainage pattern of low density.
- On satellite images of the area, various structurally controlled intermittent drainage channels could be identified (Jamison *et al*., 2004).
- The southern part of the COHWHS is drained towards the north-east by the Blaauwbankspruit and its tributaries to the Crocodile River, which feeds the Hartebeespoort Dam.
- In the central part of the COHWHS the riverbed of the Skeerpoort drains north to Magalies River; it is fed from springs, as well as by surface runoff during periods of high rainfall.
- Several perennial springs are present, namely Danielsrust-, Kromdraai- and Zwartkrans eye, with discharges of more than 5 l/s, but are not yet monitored on a continuous basis.

The only significant DWAF gauging stations in the study area are the one at the Blaauwbankspruit's confluence with the Crocodile River (A2H049) and the Nouklip eye at Skeerpoort (A2H033) (Figure 4.1). Both these stations have long term flow and chemical data.

### 4.1.2 Climate

Climate plays a major role in controlling rainfall and potential recharge, as shown by differences in recharge sources and rates between arid and humid settings (Scanlon et all, 2002). The climate in the area is typical South African "Highveld", characterised by warm summers, when 80% of the rainfall is experienced as thunderstorms, and cool dry winters with cold nights. Frosts are experienced for up to five months of the year and hail falls often.

Long term rainfall records exist at several South African Weather Bureau (SAWB) and agricultural meteorological stations distributed throughout the area (Figure 4.2), unfortunately only a few stations have continues rainfall records. None of the DWAF rainfall stations is within the study area and could therefore not be used in the borehole hydrograph investigations. For this reason it was decided to utilise the rainfall data (August 2005 – November 2006) from the rainfall collectors installed by Gauteng Department of Agriculture & Environment at Amazingwe game farm and Sterkfontein caves respectively (Figure 4.2).

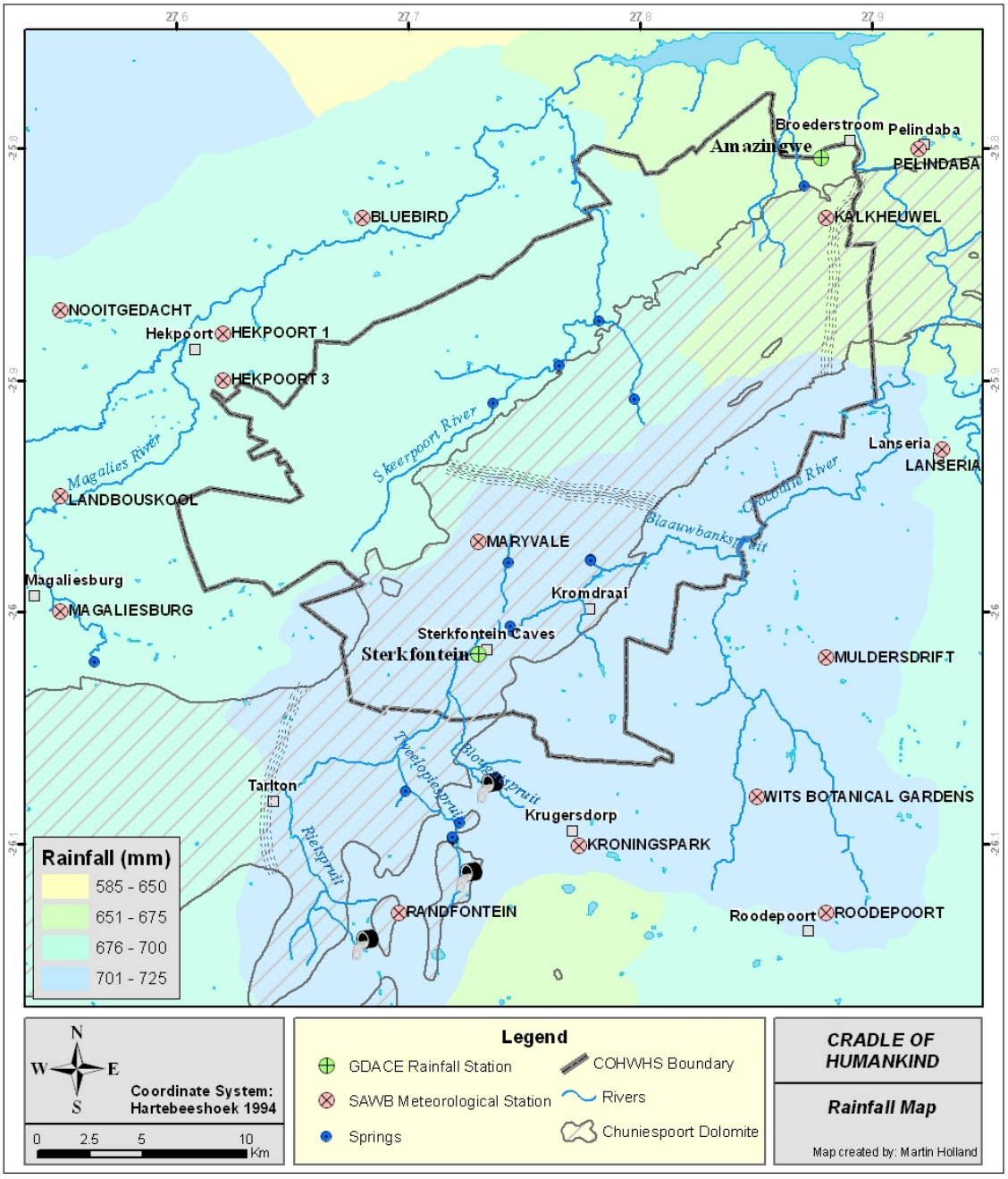


**Figure 4.2.** Location of rainfall stations together with the spatial distribution of the mean annual precipitation of the quaternary catchments as depicted by DWAF, 2005.

Table 4.1 indicates the stations with reliable continuous long term rainfall data that will be used with spring flow and borehole hydrograph interpretations. The average rainfall measured from SA Weather Services and agriculture stations has a slight spatial variability over the study area, with a higher annual average rainfall towards the south and north-west. Figure 4.3 indicates the annual rainfall relationship between the seven stations involved indicates the spatial variability of rainfall over the larger area (see for example 1988, 1996 and 2004). A correlation graph of Krugersdorp and Pelindaba meteorological stations, confirms the slight variability of rainfall over the region.

**Table 4.1.** Meteorological stations in the study area.

| (SAWS) | Rainfall Record | Coordinates | | Elevation (m.a.m.s.l) | Rainfall (mm) |
|---|---|---|---|---|---|
| | | Latitude | Longitude | | |
| Nooitgedacht | 1972-current | -25.8700 | 27.5500 | 1 463 | 782 |
| Magaliesburg | 1969-current | -26.0000 | 27.5500 | 1 480 | 637 |
| Pelindaba | 1984-current | -25.8000 | 27.9200 | 1 280 | 664 |
| Randfontein | 1955-current | -26.1300 | 27.7000 | 1 710 | 664 |
| WITS | 2001-current | -26.0800 | 27.8500 | 1 520 | 621 |
| Roodepoort | 1987-current | -26.1300 | 27.8800 | 1 656 | 758 |
| Kroningspark | 1960-current | -26.1000 | 27.7700 | 1 699 | 710 |
| **(GDACE)** | **Rainfall Record** | **Coordinates** | | **Elevation (m.a.m.s.l)** | **Rainfall (mm)** |
| | | Latitude | Longitude | | |
| Amazingwe | 2005/2006 | -25.8000 | 27.9000 | 1 274 | 584 |
| Sterkfontein | 2005/2006 | -26.0000 | 27.7000 | 1 471 | 538 |

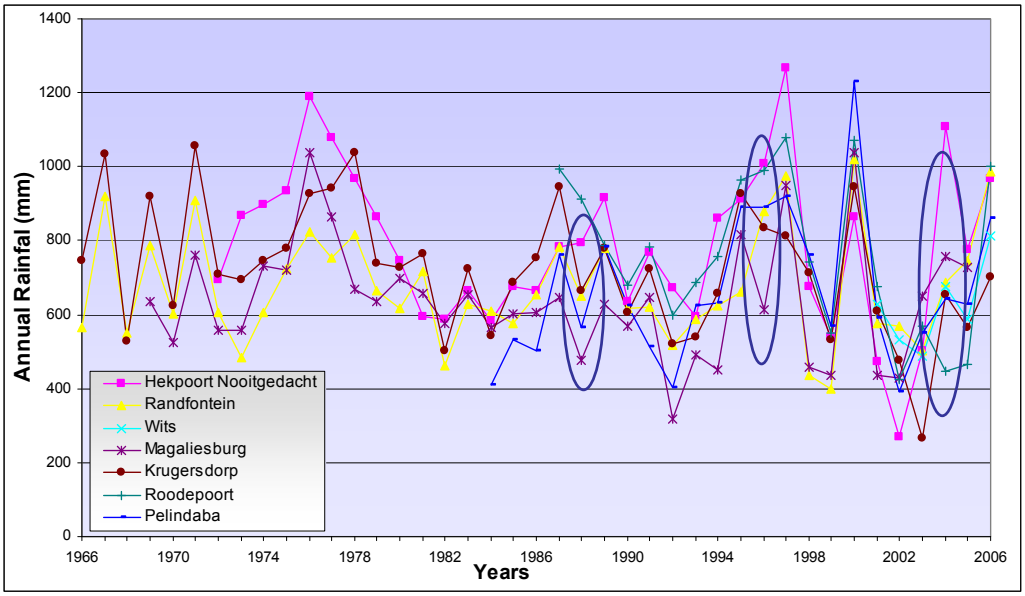


**Figure 4.3.** Long-term annual rainfall comparison between meteorological stations in the vicinity of the study area.

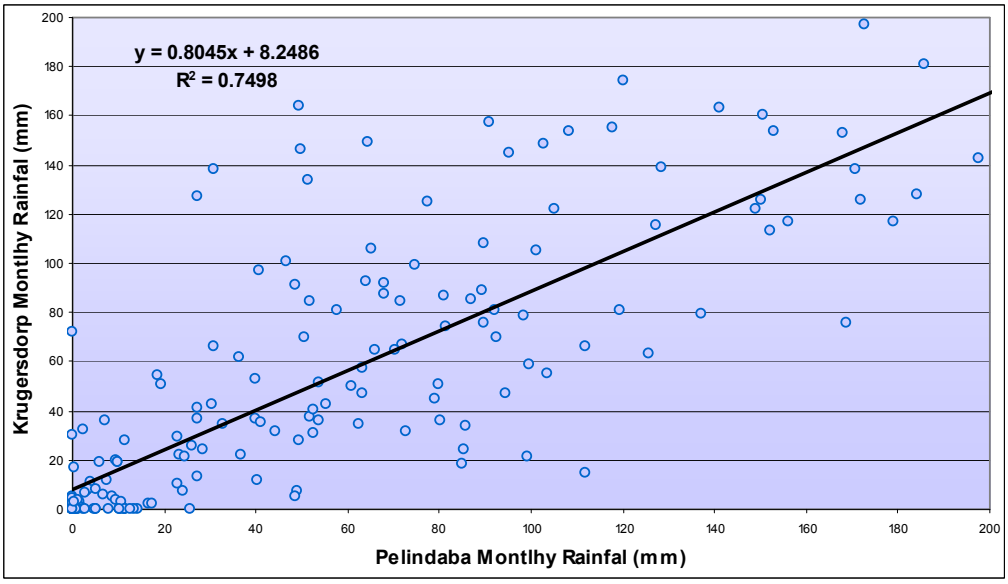


**Figure 4.4.** Monthly correlation between Krugersdorp and Pelindaba rainfall stations.

A very high potential evapotranspiration with a mean annual evaporation of about 1700 mm prevails (DWAF, 1992) and exceeds the average annual precipitation by a factor of 2.4. However, the actual evapotranspiration is much lower as the shallow soil cover limits availability of moisture to the plants, which causes excess soil water to infiltrate below the root zone, recharging the groundwater reservoir.

### 4.1.3 Geomorphology

Comparing the karst morphology of the study area to the four types of karst as distinguished by Martini and Kavalieris, 1976 in Chapter 2, both the Escarpment and Plateau type are revealed. The plateau variety of recent breccias is characterised by a flat plateau pronounced in the south-western part of the study area (Photo 3). The escarpment variety is typical of the north-eastern portion of the study area and is characterised by a rugged topography and a dendritic network of valleys where physical erosion dominates the surface morphology. This is possibly due to the slow rate of dissolution of the dolomite, to the thunderstorm character of a great part of the rainfall and to the large number of fissures and joints that are choked and thus impede the rapid seepage necessary to prevent surface flow. In this way the karst of South Africa contrasts strongly with other areas in the world characterised by more regular rainfalls and snow thawing on pure limestone, for instance in the Alps, where a karst morphology can develop even on steep slopes (Martini and Kavalieris, 1976). The dolomite is frequently concealed under a thick blanket of residual material that is derived from recent dolomite dissolution and the weathering of older karst regoliths. The surface karst features include natural springs, caves, sinkholes, dolines and shallow depressions (Photo 3).

The present karst forms and geomorphology have been created by the interplay of ancient and recent erosion cycles on lithologies that have undergone many episodes of deformation. Subsequent to the break up of the super-continent of Gondwanaland (250 million years ago), the dolomites have been uplifted into a high interior plateau and the overlying Karoo cover rocks relatively rapidly stripped off by erosion to reveal a pre-Karoo palaeo-karst surface (King, 1963; Wilkins *et al*., 1987). An episode of quaternary regional up warping on an East Northeast trending transcontinental axis has caused significant drainage reversal over the whole karst region. The emergent plateau has tilted slightly towards the north and the younger streams have aggressively incised northward draining gorges, capturing the previous drainage pattern and exploiting zones of structural weakness. Renewed karstification of this rejuvenated surface has taken place over the Pleistocene period

accompanied by climatic changes of the Highveld plateau pluvial cycles (Jamison *et al*., 2004).

**Photo 3.** A view of the undulating topography of the Cradle of humankind (left) and sinkhole formation near Sterkfontein caves (right).

## 4.2 Geology

The geology of the study area controls the occurrence, quality and flow paths of groundwater in the rock formations. The movement of groundwater is largely dependant on preferential flow paths that occurs in the primary aquifers and host rock. The 1:50 000 geological maps from the Council for Geoscience and recent mapping from Obbes, 2001 was used as starting point for the surface geology with some boreholes logs used to evaluate the geology and groundwater occurrence at depth.

The North-western boundary of the COHWHS runs along the crestal ridge of the Klapperkop quartzite of the Timeball Hill formation of the Pretoria Group. The South-eastern boundary runs over the Western part of the Johannesburg granite dome and its associated ridges of gold bearing Witwatersrand formations forming the faulted rim of the Witwatersrand basin. Dipping off the western flank of the Johannesburg Dome with a disconformable contact is the basal formation of the Transvaal Super-Group consisting of the Black Reef Quartzite formation underlying the Malmani dolomite Subgroup of the Chuniespoort Group (Figure 4.5). The improved geological map produced by Obbes (2001) is illustrated in Figure 4.5; unfortunately the study only covered the Chuniespoort Group down to the north of Sterkfontein caves.

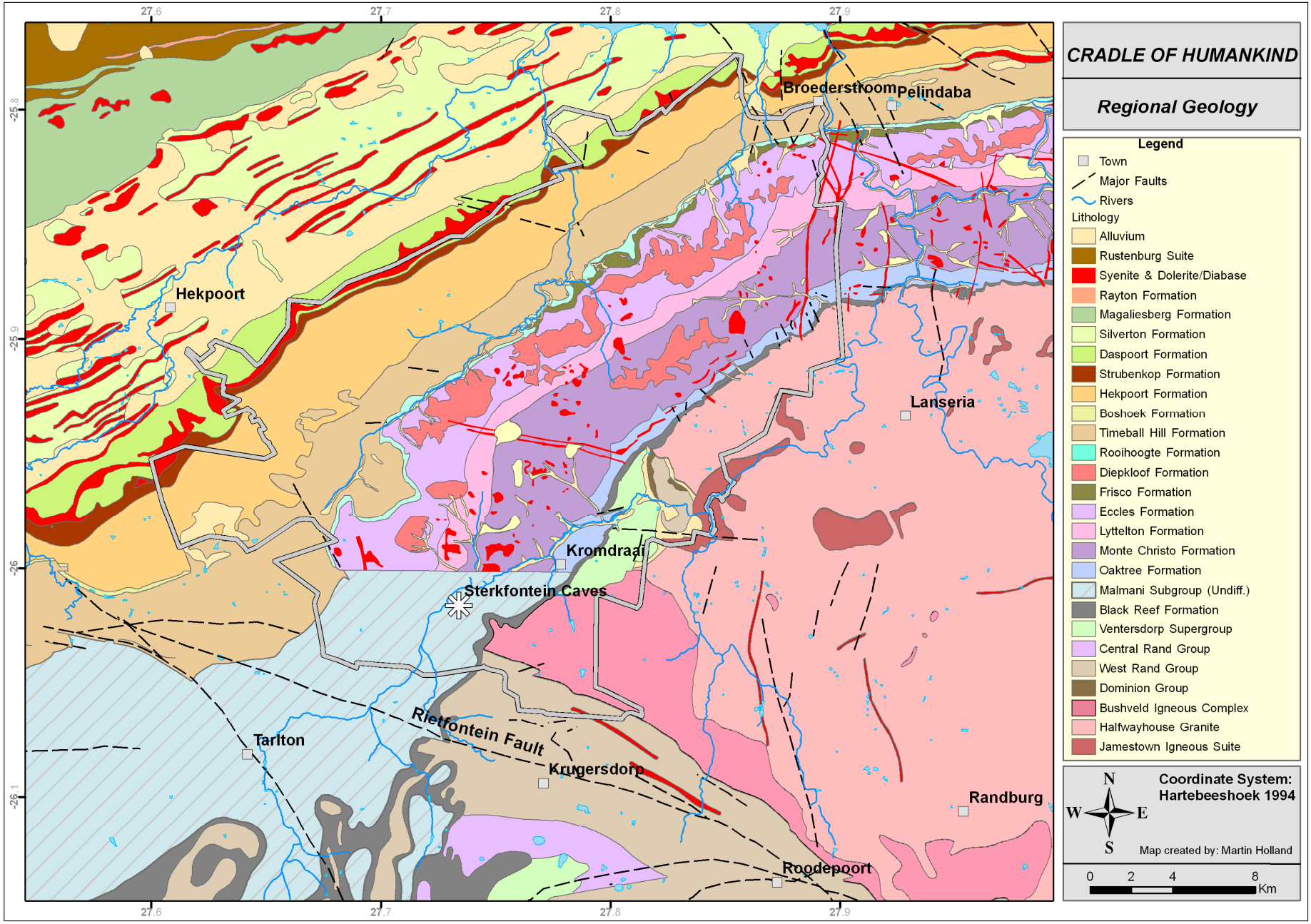


**Figure 4.5.** Geology of the Cradle of Humankind World Heritage Site.

Based on the abundance of chert, the subgroup has been subdivided into five dolomitic formations. A generalised lithostratigraphy is presented in Table 4.2. The geology pertaining to the study area is described in chronological order, from the oldest to the youngest formations.

**Table 4.2.** Lithostratigraphy of the geology of the region; area of investigation highlighted. (SACS, 1980:205; Foster, 1984; Obbes, 2001).

| Super Group | Group | Formation | Thickness (in m) | Lithology |
|---|---|---|---|---|
| | | Diepkloof | ? | (Karoo-age) Chert breccia with siliceous and ferruginous matrix. |
| TRANSVAAL | PRETORIA | Rayton | 120 | Shale, quartzite. |
| | | Magaliesburg | 300 | Quartzite. |
| | | Silverton | 600 | Shale. |
| | | Daspoort | 80-95 | Quartzite. |
| | | Strubenkop | 105-120 | Slate. |
| | | Hekpoort | 340-550 | Andesite. |
| | | Timeball Hill | 270-660 | Shale, Diamictite, Klapperkop Quartzite and ferruginous quartzite. Graphitic and sitly shale. |
| | | Rooihoogte | 10-150 | Quartzite, Shale, Bevets Conglomerate Member and Breccia. |
| | CHUNIESPOORT | Frisco | 30-158 | Chert-free dolomite with some primary limestone and carbonaceous shale at the base. |
| | | Eccles | 490 | Chert-rich dark dolomite with stromatolitic and oolitic bands. Chert increases to the top. |
| | | Lyttelton | 220-290 | Chert-free dark dolomite with large stromatolites and sometimes with wad. |
| | | Monte Christo | 740 | Alternate layers of chert-rich and chert-poor light coloured dolomite with stromatolites and oolites. |
| | | Oaktree | 190-330 | Chert-poor dark dolomite with interbedded layers of carbonaceous shale at the base, decreasing to the top and sometimes with wad. |
| | | Black Reef Quartzite | 11-30 | Shale and Quartzite. Arkosic Grit |
| VENTERS-DORP | Undifferentiated | | ? | Andesite tuff, conglomerate calcareous shale, sandstone. |
| WITWATERSRAND | CENTRAL RAND | Undifferentiated | 2 880 | Aranaceous, rudaceous rocks. |
| | WEST RAND | | 5 150 | Quartzite, reddish and ferruginous magnetic shales. |
| | DOMINION | | ? | Quartzite, conglomerate, shale, interbedded lava. |
| BASEMENT COMPLEX | | | | |

### 4.2.1 Basement Complex

The geological basement in the study area consists of Archaean rocks, known as the Kaapvaal Craton. The Halfway House granite that outcrops in the northwest of the study area is representative of the Archaean Basement and consists of gneiss, granite and granodiorite. It is the oldest rock formation in the vicinity as it forms part of the Archaean era which is about 3100 Ma old. On the Kaapvaal Craton unmetamorphosed sequences ranging in age from 3 000 to 1 750 million years have accumulated in basins from oldest to youngest (Truswell, 1977). In this study they are the Witwatersrand, Ventersdorp and Transvaal Sequences.

### 4.2.2 Witwatersrand Super-Group

In this study the rocks of the Witwatersrand Super-Group are mentioned as they underlie the Black Reef Formation at the base of the Transvaal Super-Group. The Witwatersrand Basin, deposited in a fluvial system some 2 800 million years ago, is a thick sedimentary sequence of shale, quartzite and conglomerate (Trustwell, 1977). There are two main divisions, a lower predominantly argillaceous unit, known as the West Rand Group and an upper unit, composed almost entirely of quartzite and conglomerates, known as the Central Rand Group. The latter contains the economic gold deposits (reefs) that were mined extensively not only in the West Rand, but throughout the Witwatersrand Basin.

### 4.2.3 Black Reef Formation

The Black Reef Quartzite's lies unconformable on the Witwatersrand Super-Group to the south and to the north on the Ventersdorp Super-Group or Basement Complex. The Black Reef Formation is composed of quartzite, lenticular beds of grit and conglomerate with shale at the top (Barnard, 2000).

### 4.2.4 Chuniespoort Group

Overlying the Black Reef Formation conformably is the dolomite of the Malmani Subgroup of the Chuniespoort Group. The Malmani Subgroup is subdivided into the Oaktree, Monte Christo, Lyttelton, Eccles and Frisco Formations (SACS, 1980). Karstification, has been more active in the chert-rich dolomite, due to higher porosity developing in the brittle, fragmented, cherty horizons. Therefore, the chert-rich Eccles formation and especially the Monte Christo formations have good water bearing and storage characteristics. The low groundwater potential Oaktree and Lyttelton formations are characteristically chert poor with only the occasional thin band of chert.

*Oaktree Formation*

The Oaktree Formation consists of dark-grey, chert free dolomite and is characterized by large stromatolitic domes, shale marker beds and a tuffite unit (Obbes, 2001). The formation has a uniform dark colour and can be identified by its elephant skin appearance after weathering to a dark brown colour. It is exposed throughout the study area except in the south-west where a residual soil cover marks the sequence. The top part of the formation near the Monte Christo formation becomes more light grey and the chert layers becomes thicker as it gradually changes towards Monte the Christo formation (Bredenkamp *et al*., 1986)

*Monte Christo Formation*

Obbes's (2001) detailed field mapping identified four members (Rietfontein, Mooiplaats, Reitspruit and Crocodile River) of the Monte Christo Formation. The subdivision of the Formation is based on the chert-in-shale breccias, certified stromatolite marker beds and the presence or absence of stromatolites. For the purpose of this study the Formation will described as one. The chert-rich Monte Christo Formation consists of dark grey dolomite at the top which becomes lighter towards the lower parts consisting of creamy to white dolomite rich in oolites.

**Photo 4.** Typical chert rich dolomite associated with the Monte Christo Formation, outcrop near Sterkfontein quarry.

*Lyttelton Formation*

The Lyttelton Formation largely represents the Oaktree formation and consists of chert-poor dark-grey dolomite which weathers to a chocolate-brown colour. The unit is characterized by a dark tone, a relatively subdued topography and poorly defined bedding traces on aerial photographs. The lower part of the succession contains more chert than the central portion.

*Eccles Formation*

The Eccles Formation consists of light-grey interbedded dolomite and chert bands. The upper part of the Eccles Formation consists of a silicified chert breccia, named the Leewenkloof member (Obbes, 2001).

*Frisco Formation*

The poorly exposed Frisco Formation consists of a chert poor, dark-grey dolomite and weathers to a dark-brown colour. Obbes, 2001 mapped the Formation for the first time in the area and was not previously recognized. The upper contact in the Tweefontein compartment is an erosional unconformity overlain by the Rooihoogte Formation.

### 4.2.5 Pretoria Group

The Chuniespoort Group is unconformably overlain by the Pretoria Group and this succession buries a palaeokarst landscape developed on exposed dolomites during a depositional hiatus of at least 80 Ma. The Pretoria Group is predominantly an alternating sequence of mudrock and sandstone formations with subordinate conglomerates, diamictites and carbonate rocks and significant interbedded basaltic-andesitic lavas (Erikkson and Reczko, 1995). The basal Rooihoogte Formation is a silicified chert breccia derived from insoluble chert residue resulting from the erosion of the Chuniespoort Group. Obbes (2001) mapped this unit of residual breccia as the Diepkloof Formation which consists of chert clasts set in siliceous-ferruginous matrix. It forms a prominent capping on the topographically high-lying areas and is interpreted as a weathered product of the underlying carbonate sequence.

### 4.2.6 Mafic Dykes and Lineaments

Aeromagnetic data sourced from the Council for Geoscience for the 1:50 000 map sheets 2527DC, 2527DD, 2627BA and 2627BB was used for the identification of linear anomalies in the region (Figure 4.6). These magnetic anomalies was compared to the dykes mapped by Bredenkamp *et al.* (1986) and the two dyke sets mapped by Obbes, 2001. The lineaments were additionally compared to fractures and dykes mapped by Jamison *et al.* (2004). Dykes displayed two different magnetic signatures (positive and negative). Obbes (2001) noted the negative aeromagnetic anomalies of the north-south trending dykes north of Tweefontein compartment and the positive aeromagnetic anomalies of the east-west trending dyke which constitute the border between the two compartments. The dyke compositions vary from syenite to diabase/dolerite and composite dykes are present. Interpretation of LANDSAT imagery by Jamison, in conjunction with enlarged aerial photographs and ground truth mapping investigations, has provided abundant evidence of anomalous and undocumented structures, dykes, faults and shear zones transecting this area (Figure 4.6).

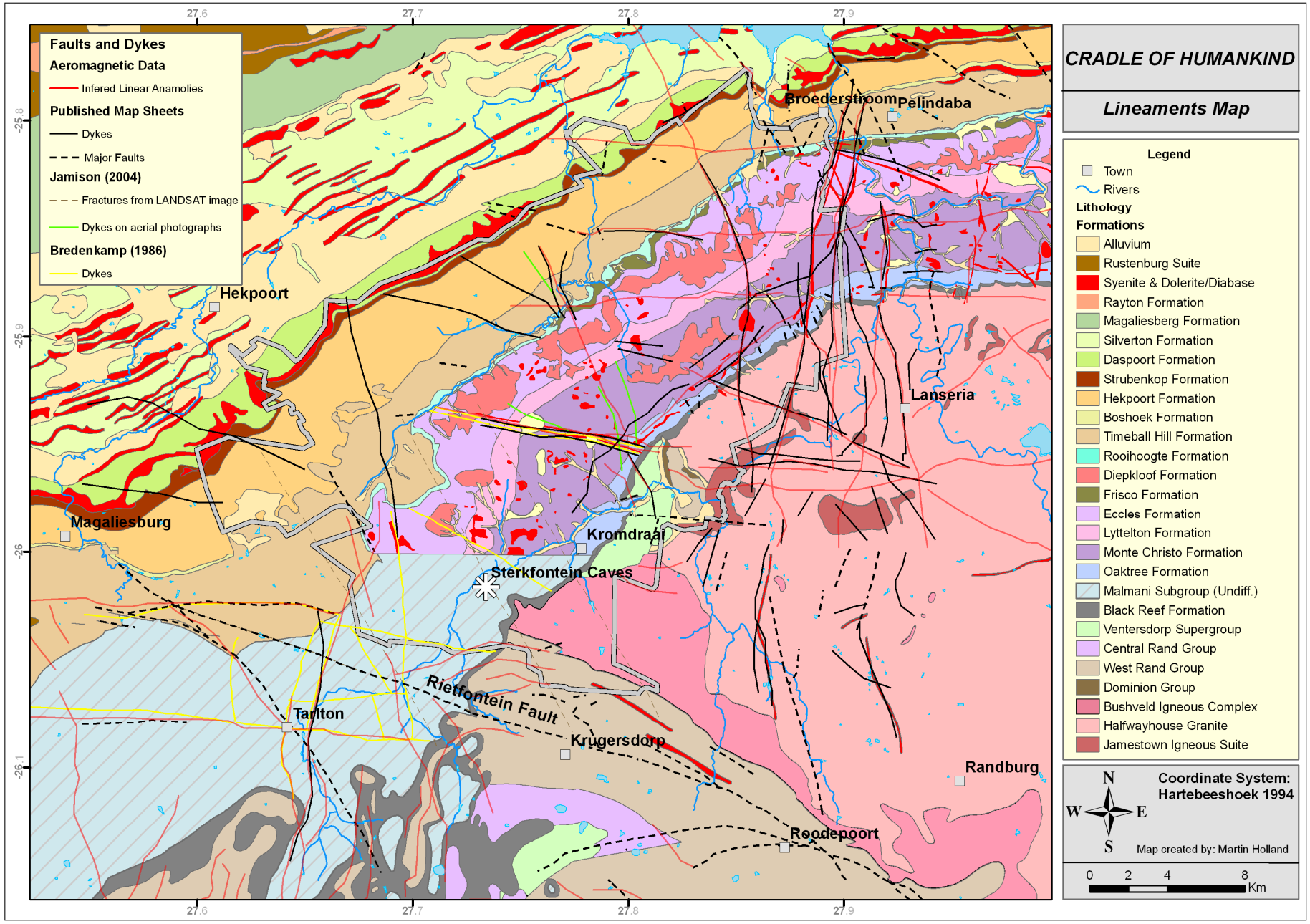


**Figure 4.6.** Faults/Dykes from published geology maps together with the linear anomalies interpreted from high resolution aeromagnetic data.

### 4.2.7 Regional Structure

Recent detailed mapping and analysis in the greater COHWHS has identified pre-Bushveld folding and late-Bushveld bedding sub-parallel ductile deformation mylonites which slice the stratigraphy into an imbricate stacked duplex (parts overlapping like roof-tiles) (Courtnage, 1995). Mylonites are formed as fine grained laminated rock by extreme plastic deformation and milling of rocks during movement on faults, under high strain in deformation zones at depth. The dolomites and Pretoria Group have subsequently been folded and fractured by a re-activated left lateral WNW trending shear system which has imprinted sub-parallel deformation zones at +/-10 km intervals parallel to the Rietfontein Wrench Fault System as the principle control of cavern and karst form development upon the area (Holland *et al*., 2005) (Figure 4.7).

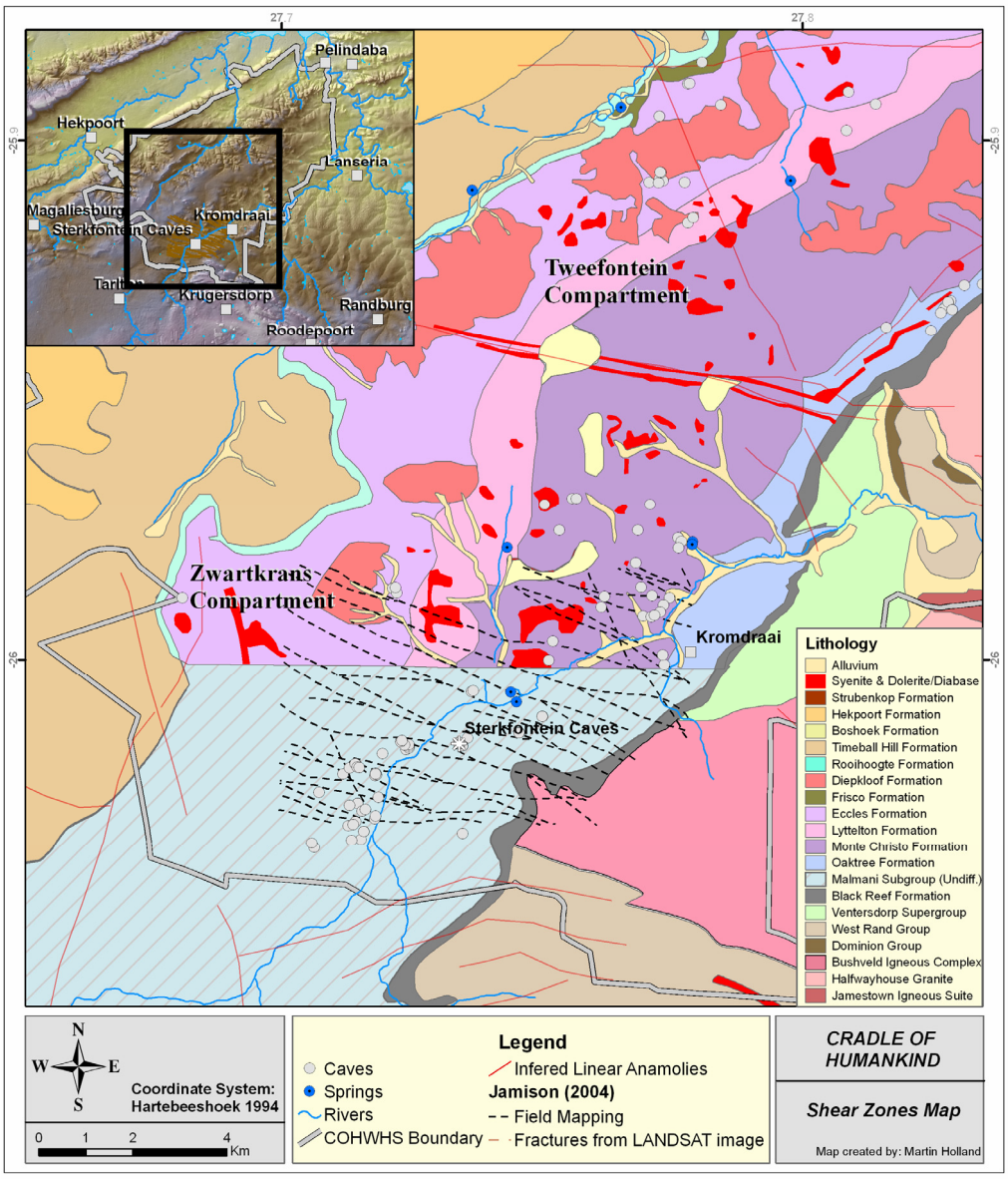


**Figure 4.7.** Locality of Caves in relation to major faults (data from Jamison *et al*., 2004).

Most of the caves, dolines, sinkholes and fissures are located on the WNW shear zones and in close relationship to impervious bedding sub-parallel mylonitic cherty slate horizons (Jamison *et. al*., 2004). The final phase of re-juvenating of these fractures occurred as a result of epeirogenic warping and uplift along the Griqualand-Transvaal axis (Partridge and Maud, 1987), during the late Cretaceous era which initiated the present Karst cycle on the Craton interior.

Therefore, the dolomites are not only compartmented by near vertical dykes and silicified faults but also by bedding sub-parallel ductile mylonitic thrust planes and refolded folds (Holland *et al*., 2005). As a result of fracture reopening in the Tertiary epeirogenic warping of the dolomite plateau, solution along the WNW trending fracture zones was enhanced and a new cycle of karstification of the dolomite ensued. The present caves and karst features would thus be expected to occur as stacked perched water tables, and complex recharge and flow regimes within and between compartments are controlled by an inherited structural and lithological framework (Jamison *et al*., 2004).

## 4.3 Hydrogeology

### 4.3.1 Groundwater Level

Groundwater level data are of fundamental importance in the evaluation of the characteristics of any groundwater resource. Groundwater level data provide evidence of actual recharge due to water reaching the water table (Scanlon *et al*, 2002; Bredenkamp *et al*, 1995). Generally, groundwater levels fluctuate according to the characteristics of precipitation events (i.e. amount, duration, and intensity) and various hydrogeological variables (e.g. topography, thickness of the unsaturated zone, and matrix composition of saturated and unsaturated materials) (Moon *et al*., 2004). Analysis of water level fluctuations can be useful for determining the magnitude of long-term changes in recharge caused by climate or land-use change (Scanlon *et al*, 2002). Groundwater level data will be used to determine the groundwater flow by constructing a map of the potentiometric surface, in addition, to the analysis of borehole hydrograph's.

Static water level measurements of 43 boreholes were undertaken with a water level dipper during summer 2006/2007. An additional 24 static water levels were measured by the CSIR during early 2007 which was incorporated into one dataset (Appendix A). Continuous groundwater level loggers (transducers) and a barometric logger were installed in four

boreholes within the karst aquifer. These loggers were set to 30 minute intervals and logged for a period of 18 months from Aug 2005 to April 2007. The positions of the boreholes monitored in this study are shown in (Figure 4.8).

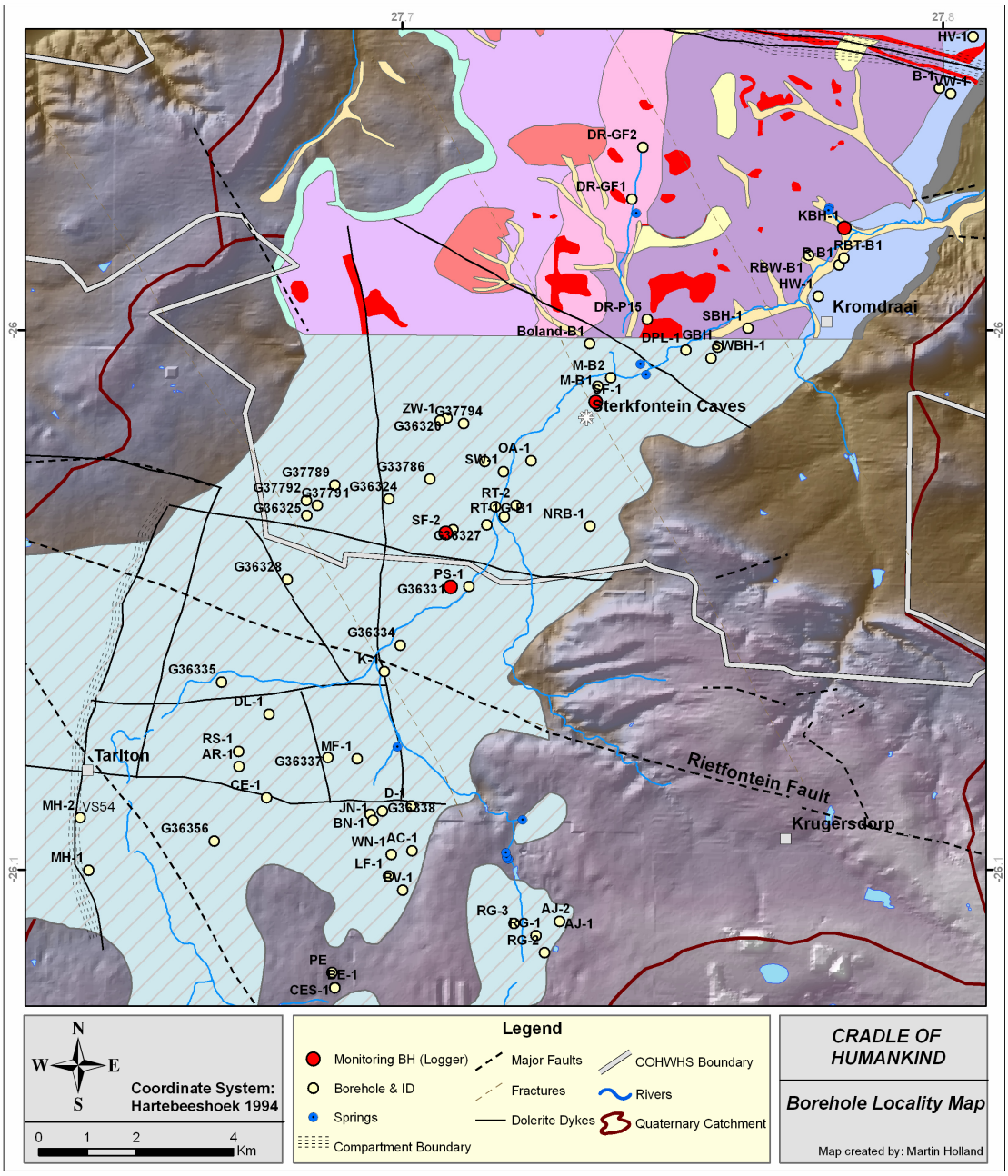


**Figure 4.8.** Map with monitoring boreholes where continuous water level loggers were installed.

*Groundwater Flow*

The spatial distribution of groundwater levels is used to visualize the variations in groundwater elevations, determine groundwater flow directions and define aquifer boundaries. A correlation between the surface topography and the groundwater levels in the dolomitic compartment is illustrated in (Figure 4.9). In general the groundwater level often

follows the surface topography. However, three grouping of boreholes (A, B and C) indicate a poor relationship between groundwater levels and topography. Group A can be associated with boreholes located at the dolomitic outlier and the surrounding high relief Black Reef Quartzite's. Grouping B and C can be attributed to the water table in the dolomite flattening out because of the hydraulic properties of the chert rich layers. The uneven weathering of the chert rich dolomite results in highly permeable coarse debris and is likely to develop greater concentration of joints which will in turn promote the process of weathering.

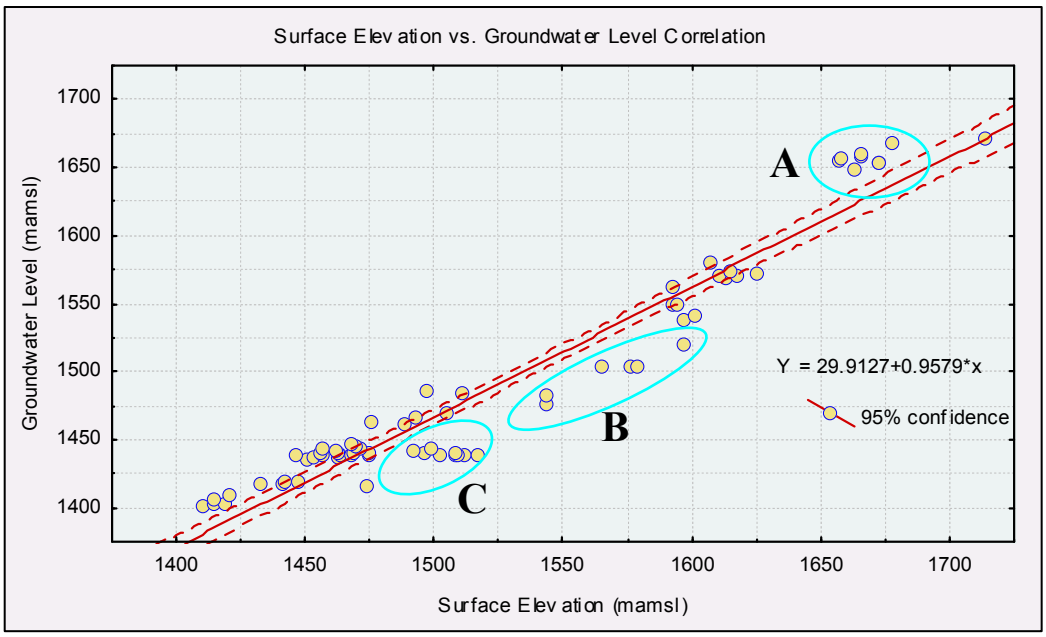


**Figure 4.9.** Correlation between surface topography and groundwater levels.

Figure 4.10 shows the water level distribution across the study area, plotted relative to sea level. The digital elevation model (DEM) of 50m intervals were used to estimate borehole elevations above mean sea level. The inverse distance weighting (IDW) interpolation method was applied to generate the groundwater level contour map. Inverse distance weighting (IDW) is an algorithm for spatially interpolating, or estimating values between measurements (Mathes and Rasmussen, 2006).

From this data it seems that there is a general gradient from the south towards Ritespruit on the north where after the gradient gently sweeps towards the SE to NW striking dyke in the northeast. The following further interpretations could be made from (Figure 4.10).

- The large groundwater gradient in the south is due to the low transmissivity of the quartzite ridges of the Black Reef Formation and West Rand Group. Groundwater flow over the quartzite's ridges is not confirmed but it is suggested that no inflow occurs.

- The most southern EW striking dyke has a definite influence on groundwater elevation confirming the dyke as a hydrogeological barrier.

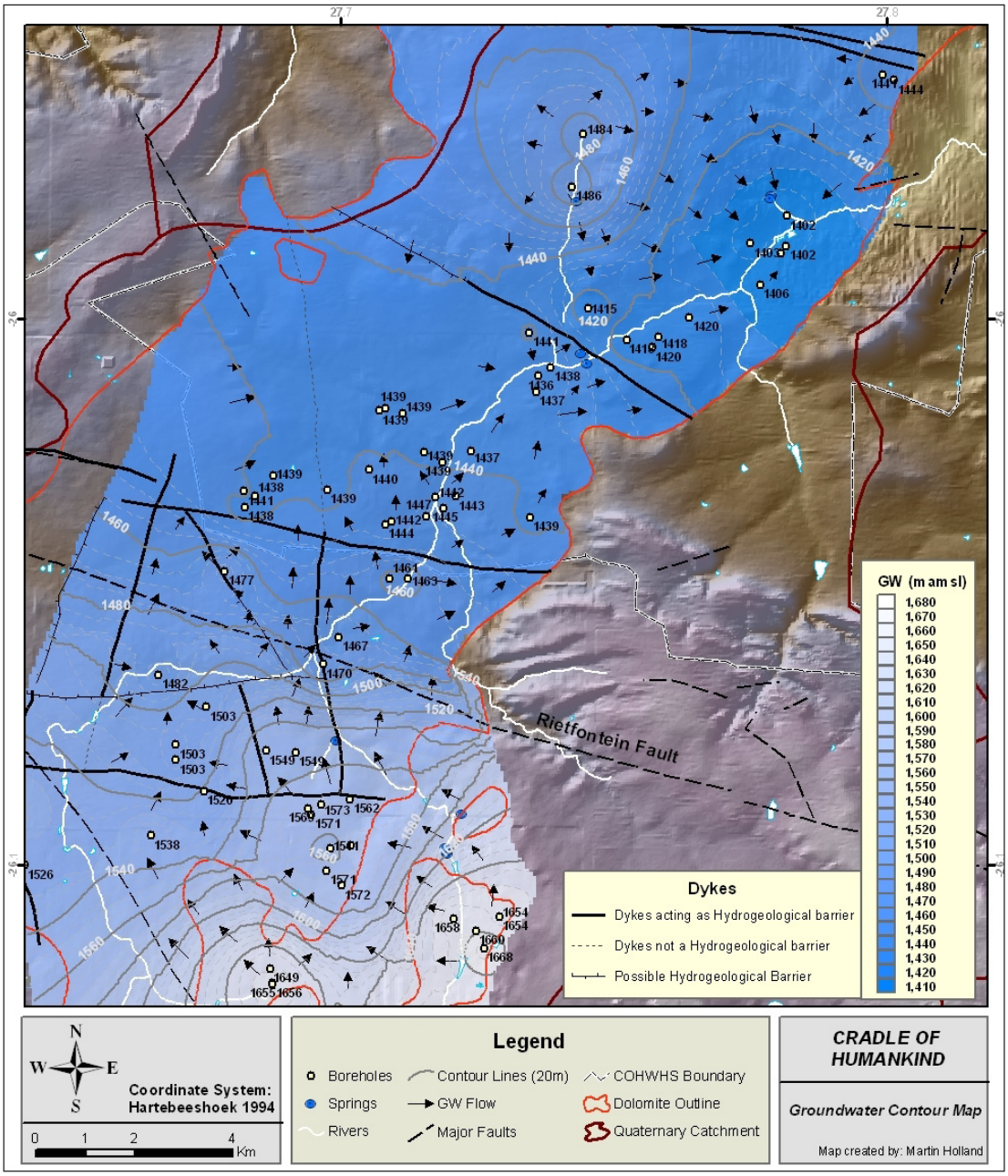


**Figure 4.10.** Groundwater level elevation contours of boreholes measured during Dec/Jan 2006/2007 (Inverse Distance Weighting - Interpolation).

- The parallel NS striking dyke's convergence with the EW striking dykes forms sub-compartments as depicted by Bredenkamp *et al*., (1986). It is evident that these sub-compartments are isolated hydrogeological from each other due to groundwater elevation differences.
- Further sub-compartments is evident by the cross cutting of the dolomites by SE to NW striking dykes in the north and northeast of the Zwartkrans compartment.

- Groundwater levels may have been impacted by large scale abstraction at site-specific places in the southern sub-compartment with a slight impact on flow direction.
- A significant levelling of the water table is seen in the centre portion of the dolomitic compartment suggesting high transmissivity values significant to karst systems (this is mainly attributed to the good water bearing characteristics of the chert-rich dolomite formations).
- Increases in water level depth were found in the regions of high relief's and hills. This could be due to karst conditions where cavities occur and gives an easy flow path for the groundwater. The water gradient is then lowered because very low capillary forces act on water to force water to flow accordingly to the topography.
- Several karst springs act as natural outflows for groundwater within the sub-compartments; this is especially evident in the most northern sub-compartment.
- The data suggest that groundwater levels are influenced by the cross-cutting dykes forming hydrogeological barriers, and not by the different dolomitic formations. Further geological mapping of the dolomitic formations and more groundwater level data is needed to confirm this statement.

### 4.3.2 Groundwater Recharge

High intensity rainfall during January and February commonly generates recharge. The absence of surface drainage channels and low surface run-off from the karst, suggest that most of the recharge emanate from rainfall infiltration. However, large amount of effluent return flow enters the underground network of the karst system via swallow holes and leaching beneath the riverbed. Bredenkamp et al., (1986) indicated that this artificial recharge significantly impacts the water balance estimation of the Zwartkrans compartment.

*Chloride Mass-Balance Method*

The rainfall analysis of rainwater showed chloride concentrations of <1 mg/l. Unfortunately the result was below the detection limit of laboratory. Van Tonder and Xu, (2002) assumed a chloride concentration of 1.24 mg/l for inland rainfall which is higher than the value obtained by the chloride analysis; therefore a chloride concentration in rainfall of 0.6 mg/l will be used. No previous recharge estimation has been conducted for the Tweefontein compartment. Chloride samples showing an anthropogenic signature were excluded from the dataset. The result of the CMB analysis for the Zwartkrans and Tweefontein compartments is illustrated in Table 4.3 and Table 4.4. Site specific recharge estimation is based on Equation 3-1 and the regional recharge estimation is based on the

harmonic mean (Equation 3-2) of chloride concentrations in groundwater. The dry deposition of chloride was excluded from the equation due to the uncertainty that exist in the estimation of atmospheric deposition.

**Table 4.3.** CMB results for the Zwartkrans compartment.

| Borehole ID | Cl (groundwater) (mg/l) | Cl (rainfall) (mg/l) | Average Annual Rainfall (mm) | Average Annual Recharge (mm) | Recharge % |
|---|---|---|---|---|---|
| KBH-1 | 5.00 | 0.6 | 710.2 | 143.74 | 12.0 |
| G36356 | 5.00 | 0.6 | 710.2 | 143.74 | 12.0 |
| G36325 | 5.00 | 0.6 | 710.2 | 143.74 | 12.0 |
| G36336 | 4.04 | 0.6 | 710.2 | 177.90 | 14.9 |
| KGR-5 | 2.50 | 0.6 | 710.2 | 287.49 | 24.0 |
| QC-2 | 2.12 | 0.6 | 710.2 | 339.02 | 28.3 |
| BF-1 | 2.00 | 0.6 | 710.2 | 359.36 | 30.0 |
| NRB-1 | 1.00 | 0.6 | 710.2 | 718.72 | 60.0 |
| BC-1 | 1.09 | 0.6 | 710.2 | 659.38 | 55.0 |
| BC-2 | 1.67 | 0.6 | 710.2 | 430.37 | 35.9 |
| DG-S | 3.00 | 0.6 | 710.2 | 239.57 | 20.0 |
| DR-GF1 | 2.00 | 0.6 | 710.2 | 359.36 | 30.0 |
| DR-S | 2.00 | 0.6 | 710.2 | 359.36 | 30.0 |
| DR-GF2 | 4.50 | 0.6 | 710.2 | 159.72 | 13.3 |
| KC-3 | 1.13 | 0.6 | 710.2 | 636.04 | 53.1 |
| RLPC-1 | 2.00 | 0.6 | 710.2 | 359.36 | 30.0 |
| WC-1 | 6.26 | 0.6 | 710.2 | 114.81 | 9.6 |
| WT-1 | 3.00 | 0.6 | 710.2 | 239.57 | 20.0 |
| KR-S2 | 3.31 | 0.6 | 710.2 | 217.14 | 18.1 |
| KR-S1 | 3.00 | 0.6 | 710.2 | 239.57 | 20.0 |
| PL-3 | 2.36 | 0.6 | 710.2 | 304.54 | 25.4 |
| KDB-1 | 3.14 | 0.6 | 710.2 | 228.89 | 19.1 |
| KD-1 | 4.36 | 0.6 | 710.2 | 164.84 | 13.8 |
| VW-2 | 9.00 | 0.6 | 710.2 | 79.86 | 6.7 |
| VW-3 | 14.00 | 0.6 | 710.2 | 51.34 | 4.3 |

The regional recharge estimation of the Zwartkrans compartment is estimated by using the harmonic mean (2.51 mg/l) of the 25 chloride concentrations sampled. Regional recharge of the Zwartkrans compartment is estimated at 23.9% which is consistent with the 21% of the chloride balance study conducted by Bredenkamp *et al*., (1986) for the same compartment. It is important to note that the authors used a chloride concentration in rainfall of 0.525 mg/l and an average annual rainfall of 660 mm.

**Table 4.4.** CMB results for the Tweefontein compartment.

| Borehole ID | Cl (groundwater) (mg/l) | Cl (rainfall) (mg/l) | Average Annual Rainfall (mm) | Average Annual Recharge (mm) | Recharge % |
|---|---|---|---|---|---|
| NFS-02 | 1.00 | 0.6 | 664 | 671.97 | 60.0 |
| NFR-02 | 2.00 | 0.6 | 664 | 335.98 | 30.0 |
| RLK-1 | 12.00 | 0.6 | 664 | 56.00 | 5.0 |
| NK-1 | 2.00 | 0.6 | 664 | 335.98 | 30.0 |
| NA-1 | 2.50 | 0.6 | 664 | 268.79 | 24.0 |
| RHL-01 | 1.71 | 0.6 | 664 | 392.96 | 35.1 |
| NM-02 | 1.85 | 0.6 | 664 | 363.23 | 32.4 |
| HV-1 | 5.00 | 0.6 | 664 | 134.39 | 12.0 |
| BR-S | 2.20 | 0.6 | 664 | 305.44 | 27.3 |

The regional recharge of the Tweefontein compartment is estimated at 28.4 % with a groundwater chloride concentration harmonic mean of 2.11 mg/l. Figure 4.11 shows the distribution of saturated chloride in the groundwater throughout the study area. The very low chloride values in the northern Tweefontein compartment and surrounding Sterkfontein caves indicate effective recharge zones.

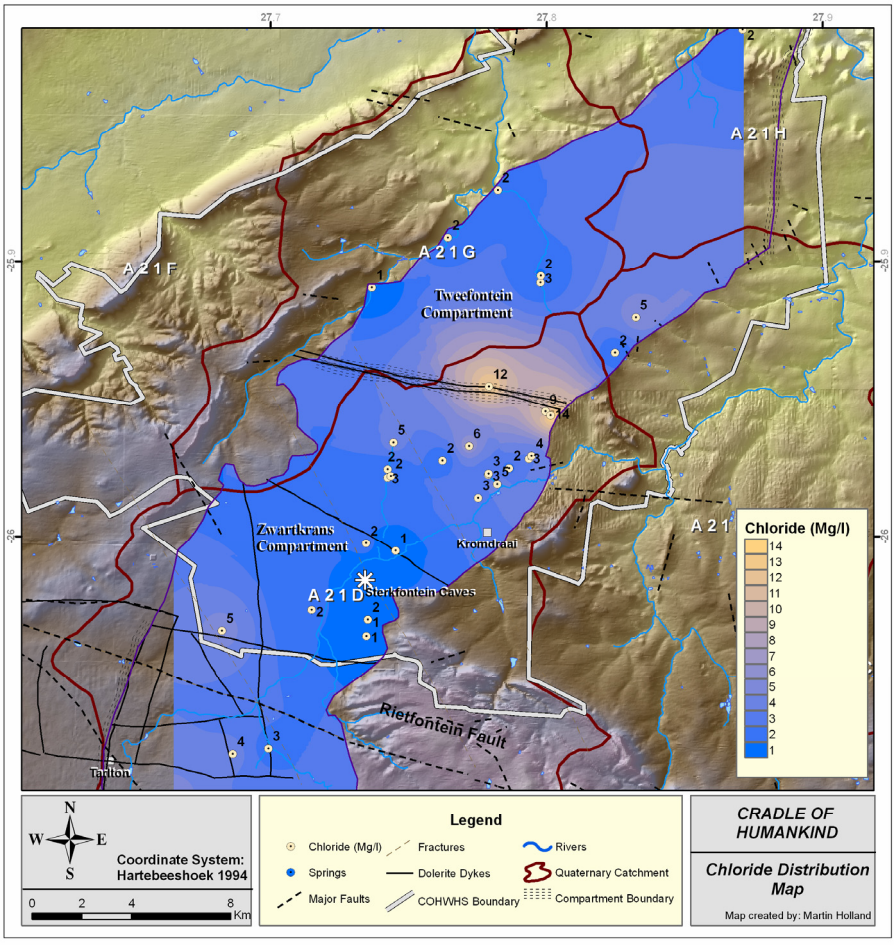


**Figure 4.11.** Chloride sample locations for determining recharge.

*Cumulative Rainfall Departure Method (CRD)*

The CRD method is based on the response of groundwater level changes due to rainfall. The Recharge spreadsheet (by Xu and Van Tonder, 2001) is used to simulate recharge for the compartment. The water balance of an aquifer can be conveniently expressed through the equation (Wright and Xu, 2000):

$$RE = Q_{off}^{gw} - Q_{on}^{gw} + Q^{bf} + ET^{gw} + \Delta S^{gw} \quad (4\text{-}1)$$

This equation simply states that all water arriving at the water table ($RE + Q_{on}^{gw}$) either flows out of the basin as groundwater flow ($Q_{off}^{gw}$), is discharged to surface ($Q^{bf}$), is evapotranspired ($ET^{gw}$) or is retained in storage ($\Delta S^{gw}$). The simulation requires average groundwater levels in the compartment and not individual monitoring boreholes. The large water level variation between sub-compartments within the Zwartkrans compartment made it more practical to apply the water level simulation on a specific sub-unit. Figure 4.12 illustrates the subdivision of the Zwartkrans compartment in to sub-units based on the work of Bredenkamp *et al*. (1986).

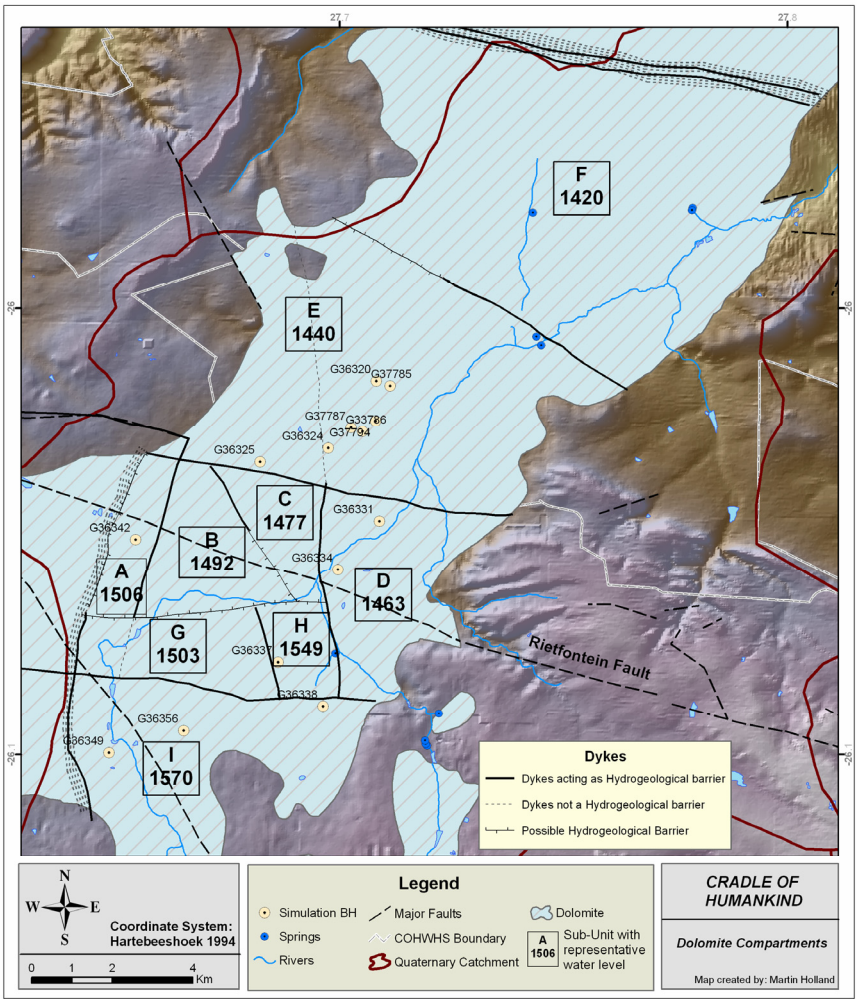


**Figure 4.12.** Hydrogeological isolated compartments created by vertical cross-cutting dykes with representing water levels.

Boreholes illustrated in Figure 4.12 had long term water level data (Apr 1990 to Dec 2004) available from the National Groundwater Database (NGDB). Rainfall data from the Kroningspark rain gauge in Krugersdorp were used in the CRD simulation (Apr 1990 to current). No actual groundwater abstraction data exist for the study area; however data from Schoeman and Associates civil engineers (Krige, 2006) calculated the amount of water required from the aquifer for irrigation from satellite images. The data covered mainly five years and included the entire Zwartkrans compartment. Sub-unit E was chosen for the CRD simulation due to the availability of the mentioned abstraction data and water level data. Table 4.5 indicates abstraction rates determined by Schoeman and associates (Krige, 2006) for sub-unit E.

**Table 4.5.** Abstraction for irrigation in Sub-Unit E.

| Month | 1970 ($m^3$/month) | 1974 ($m^3$/month) | 1986 ($m^3$/month) | 1998 ($m^3$/month) | 2004 ($m^3$/month) |
|---|---|---|---|---|---|
| October | 32560 | 70231 | 43696 | 108593 | 80778 |
| November | 47141 | 20674 | 107277 | 106415 | 139168 |
| December | 94058 | 71513 | 82928 | 113109 | 205007 |
| January | 99383 | 29429 | 116830 | 60229 | 118431 |
| February | 66774 | 35012 | 78476 | 43141 | 52132 |
| March | 56915 | 40181 | 55917 | 63163 | 78932 |
| April | 48228 | 20167 | 51861 | 84263 | 52030 |
| May | 62821 | 69897 | 77191 | 84484 | 94547 |
| June | 52380 | 53786 | 56131 | 65010 | 72752 |
| July | 52849 | 54265 | 59927 | 65591 | 73402 |
| August | 67485 | 69293 | 73811 | 83754 | 93730 |
| September | 50805 | 52163 | 57608 | 60687 | 70560 |
| **TOTAL: ($Mm^3$/a)** | **0.73** | **0.59** | **0.86** | **0.94** | **1.13** |

To derive lumped estimates of recharge from water balance studies, like the CRD method, simplifying assumptions must be made. It was assumed that Sub-unit E act as a hydrogeological isolated compartment. Therefore inflows occur via surface flow with no lateral groundwater inflow. The Zwartkrans and Boland springs discharges the unit with an estimated 22191 $m^3$/day. The estimated groundwater abstracted from sub-unit E accounts to an estimated 3142 $m^3$/day, inflows from losing surface streams (artificial recharge from effluent return flow) is predicted at 9650 $m^3$/day (Krige, 2006). The diminishing flow of the Blaauwbankspruit is clearly visible throughout the study area indicating a significant artificial recharge from sinking surface streams. The CRD simulation showed an effective recharge of 16 % of the rainfall (Figure 4.13). A storativity value of 2.3% (Bredenkamp *et al.*, 1995) was assumed initially however the model required a higher storage coefficient (6.5%) to simulate the water level fluctuations.

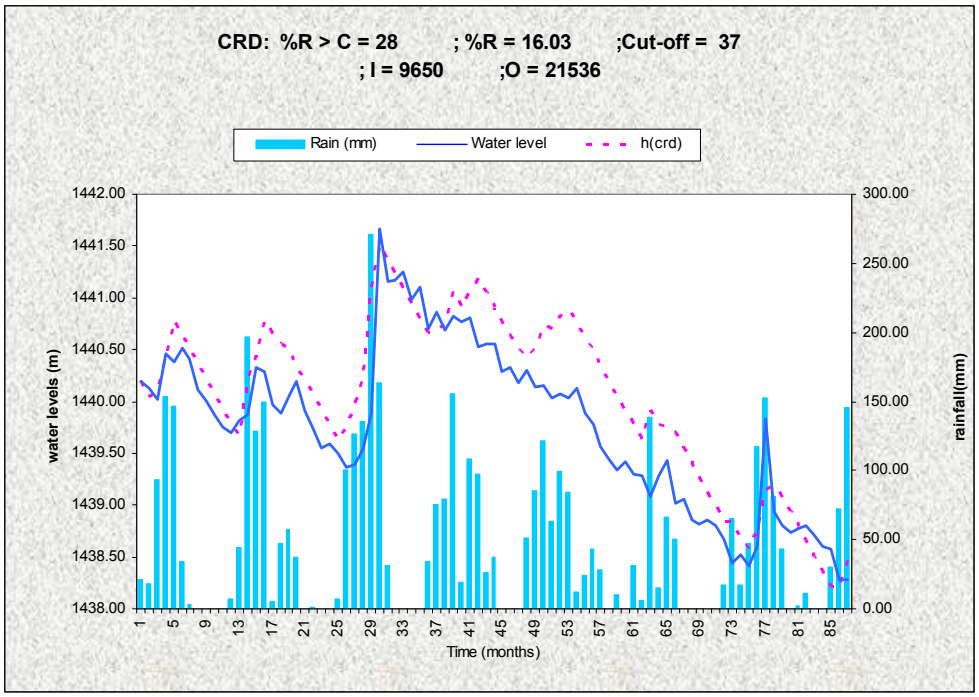


**Figure 4.13.** CRD simulation of sub-unit E of the Zwartkrans compartment.

*Recharge estimates based on best estimates*

Qualified guesses of recharge are obtained by using existing data, expert opinions and interpolation of known values. The results of all available qualified guesses and recharge calculations for the study area are summarised in Table 4.6.

**Table 4.6.** Recharge estimations based on qualified guesses and previous reports.

| Method | Recharge (mm/a) Rainfall=710.2 mm/a) | Recharge % |
|---|---|---|
| **Soil information** | 93.8 | 13.2 |
| **Geology** | 58.9 | 8.3 |
| **Vegter's Recharge Map (1995)** | 95.0 | 13.4 |
| **Harvest Potential Map** | 69.5 | 9.8 |
| **Specialist report: Bredenkamp et al. (1986)** | 99 - 120 (rainfall - 660mm) | 15.0-21 |
| **Average** | 85.64 | 11.94 |

### 4.3.3 Hydrograph Analysis

The spring flow analysis was based on the daily discharge flow recorded at the Nouklip DWAF gauging station. Borehole hydrograph analysis is based on water level data obtained from four water level loggers installed in boreholes during September 2005 to February 2007 (Figure 4.14).

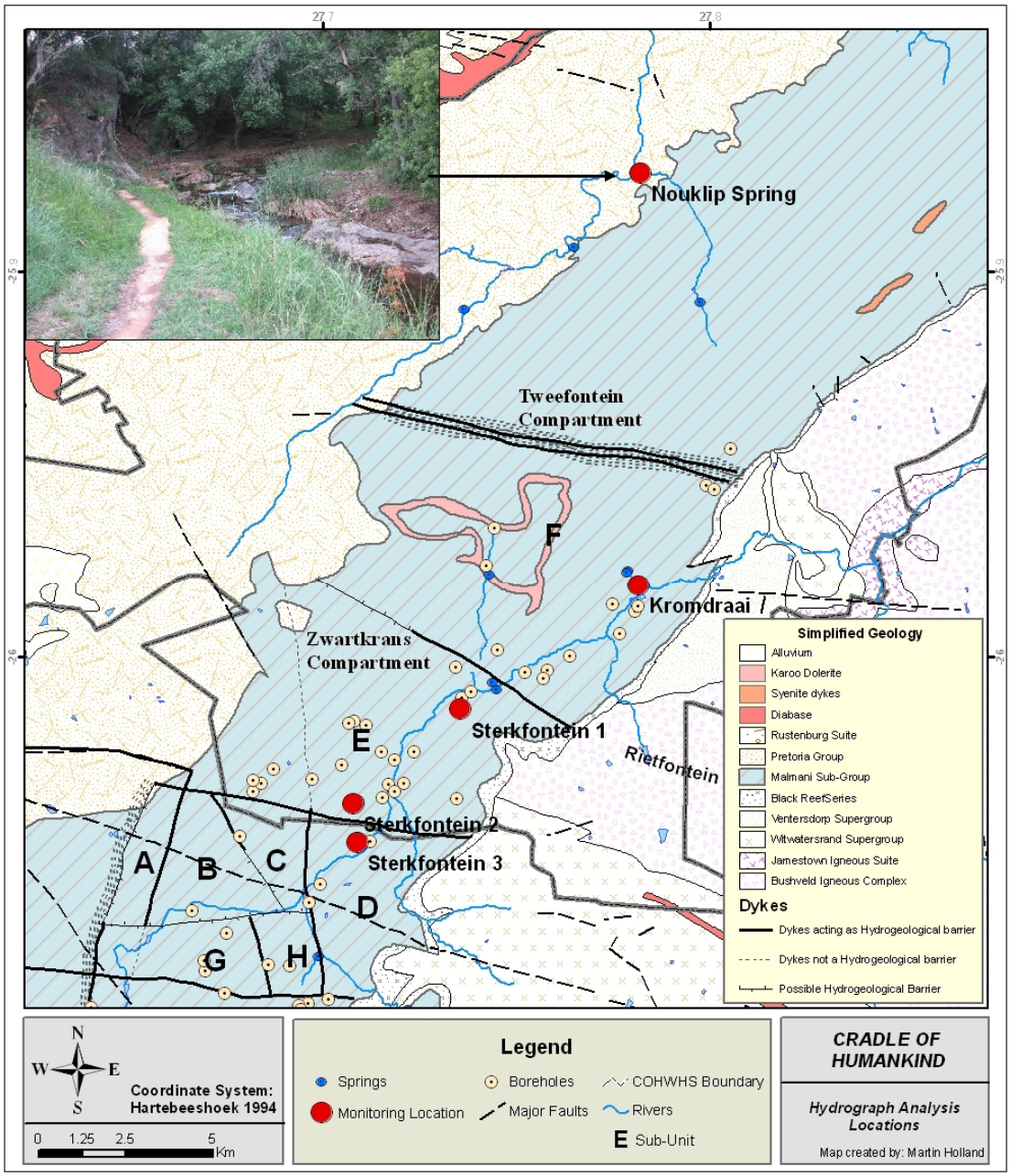


**Figure 4.14.** Monitoring locations for hydrograph analysis.

*Baseflow separation*

The hydrograph of a stream during a period with no excess precipitation will decay, following an exponential curve. Using a streamflow hydrograph where discharge is plotted on a semi-log scale, the recession slope usually is reported as the number of days it takes for the recession line to cross one log cycle of discharge. A visual inspection of the long-term discharge record of the Nouklip gauging station allowed us to identify two seasonal recession curves for the hydrograph analysis (Figure 4.15).

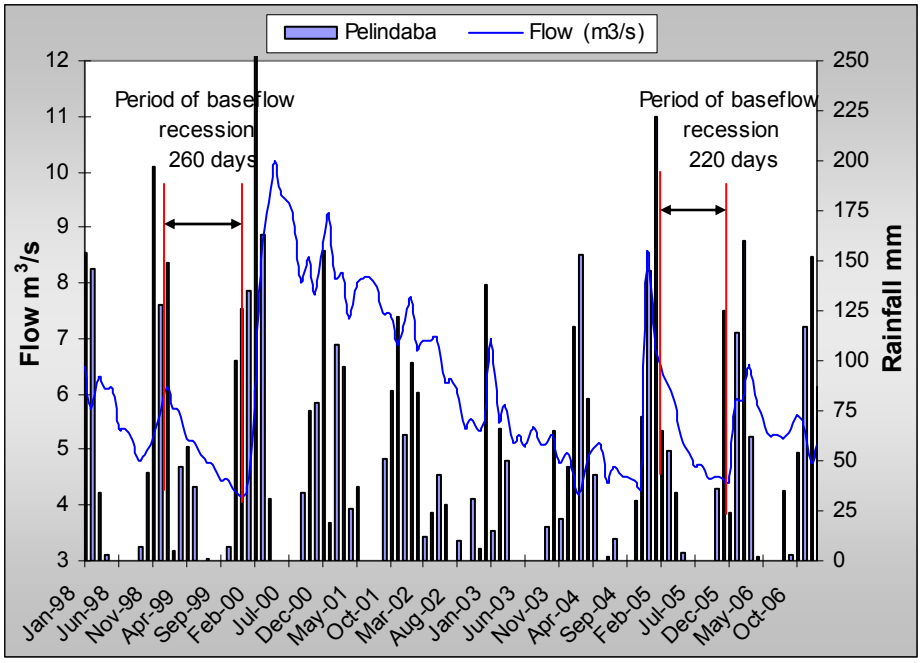


**Figure 4.15.** Long-term hydrograph for Nouklip flow gauge station.

As a first step, the recession segments had to be identified in a semi-logarithmic plot of the discharge $Q$ against time. Thereafter the methods presented in Chapter 3.3.1 were applied to the data of the recession segments. Figure 4.16 shows the semi-logarithmic hydrograph plots that were used to determine the parameters characterising the recession curves. Appendix B contains the remainder of the recession analysis graphs.

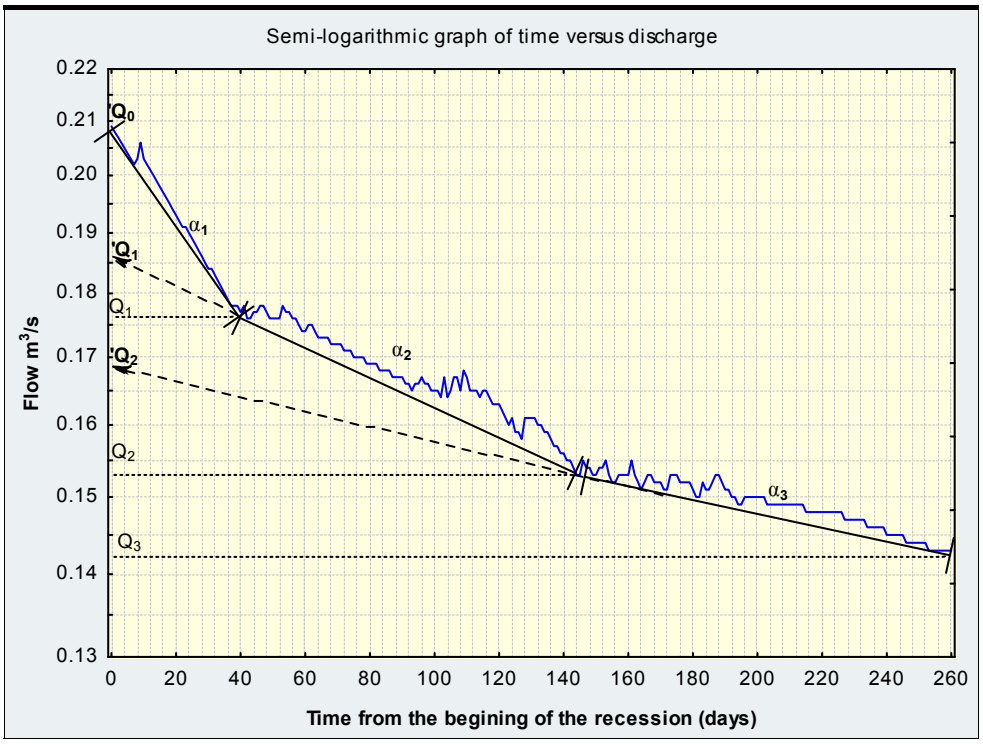


**Figure 4.16.** Response curve of the discharge over time for the 1999 hydrological year for the Nouklip gauging station according to the Maillet equation.

The mild slopes of the 1999 and 2005 hydrograph were analyzed by the Mailet equation. The hyperbolic relation of Boussinesq, seemed not to fit the data correctly and was therefore not used in the analysis (Appendix B). A summary of the two recession analysis results are presented in Table 4.7.

**Table 4.7.** Parameters characterizing the recession analysis based on the Mailet equation.

| **Recession Curve** | $Q_0$ ($m^3/s$) | $Q_1$ ($m^3/s$) | $Q_2$ ($m^3/s$) | $Q_3$ ($m^3/s$) |
|---|---|---|---|---|
| **1999** | 0.209 | 0.178 | 0.153 | 0.143 |
| **2005** | 0.233 | 0.200 | 0.169 | 0.155 |
| **Coefficient** | **$\alpha_1$ ($day^{-1}$)** | **$\alpha_2$ ($day^{-1}$)** | **$\alpha_3$ ($day^{-1}$)** | |
| **1999** | 0.004 | 0.0014 | 0.0005 | |
| **2005** | 0.010 | 0.0017 | 0.0008 | |
| **Discharge** | **'$Q_0$ – '$Q_1$ ($m^3/s$) graph** | **'$Q_1$ – '$Q_2$ ($m^3/s$) graph** | **'$Q_2$ – '$Q_0$ ($m^3/s$) graph** | |
| **1999** | 0.023 | 0.017 | 0.169 | |
| **2005** | 0.030 | 0.019 | 0.184 | |
| **Volume** | **$V_1$ ($m^3$)** | **$V_2$ ($m^3$)** | **$V_3$ ($m^3$)** | |
| **1999** | $4.97 \times 10^5$ | $1.05 \times 10^6$ | $2.92 \times 10^7$ | |
| **2005** | $2.59 \times 10^5$ | $9.59 \times 10^5$ | $1.98 \times 10^7$ | |
| **Discharge of recession** | **$V_0$ ($m^3$)** | **$V^*$ ($m^3$)** | **$V = V_0 - V^*$ ($m^3$)** | |
| **1999 (260 days)** | $2.98 \times 10^7$ | $2.4 \times 10^7$ | $5.09 \times 10^6$ | |
| **2005 (220 days)** | $2.1 \times 10^7$ | $1.6 \times 10^7$ | $5 \times 10^6$ | |

The volume of groundwater stored in the aquifer at the beginning of the recession is represented by $V_0$ and from the results it can be seen that water stored in fine storage ($V_3$) is the main contributor to discharge during the recession. The volume of water remaining in the aquifer above the spring level (free gravitational water) is represented by $V^*$. The difference between volumes $V_0$ and $V^*$ is the volume of all groundwater discharged during the recession period. The total potential groundwater discharge is estimated at $5.09 \times 10^6$ $m^3$ after 260 days of discharge for 1999 and $5.0 \times 10^6$ $m^3$ after 220 days for 2005. Based on the results an extrapolated groundwater contribution to baseflow in 2005 is estimated at $8.3 \times 10^6$ $m^3$.

It is accepted in practice that α of the order of $10^{-2}$ indicates rapid drainage of well interconnected large fissures/fractures (karst channels), while milder slopes of the recession curve (α of the order of $10^{-3}$) represent slow drainage of narrow fissures and aquifer matrix porosity (Krešić, 1997). Accordingly, an initial contribution to discharge with a quick interconnected drainage gives way to a discharge predominantly of small voids, suggesting a piston effect which confirms the duality of the karst system. The fast flow of the hydrograph could represent storage in the epikarst zone, which were drained into the karst conduit network after sufficient saturation from continuous rainfall events. The dolomite aquifer

contributes substantially to groundwater baseflow, and there is a direct hydraulic connection with the river.

*Borehole Hydrographs*

Similar to stream run-off and spring hydrograph analysis the borehole hydrograph analysis investigates the groundwater level with time. As a first step in the analysis, a visual inspection of the borehole hydrographs is conducted to identify the recession periods from the water level records (Figure 4.17 to Figure 4.20). The intense and concentrated summer rainfall, which constitutes up to 80% of the annual precipitation, indicates distinct seasonal fluctuations in all four hydrographs. Sterkfontein 1 and Kromdraai boreholes indicate short-term water table fluctuations that occur in response to intense storm events, in which a sharp pulse is transmitted through the karst system bypassing the epikarst zone. Rapid water level responses are indicative of conduits in the karst system, which pose little hydraulic resistance and drains recharge quickly (Kiraly, 2003). On the basis of the dual porosity concept and its role in karstic aquifers, Sterkfontein 1 has two lag times (delays) in response to rainfall events. The first response is instantaneous after rainfall events suggesting the passing of water in larger fractures (conduit flow) and the second response (lag) relates to the passage of water in finer fractures (matrix or diffuse flow). The continuous water level fluctuations observed on the Kromdraai hydrograph could be attributed to the shallow depth to water and pumping of nearby boreholes. Sterkfontein 2 and Sterkfontein 3 reflect the role of matrix porosity in diffuse flow in a karst system with a 3 month delay in the water level response as rainfall filters through the epikarst zone.

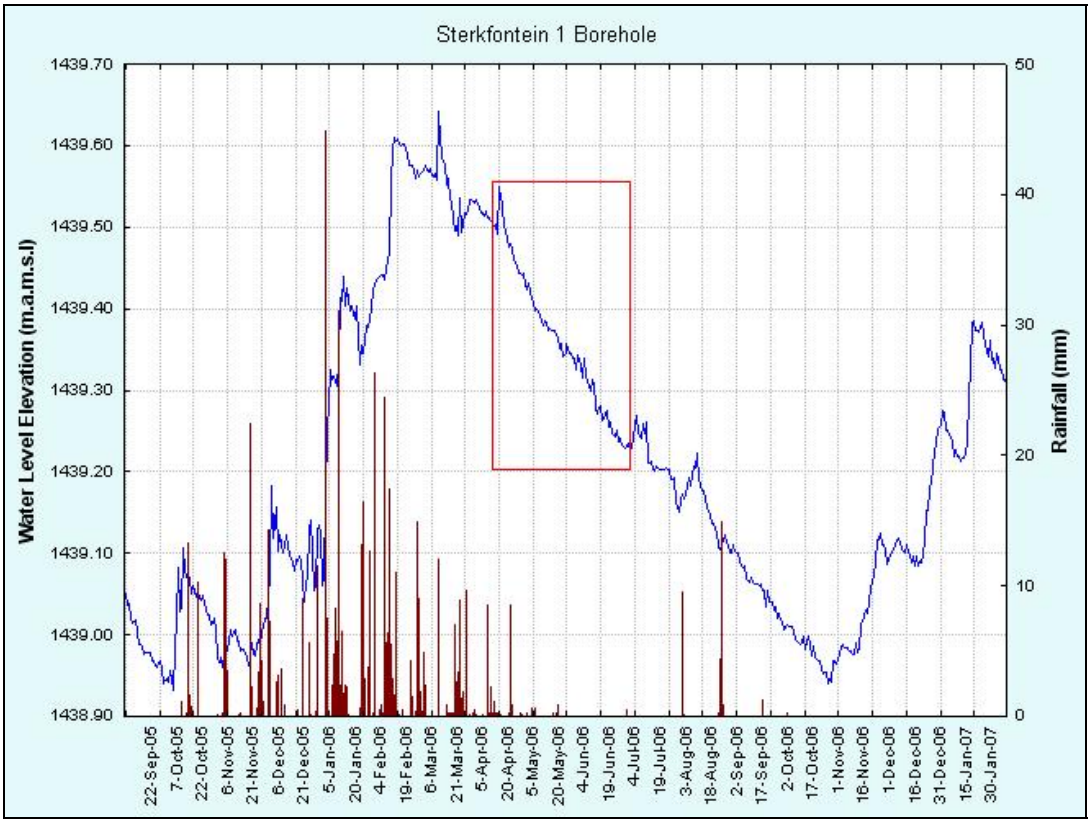


**Figure 4.17.** Sterkfontein 1 hydrograph with recession segment captured.

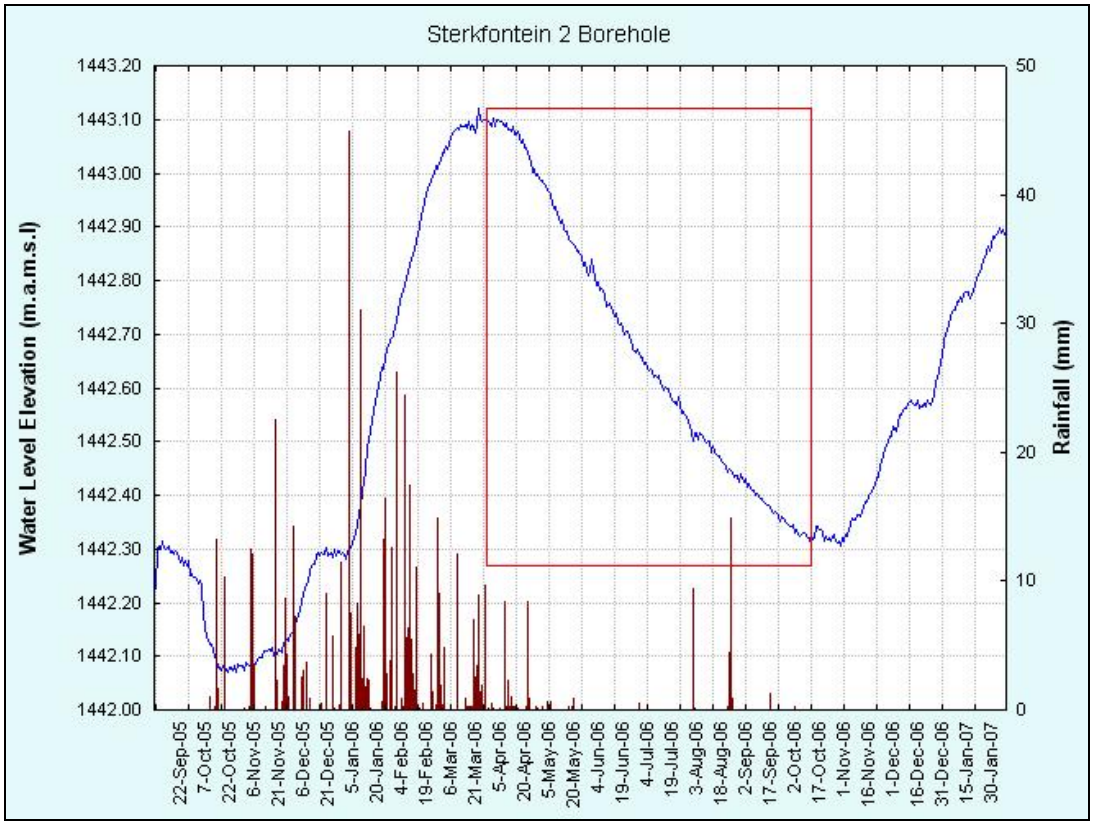


**Figure 4.18.** Sterkfontein 2 hydrograph with recession segment captured.

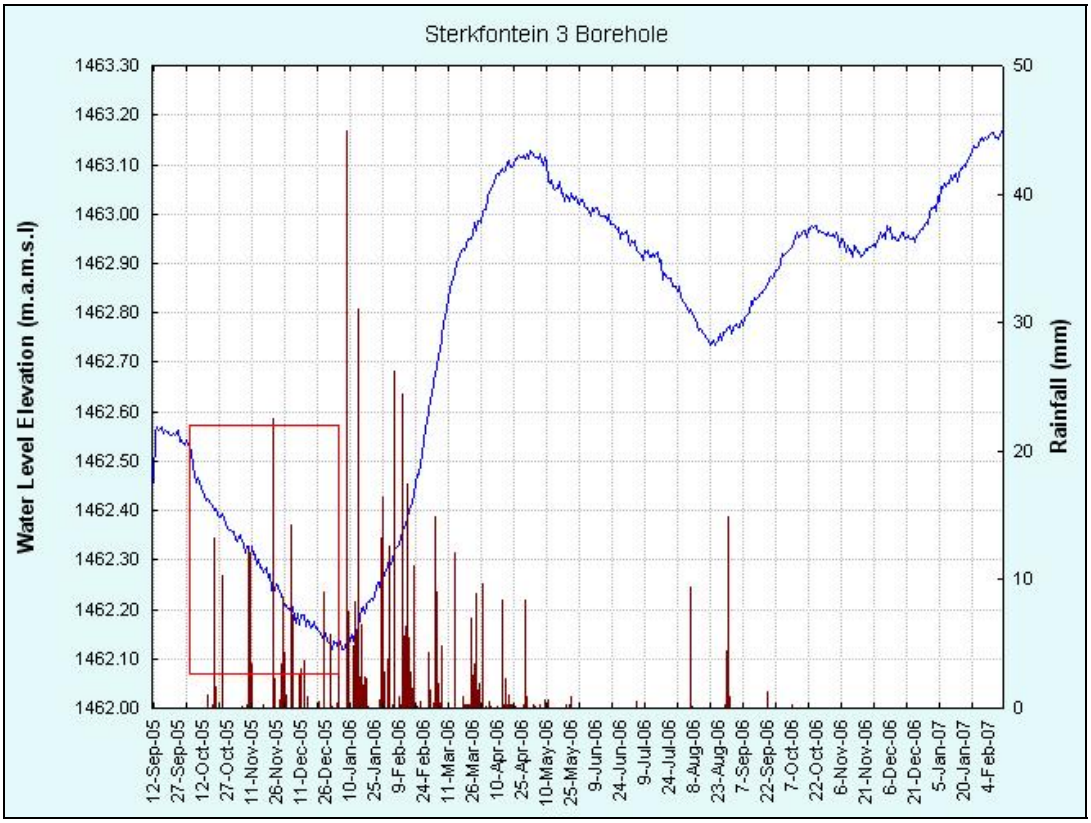


**Figure 4.19.** Sterkfontein 3 hydrograph with recession segment captured.

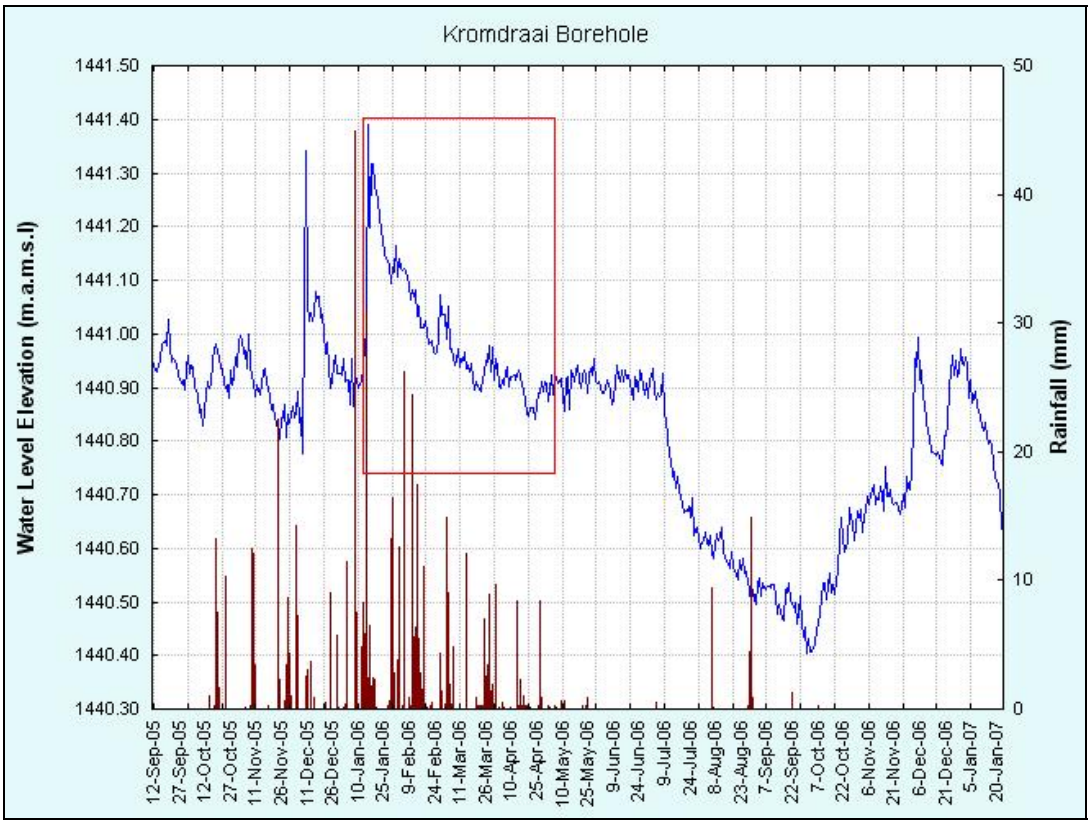


**Figure 4.20.** Kromdraai hydrograph with recession segment captured.

The recession curves from the hydrographs were chosen based on the quick response of water levels after intense storm events. Where no abrupt changes in water levels over short time intervals occurred the seasonal recession limb was used in the exponential function. The recession segments selected from the set of recession periods is more clearly illustrated on plots of semi-logarithmic graphs of water level versus time in Appendix B and the results of the hydraulic parameters calculated from the hydrographs are summarised in Table 4.8. The methods are based on discussions in Chapter 3.3.2. The equation necessitates the approximation of the drainage area of the monitoring borehole (Shevenell, 1996). In the calculations the drainage area were taken as the dolomitic compartment and its influencing boundaries. An assumed storativity, *S*, coefficient is used to get an initial value for transmissivity, *T*, which is compared to, *T*, values from other test such as pump or slug tests. In this case the assumed *S,* is based on the fitting of the CRD simulation.

**Table 4.8.** Hydrogeologic parameters calculated from monitoring borehole hydrograph data.

| Borehole | Distance Divide | $T_1/S_{y1}$ ($m^2/h^{-1}$) | $T_2/S_{y2}$ ($m^2/h^{-1}$) | $T_3/S_{y3}$ ($m^2/h^{-1}$) | $T_1$ ($m^2/day^{-1}$) Segment | | | $S_{y3}$ |
|---|---|---|---|---|---|---|---|---|
| | | | | | $T_1$ | $T_2$ | $T_3$ | |
| **Sterkfontein 1** | 7000m | 7456 | 1869 | 776 | 447 | 112 | 46 | 0.06 |
| **Sterkfontein 2 (SBH-2)** | 7000m | 4458 | 1469 | 2040 | 267 | 88 | 122 | 0.06 |
| **Sterkfontein 3** | 5000m | 32861 | 13429 | 10834 | 1971 | 805 | 650 | 0.06 |
| **Kromdraai (KBH-1)** | 3000m | 19190 | 3892 | 2345 | 161 | 33 | 19 | 0.06 |

It is evident that the conduit portion of the recession curve hosts greater *T/S* values than the flattening section of the curve which represents fracture and matrix drainage due to the initial high *T* (flow) and low *S* (storage). Comparing the results obtained with the results from Shevenell (1996) for estimating transmissivity in karst aquifers from well hydrographs a few difference must be highlighted. Shevenell (1996) used a study site with relatively small drainage basins with groundwater flow that mimics the topography. The study site had a shallow karst aquifer with long distance flow unlikely to occur. In contrast, the karst aquifer under investigation consists of a large drainage basin (147 $km^2$) with groundwater flow highly influenced by dykes and springs as outflow points. In some areas sharp increases in water level depth can be expected. Other limitations noted by Shevenell (1996) include, 1) long storms forming broad peaks tend to mask some of the quick flow characteristics, 2) recession curves should be complete 3) the logarithm of water level is used (WL above transducer) 4) it is assumed that the drainage areas corresponding to volume changes represented by the three line segments are the same (drainage through a sinkhole will therefore be much smaller than the interpreted area). Nevertheless the method applied is valuable in estimating aquifer

diffusivity and providing qualitative values for transmissivity (*T*) for different portion of the flow regime when corresponding stream or spring discharge rates are not available.

### 4.3.4 Aquifer Parameters

A slug with known volume was used to determine the hydraulic conductivity determined from the rate of rise of the water level in a borehole. A Solinst water level logger was used to record the head of water, at preset increments of time until the water level in the borehole has recovered to or near static water level. The large diameter boreholes required a large slug to displace a significant amount of water. The size of the slug made the operation difficult and the results of these large diameter slug tests could not be used in the conductivity analysis due to inaccurate results. From the initial seven slug tests conducted on boreholes throughout the study area; four tests could be used to determine the hydraulic conductivity. Table 4.9 summarizes the borehole construction details used in the analysis and the aquifer parameters determined by the various methods of slug test interpretation. The slug test response graphs are included in Appendix C.

**Table 4.9.** Summary of Aquifer parameters, K and T from slug test interpretations.

| Borehole ID | BH Depth (m.b.g.l) | Casing Diameter (mm) | Water Level (m.b.g.l) | Hydraulic conductivity K (m/day) | Transmissivity T ($m^2$/day) | Method |
|---|---|---|---|---|---|---|
| KBH-1 | 78 | 165 | 8.30 | 0.89 | 160 | Bouwer & Rice (1976) |
| | | | | 1.08 | 200 | Butler et al. (2003) |
| BBH-1 | 120 | 165 | 22.15 | 19 | 1900 | Van der Kamp (1976) |
| | | | | 26.54 | 7400 | Butler et al. (2003) |
| SBH-2 | 73 | 165 | 54.5 | 4.3 | 780 | Bouwer & Rice (1976) |
| | | | | 6.72 (Inserted) | 1200 | Butler et al. (2003) |
| | | | | 4.19 (Ejected) | 760 | |
| VWBH-3 | 35.5 | 165 | 13.32 | 0.26 | 46 | Bouwer & Rice (1976) |
| | | | | 0.21 | 37 | Butler et al. (2003) |

Bredenkamp et al. (1986) measured transmissivity values ranging from 1 to 25 100 $m^2$/day based on more than 30 pump test analysis in the Zwartkrans compartment. The values are indicative of the highly anisotropic and heterogeneous character of the karst aquifer. Values obtained from slug test vary between 37 and 7400 $m^2$/day. The results indicated that the Bouwer and Rice (1976) approach may lead to under prediction of the hydraulic

conductivity in permeable aquifers as proposed by Butler et al., (2003). The location of the slug test boreholes are plotted on the geological map for easier interpretation (Figure 4.21).

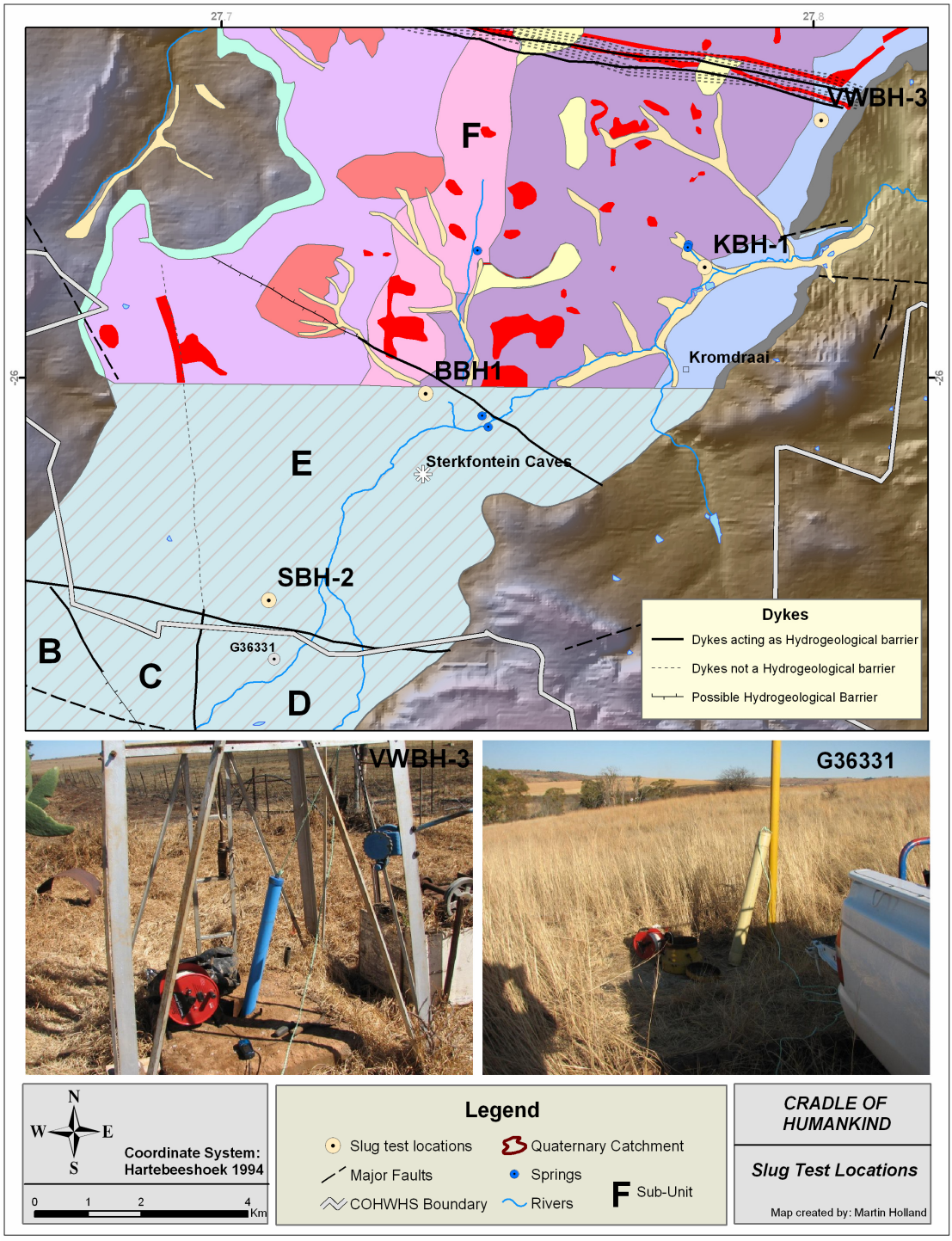


**Figure 4.21.** Location of boreholes which was subjected to slug testing (photos indicating slugs).

The evaluation of the slug tests in relationship with its spatial distribution reveal that the chert content in the aquifer has an influence on the transmissivity (*T*) values. VWBH-3 is situated in the chert poor Oaktree formation with transmissivity value of 46 $m^2$/day. KBH-1

drilled into the overlying alluvium and the chert rich Monte Christo formation reveal higher transmissivity values of 200 $m^2$/day. Boreholes BBH-1 and SBH-2 represents *T* values in the thousands suggesting an excellent aquifer with high permeability. The chert poor formations weather evenly to produce a low storage potential residue of silty clay. The chert rich formations weather quite differently. The dolomite weathers faster than the chert leaving the rock supported by chert structures. Eventually the chert will weather and collapse under its own weight leaving a permeable coarse chert breccia. Chert rich formations develop a greater concentration of fissures and fractures which will enhance the process of weathering. KBH-1 corresponds well to the *T* estimates obtained from the hydrograph analysis. SBH-2 indicates a higher *T* value compared to the hydrograph analysis. The slug test results are probably not as reliable given that the water level response was caused by a sharp, instantaneous injection rather than a regional pressure pulse of the aquifer.

## 4.4 Chemical Hydrogeology

### 4.4.1 Geochemical Description

Karst aquifers are characterized by an extreme spatial heterogeneity that strongly influences their hydraulic behaviour and the transport of pollutants (Jaquet et al., 2004). The investigated karst aquifer demonstrates the existence of heterogeneity in groundwater mineral contents related to anthropogenic activities. Degradation of groundwater quality is observed in most parts of the karst catchment, where anomalous high concentrations of sulphate, chloride and nitrate were measured. An integrated approach relying on conventional graphical displays such as schoeller and piper diagrams in collaboration with multivariate statistical analysis was used to delineate potential anthropogenic sources and determine the influence they have on the groundwater chemistry (Holland and Witthüser, 2007).

The study was carried out by combining three ground and surface water chemical datasets for the COHWHS. These included data from the Council for Geoscience, University of Pretoria and the National Groundwater Database. The water quality sampling was performed according to SABS ISO 5667 Standards. Field measurements included pH, electrical conductivity (EC), temperature, and dissolved oxygen content. While the CGS and the University of Pretoria's samples were generally analyzed for major ions (Ca, Mg, Na, K, $SO_4$, Cl, $HCO_3$, $NO_3$, $PO_4$, and F) and trace elements, only selected samples from the NGDB were analyzed for trace elements. For specific ions like sulphate a high percentage of the data are below the analytical detection limit (censored data), these values were replaced with half

the specific detection limit as a best guess for the real concentration (Pannatier et al. 2000). If a sample wasn't analyzed for an element, typically one or all of the trace elements, no substitution was done. Data with unacceptable errors in the ion balance were excluded from the database and further analysis:

$$\text{E.N.}[\%] = 100\% \cdot \left|(Cations - Anions)/(cations + Anions)\right| < 5\% \quad (4\text{-}2)$$

Errors of 5 % were considered as acceptable, however highly mineralised water (AMD) with errors of 10% was also considered. The location of the sampling points in relation to the geology is indicated in Figure 4.22.

*Hierarchical Cluster Analysis*

Very few boreholes have been sampled on a continuous basis and the data are highly variable in content. The database contains single, multiple and temporal chemical analyses which make the use of only conventional display diagrams impossible. Multivariate statistical techniques can be applied on large datasets and use any combination of chemical and physical parameters (e.g., temperature) to classify water samples (Heikinien *et al*., 2002; Hussein 2004; Lambrakis *et al*., 2004; Singh et al. 2003; Thyne *et al*., 2003). Since most of the applied statistical analysis assumes normally distributed data (Güler *et al*., 2002), a studentized range test (n > 1000 valid samples) for normality with a level of significance of 0.01 was performed. The distribution characteristics of each variable in the database were evaluated by histograms and their measures of location and dispersion. The studentized range test compares the ratio of the sample range and standard deviation to tabulated critical values (Pearson and Hartley, 1970).

The following variables were log-transformed so they more closely correspond to a normal distribution: Na, K, HCO3, and pH. Variables $NO_3$, Cl,, Ca, $HCO_3$, $SO_4$ and Electrical Conductivity (EC) follow a normal distribution, so were not log-transformed. These were the only variables with continuous data that could be used in the cluster analysis. Ward's linkage rule was used to analyze the distances among linkages for the entire group of observations and the squared Euclidean distances were used to determine the distance between observations. The data were standardized by calculating their standard scores (*z*-scores). The hierarchical cluster method provide a graphical result, which is useful for determining the number of clusters that adequately describe underlying processes that lead to the identification of homogeneous groups (dendrogram). The graphical display of the dendrogram is included in Appendix C. Based on the visual assessment of the resulting dendrogram, three distinct hydrochemical groups were identified. Clusters 1 and 3 could be further sub-divided into two-subgroups for easier interpretation. A summary of the chemical data is presented in (Table 4.10).

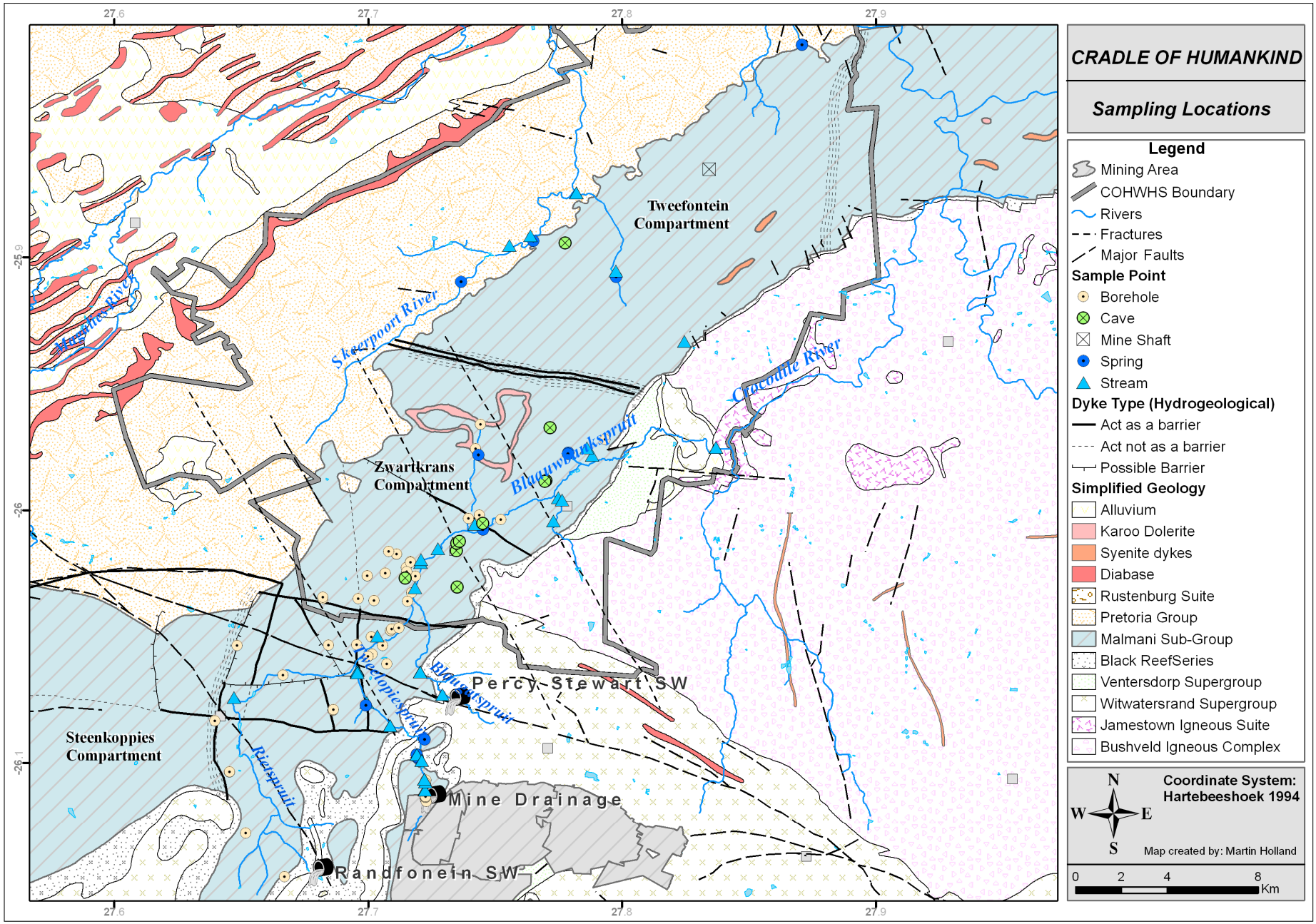


**Figure 4.22.** Sampling location in relation to geology.

In general terms, Group I with the highest number of samples is characterized by elevated sodium, chloride, bicarbonate, nitrate and sulphate concentrations, indicating the influence of a combination of anthropogenic sources. The subgroups of Group I are separated based on nitrate, sulphate and bicarbonate concentrations. SG-1a has characteristic high nitrate concentrations suggesting run-off of fertilizers and livestock excrement in the agricultural areas however; domestic effluents from leaking sewage systems and septic tanks cannot be excluded. SG-1b is highly mineralised with elevated concentration of all major ions especially sulphate, this signature which could be attributed to the mine drainage.

**Table 4.10.** Mean values for the groups distinguished by the hierarchical cluster analysis.

| PARAMETER (mg/l) | TOTAL POPULATION | GROUP I | | | GROUP II | GROUP III | | |
|---|---|---|---|---|---|---|---|---|
| | | Total Group I | SG-1a | SG-1b | Total Group II | Total Group III | SG-3a | SG-3b |
| Valid N | 148 | *88* | 32 | 56 | *40* | *20* | 10 | 10 |
| pH | 6.88 | *7.35* | 7.5 | 7.2 | *7.28* | *4.0* | **3.3*** | 4.8 |
| El.Cond (mS/m) | 111.15 | *85.01* | 87.88 | 83.38 | *34.09* | *380.3** | **491.8*** | 268.7 |
| Na | 53.19 | *49.34* | 53.55 | 46.93 | *3.95* | *168.59* | 262.5 | 74.68 |
| Mg | 43.85 | *30.19* | 37.55 | 25.99 | *20.04* | *151.59* | 194.3* | 108.8* |
| K | 4.68 | *4.37* | 2.80 | 5.27 | *0.97* | *13.42* | 21.9 | 4.86 |
| Ca | 110.11 | *69.28* | 67.68 | 70.19 | *30.45* | *449.1* | 489.7* | 408.4* |
| HCO3 | 139.06 | *151.16* | 209.32 | 117.92 | *174.63* | *14.67* | 0.49 | 28.84 |
| NO3 | 19.01 | *27.96* | **54.2** | 12.92 | *6.04* | *5.55* | 9.02 | 2.09 |
| SO4 | 511.92 | *206.1* | 141.13 | **243.08** | *11.77* | *2858** | **4042*** | **1673*** |
| Cl | 34.25 | *48.73* | **63.25** | 40.43 | *4.25* | *30.51* | 33.63 | 27.39 |

* - exceed the acceptable limits for drinking water in South Africa (SANS, 2005).

It is suggested that Group II represents the geogenic dolomitic signature with concentrations of identified compounds in this group well within the ideal limits for drinking water in South Africa (SANS, 2005). Group I and II is also characterised by the high concentrations of bicarbonate and buffered pH values due to the dissolution of the carbonate minerals (dolomite).

Group III contains mostly water samples with a distinct high sulphate concentration which could be related to the highly mineralised mine drainage water. Average sulphate

concentration in the flooded mines is about 2858 mg/l with a pH value of 4.0. This is related to the oxidation of sulphide minerals such as pyrite in the gold-bearing strata. The low pH value promotes the dissolution of dolomite, resulting in elevated calcium and magnesium. Sulphate, calcium and magnesium concentrations as well as EC exceed the acceptable limits for drinking water in South Africa, which are 400 mg/l, 150 mg/l, 70 mg/l and 150 mS/m respectively (SANS, 2005).

*Spatial Distribution*

The relationship of the statistically defined clusters of samples to geographic location illustrates the most important message that geochemical survey datasets contain i.e. the variation in regional distribution (Reimann et al. 2005). Mapping the cluster groups based on their chemical similarity allowed us to identify the spatial relationship of hydrochemical processes and/or flow paths. Swallow holes and diffuse leakage from rivers acts as one of the main contributors to recharge of the karst system and has altered the groundwater chemistry over a large area. Based on the spatial distribution map, Figure 4.23, it is evident that Group III indicates the source of the acid mine drainage, Group I and its subgroups represent the contamination signature and are located either in the immediate vicinity of the anthropogenic sources or along the flow path of polluted waters and Group II represent the natural water of the dolomite and are either located beyond the current area of influence or related to the mixing (dilution) of surface water and groundwater of uncontaminated flow paths.

The bounding effect that the dykes impose on the flow is clearly evident. To the left of the main north-west transecting dyke a number of samples represent the background level whereas the samples towards the right of the dyke indicate the mixing of polluted water. The SE-NW striking dyke towards the east acts also as a hydrogeological barrier with mixing only occurring via surface flow paths. Water samples taken from caves along the contamination flow paths indicate a background level confirming with Jamison *et al*. (2004) that caves are expected to occur as stacked perched water tables.

*Hydrochemical Facies*

Plotting the chemical dataset on a piper diagram and labelling the water sampling types (borehole, caves etc.), produces a better visual presentation of the comparison between sampled location and the water types (Figure 4.24). Evidence of mixing of different water types can be used to confirm the boundaries of the contaminant plume (Heikkinen *et al*., 2002).

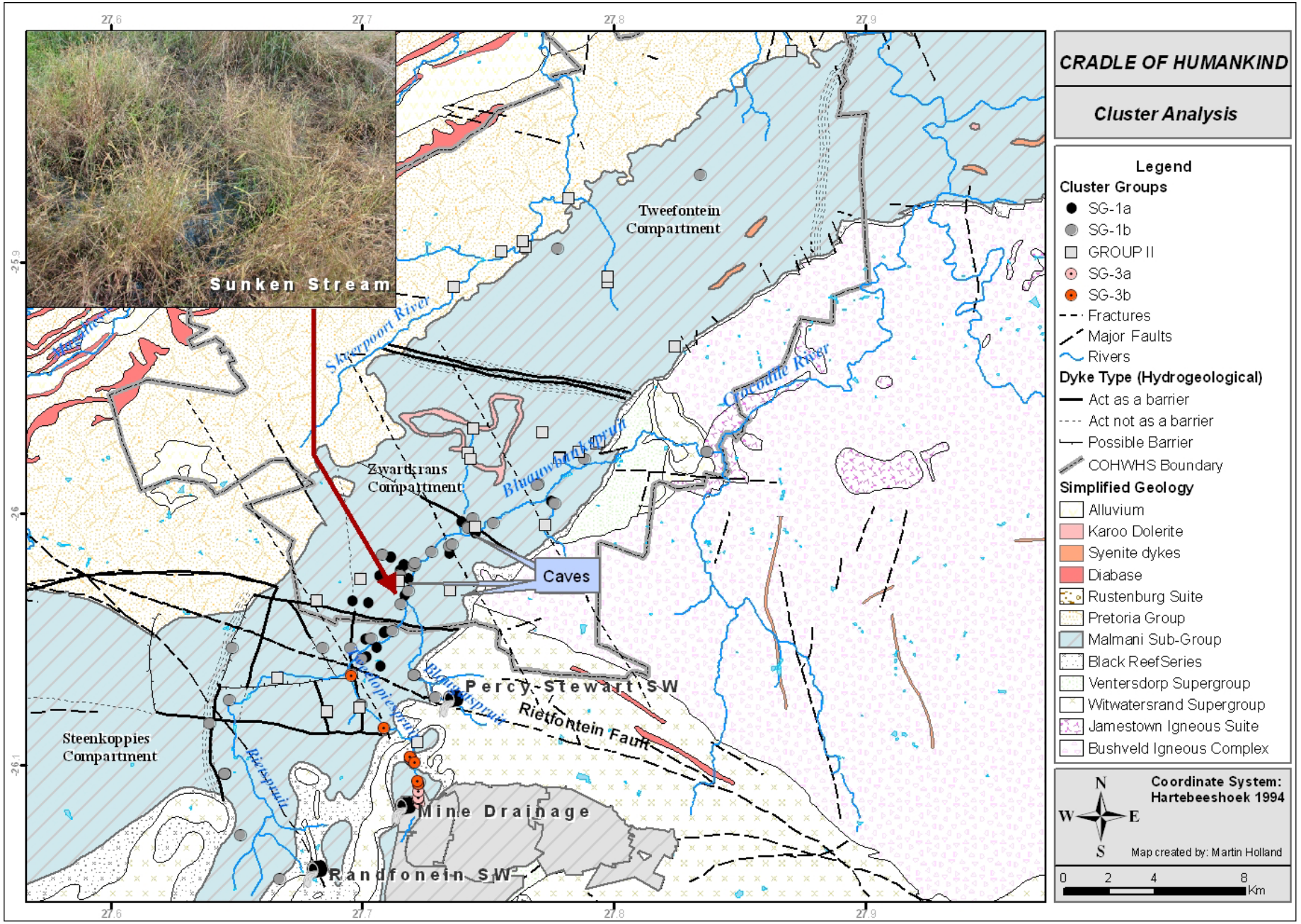
Sunken Stream
Tweefontein Compartment
Zwartkrans Compartment
Steenkoppies Compartment
Caves
Percy-Stewart SW
Rietfontein Fault
Mine Drainage
Randfontein SW
Skeerpoort River
Tweelopiespruit
Blougatspruit
Riverspruit
Tweelopiespruit
Tweelopiespruit
Tweelopiesp

From Figure 4.24 the water chemistry appears to evolve along two lines, one from a Ca-Mg-$HCO_3$ water type toward a $SO_4$ type and the other from Ca-Mg-$HCO_3$ toward Na-rich type. The direction of these trends are consistent with increasing specific conductance and total dissolved solid content of the samples and reflect increased water interaction. The Ca-Mg-SO4 facies in the upper corner of the diamond indicates the impact of acid mine drainage on the water chemistry and is defined by cluster Group III.

Water samples in the anion field vary between $HCO_3$ and $SO_4$ with a few samples shifting towards Cl (typically related to the effluent return flows). In the cation field a number of surface water samples shifts towards Na and K ions. The majority of water samples have an equivalent mole ratio of Na/Cl larger unity, clearly deviating from ratios determined by Galloway *et al*. (1983) for Atlantic rainwater (0.81–0.90) or seawater (0.86). The increase in sodium associated with several of the samples appears to reflect chemical evolution related to anthropogenic impacts from irrigation return flow, mine drainage and municipal waste water discharge. This plot illustrates that the direct drainage of large volumes of municipal wastewaters and decanting mine water into the catchment's tributaries has changed the natural chemistry of the karst aquifer.

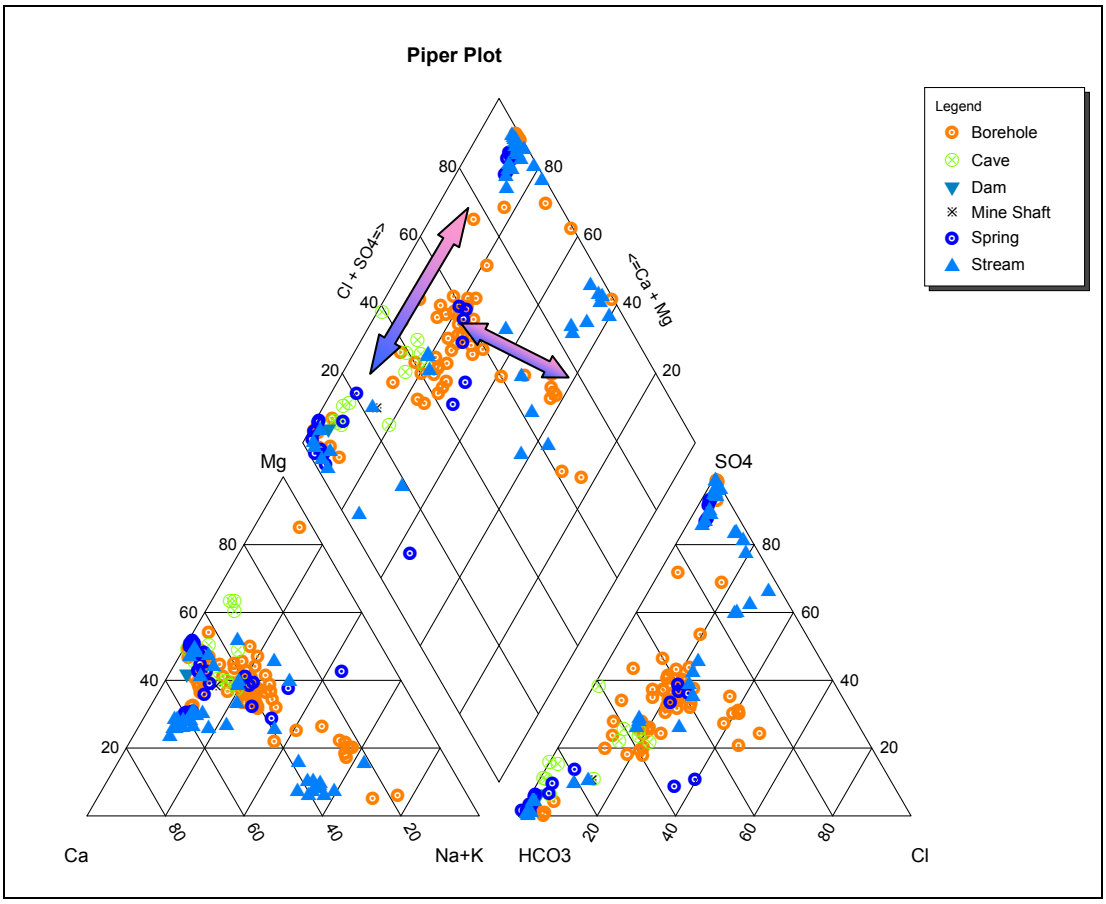


**Figure 4.24.** Piper diagram presenting the composition of 148 groundwater and surface water samples collected from 1996 to 2007.

*Nature of contamination*

As can be seen from the previous section surface streams are the main receptor of contaminants due to their easy accessibility for disposal of wastewater and run-off. The confluence of tributaries into the main drainage stream causes assimilation of contaminants in the groundwater which make it difficult to trace the anthropogenic source. Nitrate, phosphate and ammonia are normally a good indicator of sewage return effluent; however, not all samples were measured for these parameters. Similarly the chemical signatures for mining impact, such as metals, were only measured in a few samples. The hydrochemical sections on near complete sample datasets shown in Figure 4.25 to Figure 4.27 illustrate the main features of the hydrochemical environment of the karst aquifer, which allows for differentiating between possible anthropogenic sources.

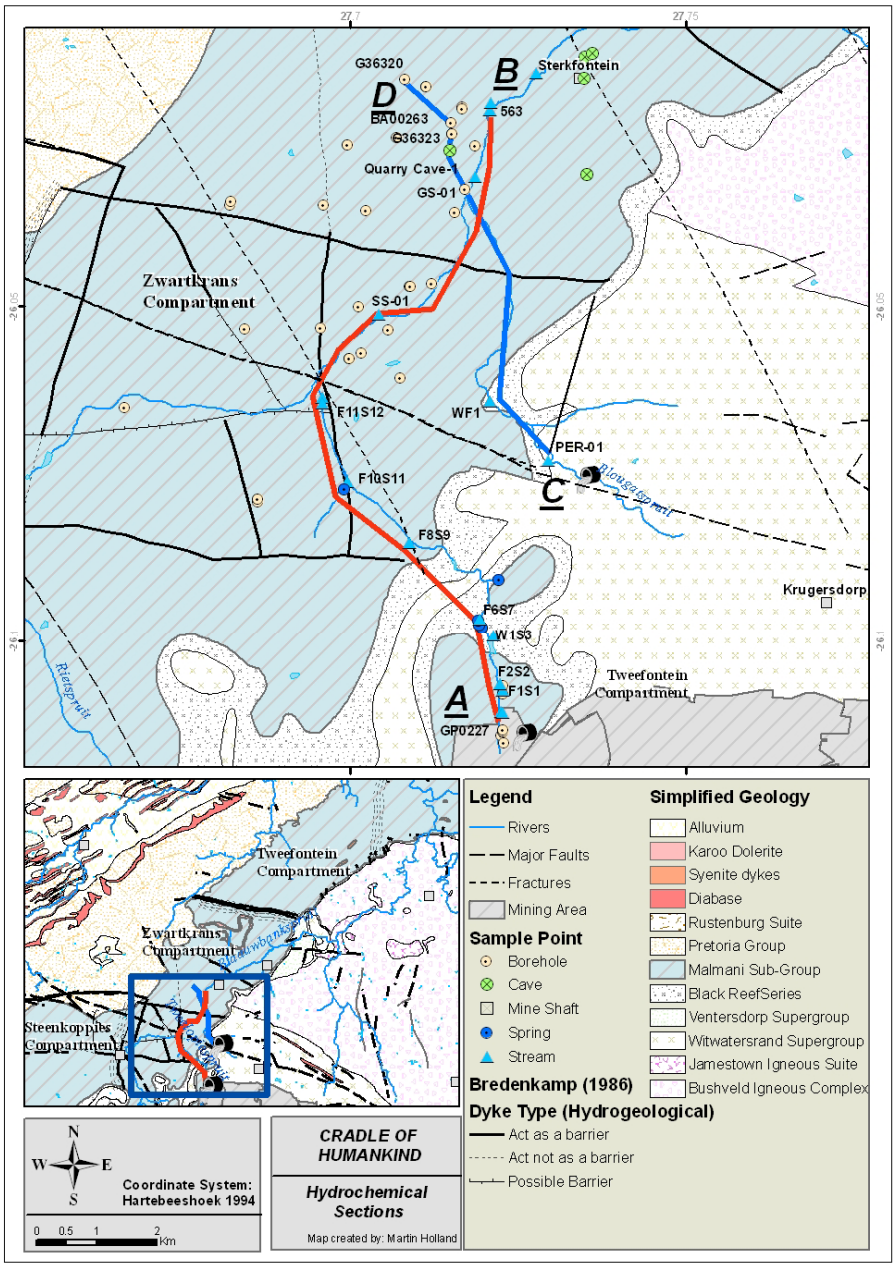


**Figure 4.25.** Hydrochemical section sampling points.

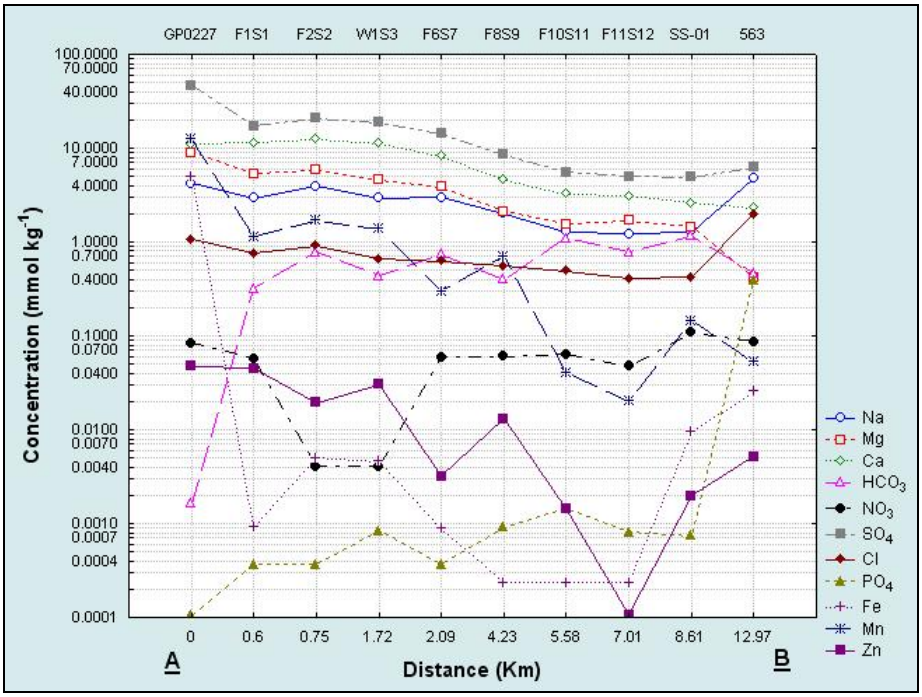


**Figure 4.26.** Schoeller plot of hydrochemical section A to B.

Section A to B represents mostly surface water samples from the Tweelopiespruit, draining the decanting acidic mine water (Figure 4.26). Springs located downstream on the contact zone between the dolomite and the Westrand Group quartzite's, dilutes the highly polluted surface water somewhat before it disappears into sinking streams as can be seen from Photo 5. The graph also indicates that the zink is transported down gradient and could act as a natural tracer for the mine drainage water. However, during dissolution of dolomite residual products such as iron and manganese are left behind. Iron precipitates immediately downstream and is clearly visible with a distinct yellow-orange colour also termed "yellow boy" (Photo 5).

**Photo 5.** Sunken stream near sample SS-01(left) and iron precipitation near sample GP-0227 (right).

It is important to note that potassium concentration increases significantly at sample '563' which is after the confluence of the Blougatspruit which drains the Percy Stewart sewage works effluent return flow. The extent to which phosphates is retained within the aquifer would be expected to vary according to the relative importance of diffuse and conduit flow.

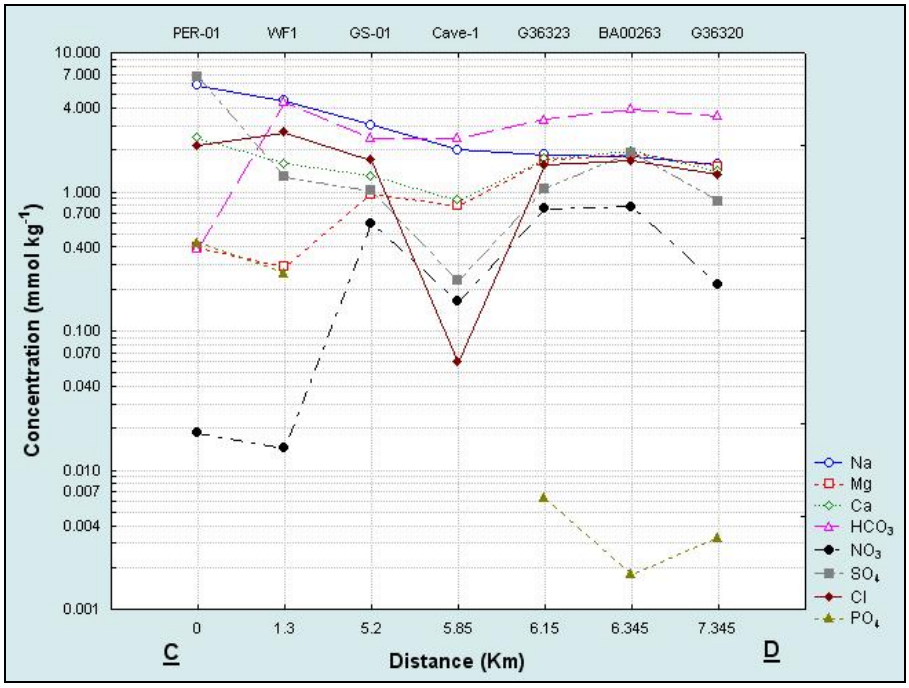


**Figure 4.27.** Schoeller plot of hydrochemical section C to D.

Section C to D describes the hydrochemical evolution from the Percy Stewart effluent return flow outlet to the groundwater samples collected from boreholes in the karst aquifer. As expected the dissolution of dolomite down gradient produces calcium, magnesium and bicarbonate. The elevated nitrate concentrations from sample GS-01 confirms that nitrate has a different anthropogenic source and could be related to the use of agricultural activities. Unfortunately phosphate weren't analysed throughout the section but the results would suggest that phosphate could be a good indicator for waters mixing with sewage works effluent, with biochemical data lacking. The sample taken from the cave indicates a different chemical signature which could be that the cave and regional groundwater is not hydraulic connected. It is suggested that an impermeable geological formation dips underneath the caves and it is possible that this groundwater barrier (aquitard) causes rainwater to accumulate in the caves forming a pocket of water. The extent of this perched aquifer appears to be localised.

### 4.4.2 Isotope Hydrogeology

Isotope samples were obtained from 14 boreholes, 6 springs and a rainfall event during 2006 (Figure 4.28). Twenty-one water samples were submitted to Ithemba Laboratories for low-level tritium ($^{3}H$) and stable isotope deuterium ($^{2}H$) and oxygen ($^{18}O$) analysis. The analytical data are presented in Table 4.11.

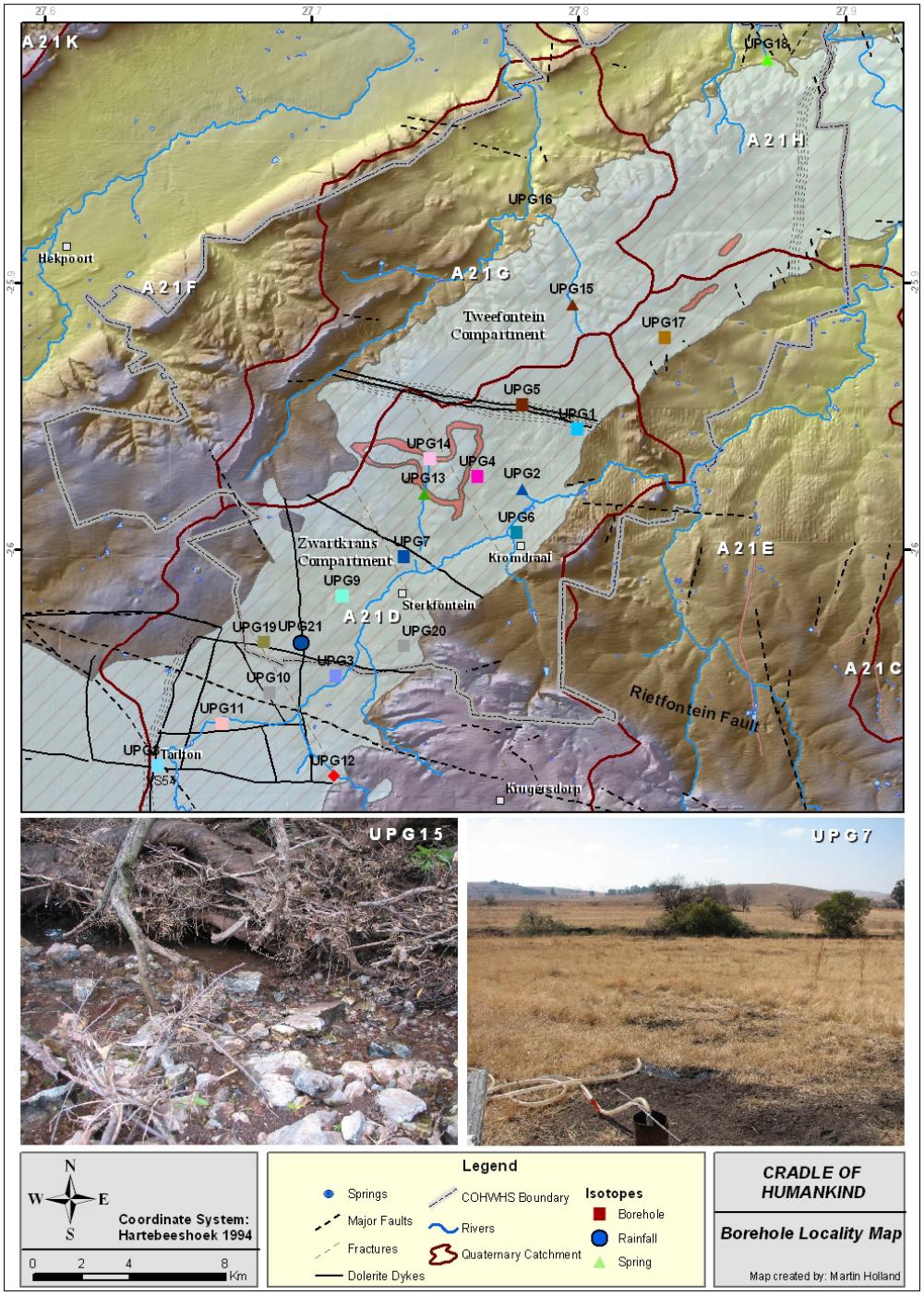


**Figure 4.28.** Isotope sample location with photos.

**Table 4.11.** Analytical results of 21 isotope samples taken from the karst aquifer.

| Lab ID | Borehole ID | Latitude | Longitude | δD[ ‰] SMOW | $\delta^{18}O$[ ‰] SMOW | Tritium ($^{3}H$) |
|---|---|---|---|---|---|---|
| **Zwartkrans Compartment** | | | | | | |
| UPG1 | VWB1 | 27.79945 | -25.95502 | -24.14 | -4.57 | 5.00 |
| UPG2 | PL-1 | 27.77890 | -25.97736 | -30.34 | -5.62 | 0.70 |
| UPG3 | PS3 | 27.68227 | -26.03161 | -18.68 | -3.45 | 2.00 |
| UPG4 | RLP1 | 27.76221 | -25.97267 | -30.36 | -5.33 | 0.80 |
| UPG6 | OBM1 | 27.77689 | -25.99381 | -18.69 | -3.32 | 4.80 |
| UPG7 | BBM1 | 27.73458 | -26.00261 | -30.47 | -5.40 | 0.20 |
| UPG8 | G36348 | 27.64216 | -26.08133 | -15.82 | -3.22 | 1.30 |
| UPG9 | G367794 | 27.71136 | -26.01740 | -17.60 | -3.35 | 1.40 |
| UPG10 | G36330 | 27.68415 | -26.05397 | -23.30 | -4.20 | 0.70 |
| UPG11 | G36335 | 27.66624 | -26.06578 | -22.59 | -4.10 | 0.90 |
| UPG12 | KGR1 | 27.70829 | -26.08533 | -21.14 | -3.84 | 1.40 |
| UPG13 | DR-S | 27.74229 | -25.97887 | -28.43 | -5.19 | 1.20 |
| UPG14 | DR-B | 27.74445 | -25.96622 | -28.92 | -5.07 | 1.00 |
| UPG19 | G36325 | 27.68215 | -26.03498 | -27.90 | -4.88 | 0.10 |
| UPG20 | NCB1 | 27.73468 | -26.03637 | -30.57 | -5.29 | 0.20 |
| UPG21 | RS-1 | 27.69619 | -26.03509 | 1.10 | -1.29 | 13.90 |
| **Tweefontein Compartment** | | | | | | |
| UPG5 | RLK1 | 27.77904 | -25.94564 | -28.56 | -5.29 | 1.20 |
| UPG15 | NFB | 27.79773 | -25.90795 | -29.24 | -5.52 | 2.10 |
| UPG16 | NFK | 27.78222 | -25.87444 | -32.12 | -5.78 | 0.60 |
| UPG17 | MB1 | 27.83221 | -25.92065 | -28.96 | -5.42 | 2.20 |
| UPG18 | BR-1 | 27.87090 | -25.81604 | -29.23 | -5.37 | 5.20 |

*Stable Isotopes*

The stable isotope data are plotted in Figure 4.29. The δD vs. $\delta^{18}O$ data points are shown relative to the Global Meteoric Water Line (GMWL, Craig, 1961). $\delta^{18}O$ ranges from -5.8‰ to -3.2‰ and δD from -30.6‰ to -15.8‰. The $\delta^{18}O$ and δD values of all samples are remarkably well correlated along an evaporation or mixing line. The long term isotopic data from the Pretoria GNIP (Global Network of Isotopes) station were used to obtain a more localised meteoric water line (PMWL, IAEA, 2004). A deuterium excess of 11.8% was assigned to this line and could hypothetically indicate the initial composition of the evaporated waters.

Samples located in the southern portion of the Zwartkrans compartment (UPG3, UPG7, UPG8, UPG9, UPG10, UPG11, UPG12, has developed enrichment in their heavy isotopic content due to significant kinetic (non-equilibrium) evaporation (Figure 4.28). This can be explained by several mechanisms, one being the recharge of groundwater by surface water. Light isotopes are preferentially transferred to the vapour phase. The resulting surficial layer enriched in the heavily isotope is then readily mixed into the bulk of the water body through connective processes. This evolutionary enrichment produces $\delta^{18}O$ and δD values

which lie to the right of the meteoric water line, and plot on an evaporation line of lesser slope and lower deuterium excess than the water meteoric water line. Groundwater derived through infiltration will carry this distinctive isotopic signal and could represent diffuse recharge in the area. All other samples plot on the meteoric water line or to the left of the PWML indicating a depleted isotopic composition, suggesting quick local recharging events typically of karst aquifers. Springs represented by UPG2, UPG15 and UPG16 may represent a more accurate local meteoric water line with an approximate deuterium excess of 15%.

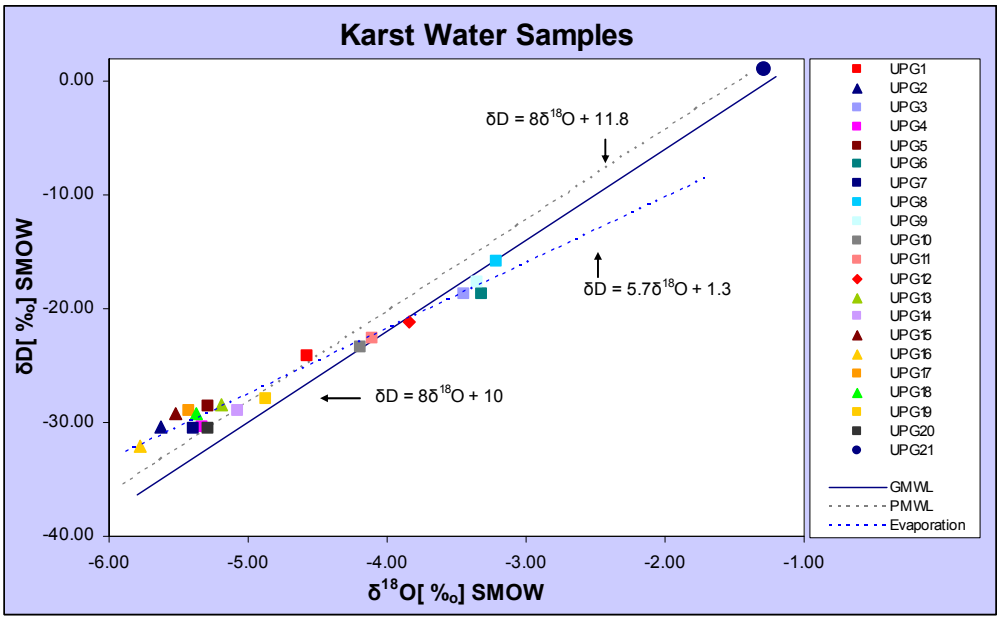


**Figure 4.29.** $\delta^{18}O$ vs. $\delta D$ of sample set relative to global meteoric water line (GMWL) (Craig, 1961) and long term Pretoria meteoric water line (PMWL).

*Tritium*

Major differences are found in the radioactive tritium contents, were it ranges from 0.1 – 5.2 *TU* and are clearly distinguished in two groups. The tritium value of the rainwater sample is unusually high at 13.9 *TU*, compared to about 3 – 4 *TU* normally found in ordinary rain water. Such values of between 10 and 14 *TU* are, however, observed occasionally in rain water sampled from the city area of Johannesburg[1]. The origin of these $^{3}H$ values could be attributed to Pelindaba nuclear technologies situated 30 km NE of the rainwater sample location. The long term tritium average from the GNIP monitoring data from the Pretoria station was added to the sample set.

[1] Horstmann, U. (2007). Personal communication, Johannesburg, 11 July.

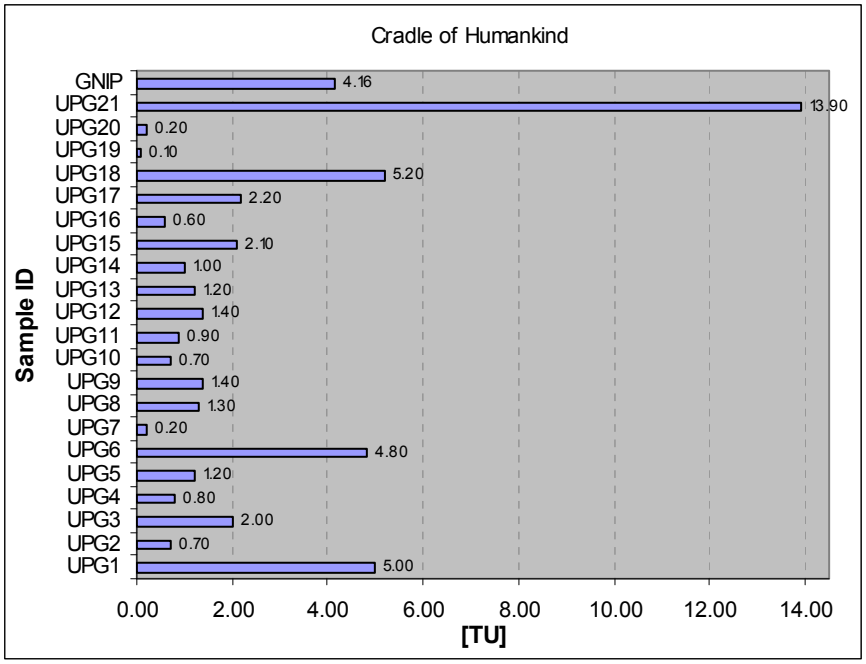


**Figure 4.30.** Tritium content of dataset in tritium units (*TU*).

Tritium is a radioactive isotope that follows a well-known law of disintegration. However, its concentration in rainfall is becoming too low for groundwater dating in karst aquifers with short residence time (Perrin et al., 2003). In this study three samples (UPG18, UPG1 and UPG6) are set of from the rest of the samples which has values of around 5 *TU* indicating recent recharge and relatively fast percolation. Waters that originated from rainfall prior to nuclear-bomb testing would have maximum $^{3}H$ concentrations of 0.2 to 0.8 *TU* by the early 1990s. Samples with tritium values lower than 2 would account for residence times in order of several decades.

## 4.5 Conceptual Model

The conceptual model describes the flow and recharge characteristics of the groundwater system. According to Scanlon *et al.*, (2002) the conceptual model should describe location, timing and likely mechanisms of recharge and provides initial estimates of recharge rates. From the results of the hydrogeological investigation and other specialist's reports the following conceptual understanding of the (146km$^2$) Zwartkrans compartment could be attained. A 3D perspective of the Zwartkrans surface is illustrated in Figure 4.31. To illustrate the conceptualisation, a section was drawn along the Tweelopiespruit and Blaauwbankspruit that shows the stream elevation and the groundwater table, as measured in the monitoring boreholes (Figure 4.32).

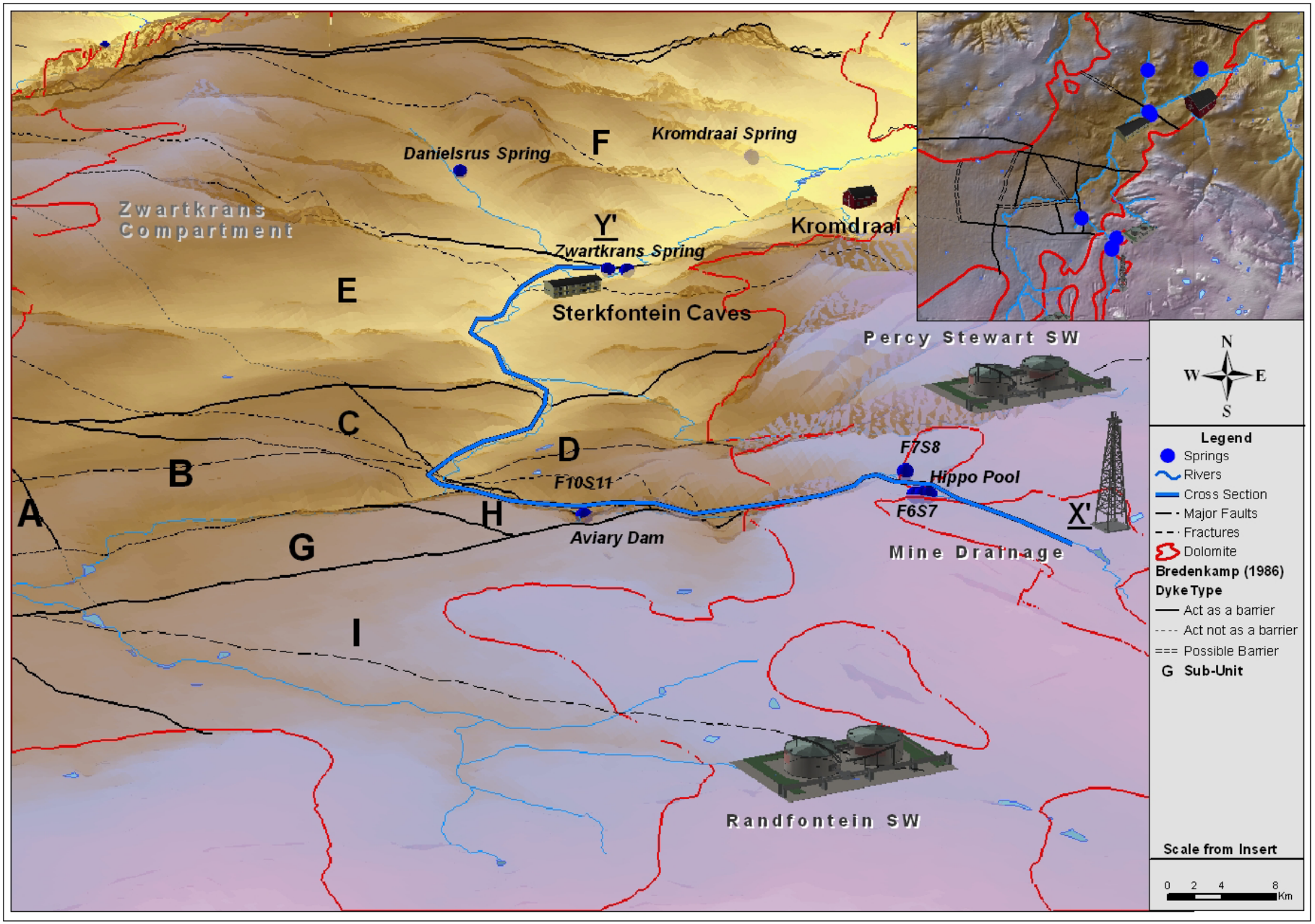


**Figure 4.31.** 3D surface terrain model of Zwartkrans compartment (vertical exaggeration x 2).

In this study the distinct master conduit flow typical of well developed karst systems could not be clearly identified, although Bredenkamp et al., (1986) estimated transmissivities of up to 25 000 $m^2$/day suggesting the hydraulics of conduit flow. The current investigation revealed two distinct types of groundwater flow (recharge) mechanisms in the study area. The first flow system could represent the epikarst zone where flowpaths are through networks of poorly integrated conduits and smaller solutionally widened fractures and fissures. This slow diffuse flow from low permeability rock blocks from the unsaturated zone demonstrates the piston effect of carbonate aquifer hydraulics. The second is a large volume, quick internal drainage of well developed integrated system of conduits and fissures. A considerable lag time is evident from the hydrograph response graph confirming the foremost and the latter is established by the significant hydraulic response to recharge events suggesting rapid and turbulent groundwater recharge.

Groundwater level contours indicate that groundwater flow is from the southwest of the study area towards the northeast. The Black Reef formation and Pretoria Group act as no-flow boundaries due to significant lower transmissivities. The influence of younger intruding dykes on the groundwater flow is clearly evident although the extent of leakage was not assessed.

*Recharge*

A distinct allogenic diffuse recharge from the sinking Tweelopiespruit which drains the mine decanting water is observed in the centre of the Zwartkrans compartment. A daily flow estimate of 2.51Ml/day at the edge of the dolomite compartment was measured by Krige (2006), but after transecting the dolomite it disappears completely, suggesting a highly variable inflow of 0.92 $Mm^3$/a. The Blougatspruit which carries effluent return flow have a similar character although not disappearing completely, a degraded flow could be observed at the R563 bridge crossing. As the initial flow of the stream flowing onto the karst system is estimated at 19Ml/day (Krige, 2006) a subjective 60% could be allowed for leakage into the underground system which cumulates to an annual inflow of 4.1 $Mm^3$/a. Both these flow values are indicated on the section diagram (Figure 4.32). Another significant inflow could be attributed to the lower Rietspruit were an estimated 4.2 $Mm^3$/a completely disappears before it reaches the town of Tarlton. From the isotope work done in this study it is established that surface water is recharging the groundwater system in the southern Zwartkrans compartment.

Further north, sub-compartment F, have a good integrated system of conduits that collects water from all parts of the recharge area and discharges it to surface streams through two large-volume springs (Figure 4.31). The stable isotopes of the Danielsrus and Kromdraai

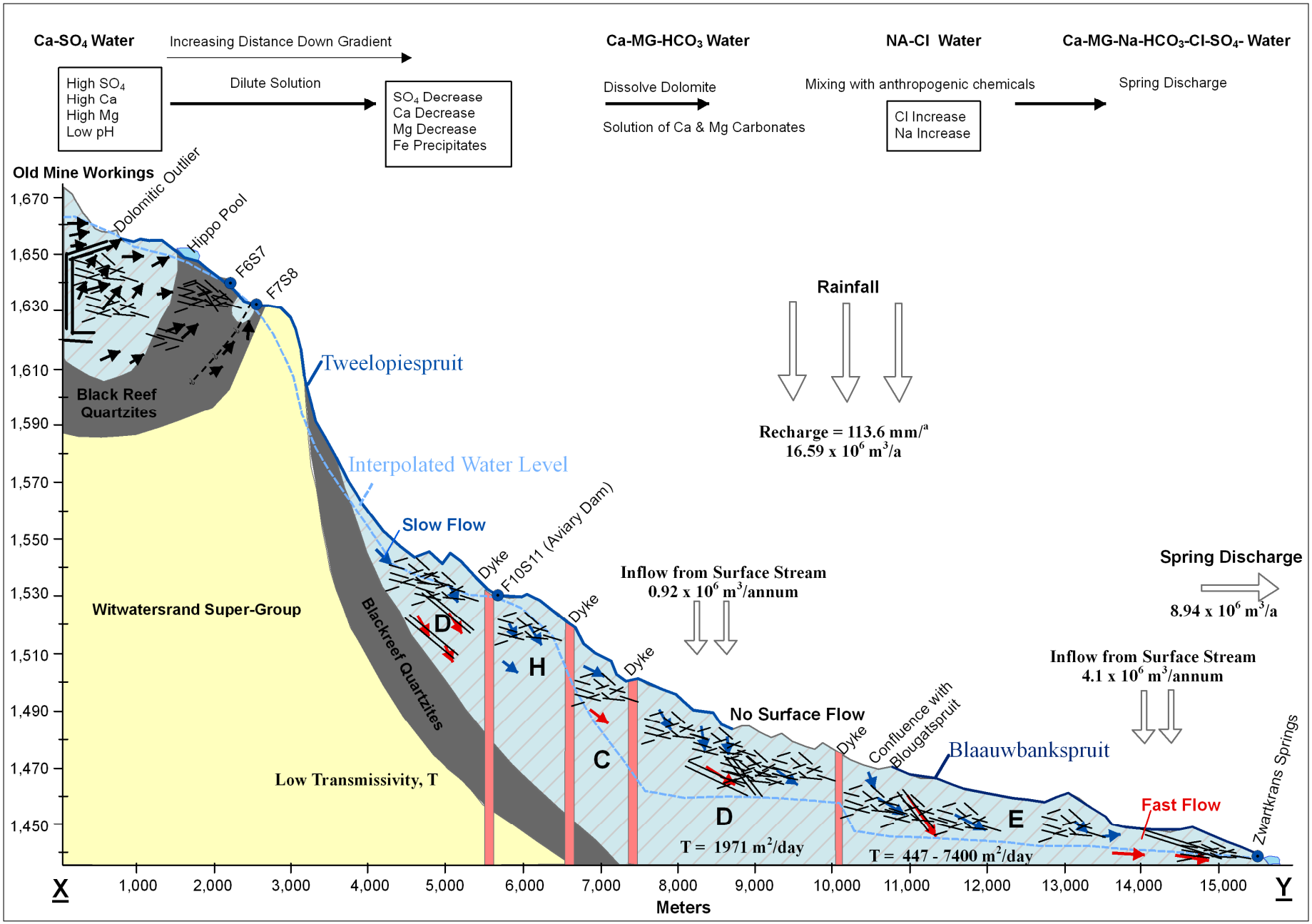


**Figure 4.32.** Cross section along the Tweelopiespruit as illustrated in Figure 4.31 indicating the major aquifer properties.

springs, and the borehole hydrograph from Kromdraai borehole confirm a local and quick recharge component. Other recharge mechanisms of the aquifer include recharge from perched groundwater systems in some caves and a concentrated direct recharge from sinkholes. Estimation of recharge methods shows a reasonable agreement and a recharge of 16% of the average annual precipitation (710mm) is projected which accounts to 16.59 $Mm^3/a$ over the Zwartkrans compartment.

*Hydrochemical Evolution*

In areas of recharge high concentrations of $CO_2$ and low dissolved solids content cause solution of dolomite (Hiscock, 2005). The dissolution of calcium and magnesium forms a Ca-MG-HCO3 water type. With this chemical evolution $SO_4$ increase and $HCO_3$ remains relatively constant. The mixing of highly polluted Ca-$SO_4$ water type has altered the natural chemical character of the aquifer and the application of fertilizers and effluent discharge added further Na, K, CL, $NO_3$ and $PO_4$ in the unsaturated zone providing opportunity for attenuation by adsorption and ion exchange. A schematic illustration of the evolution of the chemical character of groundwater in the karst aquifer is shown in Figure 4.32.

*Dolomitic Outlier*

With reference to Figure 4.32 it is also important to point out that the polluted mine water decanting area is situated within a dolomite outlier that is separated from the Zwartkrans Compartment by the Black Reef Formation and sediments of the Witwatersrand Super-Group. The dolomite outlier has similar characteristics as the dolomites discussed in the previous section but is dominated by residual products such as silica, iron and manganese oxides and hydroxides (wad) caused by the dissolution of the dolomite. This residual mass is also spongy, compressible, of low density and has a high void volume (Van Biljon, 2006). In an effort to identify groundwater flow paths from the mine workings a geophysical investigation was undertaken by Van Biljon (2006). The aim of the gravity survey was to determine preferential flow-paths along deeply weathered paleo-valleys (or grykes) in the dolomite bedrock. From the results three boreholes (RG1 to RG3) were drilled into the weathered zones to act as scavenger boreholes to create a sufficient drawdown to prevent contamination moving towards the Krugersdorp Game Reserve (KGR).

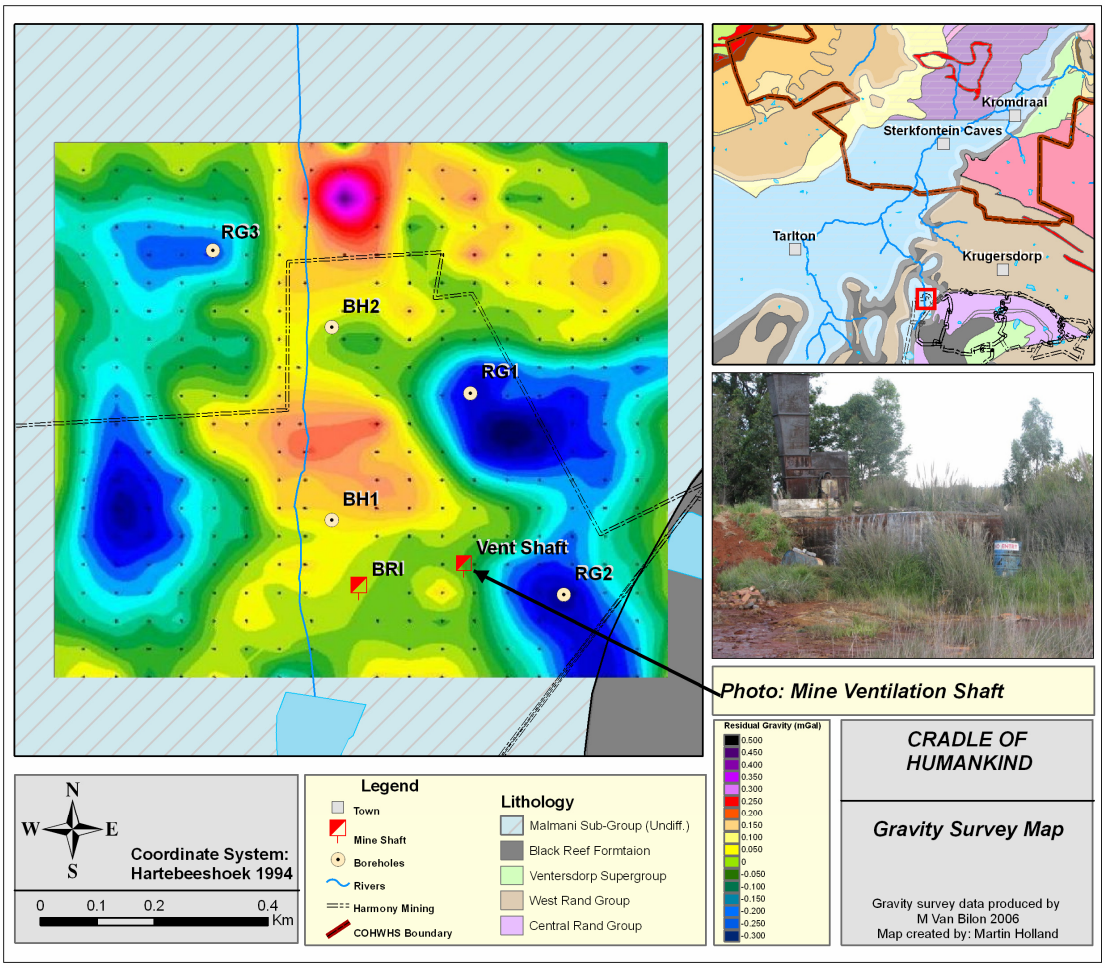


**Figure 4.33.** Gravity survey at the mine water decanting area on the dolomitic outlier (Data obtained from Van Biljon, 2006).

The dolomite outlier is the first zone affected by contaminated decant from the mine workings. The migration of contamination towards the Hippo Pool in the KGR signifies the edge of the hydraulic connection to the mine workings. Prior to 2002 before the decanting commenced the Hippo Pool was known as the dry dam as it never contained water. An investigation into management options by Harmony Gold (Van Biljon, 2006) is to lower the water level below the discharge point at the Hippo Pool. This water level is known as the Environmental Critical Level (ECL) and is set at 1636 m.a.m.s.l. It is suggested that no deeper underground migration of polluted mine water occur towards the adjacent formations (Van Biljon, 2006). However, the polluted chemical character of spring F6S7 could indicate the migration of polluted waters through fractures in the Black Reef Formation. It is important to note that the spring F7S8 discharging further downstream at the small dolomitic outlier contact zone is in pristine condition which could be attributed to groundwater flow paths different to the contamination plume.

# 5. Groundwater Resource Directed Measures (GRDM) Assessment

## 5.1. Preparatory Phase

As a result of the decanting acidic mine water from abandoned mine shafts, increasing sewage effluent return flows entering the catchment and large scale abstraction of groundwater for irrigation, the Cradle of Humankind dolomitic aquifer was recognised as a stressed aquifer. Specialist's reports by Van Biljon (2006) have noted a lowering of the water table of between 2.01m and 5.44m due to the rapid escalation of land under irrigation in the last 20 years.

The impact on groundwater quality in the aquifer, the ongoing exploitation and the Heritage status of the Cradle of Humankind suggested that the GRDM investigation be undertaken at a comprehensive level. However, the complex hydrogeology of this compartmentalised karst aquifer was not yet systematically investigated nor is it understood. This, together with a lack of monitored groundwater and spring data, results in the assessment being of low to medium confidence with a rapid to intermediate Reserve determination.

## 5.2. Description of Study Area

Full descriptions of the study area were given in Chapter 4 which included background information, physiography, climate and hydrogeological characterisation of the study area.

## 5.3. Delineation of Resource Units

The quaternary catchment is used as a starting point for delineating groundwater resource units within a study area. However, the objective of delineation is to group significant water resources with similar characteristics (Parsons and Wentzel, 2007). Consideration of location, geology and groundwater flow directions quaternary catchment boundaries as the basis for delineation weren't sufficient. The study area could be divided into two main groundwater resource units, one being the highly utilised Zwartkrans compartment and the other less utilised Tweefontein compartment. It is important to note that the Zwartkrans compartment could be delineated further into sub-units due to the compartmentalization of cross-cutting impermeable dykes. For simplicity and applicability, only the larger compartments will be used in the GRDM assessment each with its own level of confidence depending on data obtained.

### 5.3.1. Sources of Information

In response to the increasing surface-run-off from decanting acidic mine water a few investigations on groundwater resources of the karst aquifer was conducted by Van Biljon (2006) and Krige (2006). Geochemical descriptions of the karst groundwater in the Cradle of Humankind by Holland and Witthüser (2007) provide a detailed description of the source and extent of contamination. These professional studies form an important part of the GRDM assessment. Data presented in the GRDM assessment were obtained from the hydrogeological investigation that formed part of this study.

## 5.4. Resource Classification

In the absence of tools to determine the category of a resource, it was decided to incorporate the classification tools presented in Chapter 2.3. A category can be set using a stress index based on the volume of groundwater abstracted in relation to annual recharge. Further assessment is based on contamination and environmental impacts (Table 5.1).

**Table 5.1.** Categorisation of resource units in the Cradle of Humankind World Heritage Site.

| Unit | GW Use ($Mm^3/a$) | Recharge ($Mm^3/a$) | Stress Index | Classification | | | Category | |
|---|---|---|---|---|---|---|---|---|
| | | | | Reserve Quantity | Impact Indicator | Conta-mination | Management Class | Present Status |
| Zwartkrans Compartment | 14.1 | 16.6 | 0.85 | E | D | D | Poor | E |
| Tweefontein Compartment | 0.4 | 13.4 | 0.03 | A | A | A | Excellent | A |

Bredenkamp *et al* (1986) estimated an irrigation abstraction rate of 15.02 $Mm^3/a$ and Schoeman and associates estimated an abstraction rate of 14.08 $Mm^3/a$ in 2004. Krige (2006) estimated a value of 25.5 $Mm^3/a$ and founded that Schoeman and associates did not include all areas under irrigation from satellite photographs. Without the validation of true abstraction rates in the compartment this component remains critically uncertain and should be addressed. Average annual recharge of the study was set at 16.6 $Mm^3/a$ in the Zwartkrans compartment and 13.4 $Mm^3/a$ in the Tweefontein compartment respectively based on the hydrogeological investigations in Chapter 4. Other specialists studies in the Zwartkrans area determined recharge estimations of 16.8 $Mm^3/a$ (Bredenkamp et al., 1986) and Krige (2006) used a recharge value of 14.3 Million $m^3/a$ in a water balance study.

If a stress index of a unit is more than 0.65, it exceeds the lowest limit of sustainability. It's obvious from the stress index that the Zwartkrans resource unit is over-utilised and requires serious corrective management actions. The declining groundwater levels, worsening groundwater quality and heightened conflict levels implies that the resource is in a degraded state.

## 5.5. Reserve Quantification

The results of the classification phase clearly indicate the commitment of available groundwater resources for irrigation in the Zwartkrans compartment. The development of any further water supplies relies solely on the utilising of groundwater in storage of the dolomitic sub-units. From this aspect the determination for allocatable groundwater in the Zwartkrans compartment is relatively simple, as use almost exceeds input even before ecological and human needs have been taken into account. The inherent heterogeneity of the karst system and major uncertainties of inflows results in a highly suspect Reserve determination, however, an attempt towards Resource Directed Measures will at least give an account of the factors involved.

### 5.5.1. Basic Human Needs

Calculation of basic human needs in a resource unit is a simple task, where each person living within the boundaries of the resource unit is allocated 25 L/p/d. Using 2001 population census data for magisterial districts, the population of Zwartkrans and Tweefontein compartments was estimated at 9145 and 1304 respectively. The two resource units was overlaid with the municipal ward population data, which allowed the estimation of population on the resource unit based on the percentage of the ward that covers the unit. If it is assumed the entire population is dependent on groundwater as a source of supply and using a basic human need of 25 L/p/d, then the basic human need of the Zwartkrans and Tweefontein is calculated as 0.08 $Mm^3/a$ and 0.01 $Mm^3/a$.

**Table 5.2.** Population Data.

| Municipal Ward | Municipal Area | Total Population | Area on Zwartkrans | Area on Tweefontein | Zwartkrans Population | Tweefontein Population |
|---|---|---|---|---|---|---|
| Randfontein 1 | 298 | 6760 | 9.5 | | 215 | |
| Randfontein 3 | 28 | 8953 | 7.1 | | 2270 | |
| Mogale 19 | 147 | 6692 | 54.5 | | 2481 | |
| Mogale 12 | 40 | 6818 | 14.5 | | 2472 | |
| Mogale 11 | 40 | 6343 | 6 | | 951 | |
| GTDMA41 | 243 | 2291 | 80 | | 756 | |
| GTDMA41 | 243 | 2291 | | 114 | | 1075 |
| Mogale 29 | 459 | 11285 | | 9.3 | | 229 |
| | | | | **Total:** | **9145** | **1304** |

### 5.5.2. Groundwater Contribution to Baseflow

The conceptual understanding of the groundwater contribution to baseflow in South Africa Rivers is problematic (Parsons and Wentzel, 2007). Surface water – groundwater interactions are complex and do not always conforms to the classical concepts of recharge and baseflow. One of the major drawbacks in using flow data to determine the groundwater contribution to baseflow is the lack of good quality measured flow data. Where long term spring and river flow data exist, discharge, recharge and other hydraulic aquifer parameters from spring hydrograph analysis could be obtained (Perez, 1997; Amit et al, 2002; Kovacs *et al*., 2004).

In this study no continuous flow measurements were available for the Zwartkrans compartment, whereas the Tweefontein compartment had a long term gauging station installed at Nouklip spring. The groundwater contribution to baseflow in the Tweefontein compartment determined by hydrograph separation techniques in Chapter 4.3 were estimated at 8.3 $Mm^3/a$. The Tweefontein compartment is virtually devoid of surface drainage channels except for the one tributary of Skeerpoortriver which drains the Tweefontein compartment towards the north. The dolomite aquifer contributes substantially to groundwater base flow, where there is direct hydraulic connection with the river and where springs comprise the source of streams.

The groundwater contribution to baseflow of the Blaauwbankspruit which drains the Zwartkrans compartment is much more difficult to assess. Significant surface – groundwater interaction is evident from the chemical and isotope investigations. Surface streams completely disappear through swallow holes only to re-appear as springs downstream. Theoretically, the discharging springs into streams reflect a total groundwater contribution to

baseflow and that a lowering of the water table below the discharging level would decrease the flow or even dry up the spring. This obviously affects the surface water bodies that sustain the aquatic ecosystems and emphasise the need for spring discharge monitoring. In the karst system the groundwater contribution to baseflow and therefore the aquatic system is one of the main difficulties in assessing the Reserve component. In the interest of quantifying the Reserve, a spring discharge value of 8.94 $Mm^3/a$ will be used as the best estimate for baseflow in the Blaauwbankspruit. The lack of data together with the varying surface run-off caused by the anthropogenic effluent return flows resulted in low confidence baseflow estimations.

### 5.5.3. Reserve Estimation

The GRDM assessment for Tweefontein indicates a preliminary Reserve component of 62%, leaving a possible (5.4 $Mm^3/a$) allocatable groundwater (Table 5.3). In general, the Reserve accounts in both compartments for more than half of the estimated recharge, but are slightly higher in the northern parts of the study area where rainfall is lower. Based on the assessment undertaken, in theory no additional abstraction can take place in the Zwartkrans compartment. A more reliable Reserve determination could be validated if specialist reports could obtain accurate irrigation abstraction rates, groundwater contribution to baseflow estimates, and infiltration rates of surface water into the groundwater system. Up to this time it is suggested that no additional water licenses should be issued without the proper understanding of the water balance.

**Table 5.3.** GRDM assessment for both Zwartkrans and Tweefontein compartments.

| Resource Unit | Total Area ($Km^2$) | Annual Recharge ($Mm^3/a$) 16% of AR | RESERVE | | | ALLOCATION | |
|---|---|---|---|---|---|---|---|
| | | | Groundwater Contribution to Baseflow ($Mm^3/a$) | Basic Human Needs ($Mm^3/a$) | Reserve (% recharge) | Current Ground-water Use | Groundwater Allocation |
| Zwartkrans | 147 | 16.6 | 8.94 | 0.08 | 54 | 14.08 | 2.52 |
| Tweefontein | 128 | 13.4 | 8.3 | 0.01 | 62 | 0.34 | 5.4 |

It is the authors opinion that any additional water (mine and sewage works water) to the karst system is likely to cause the groundwater table to rise and replenish the water resources in storage.

### 5.5.4. Reserve for Water Quality

Methods for quantifying the groundwater quality component of the Reserve are not yet provided in the GRDM manual. However, in practice GRDM assessments include a preliminary groundwater quality assessment based on the following Table 5.4:

**Table 5.4.** General chemistry for Zwartkrans and Tweefontein compartment.

| Parameter | Ambient Ground Water Quality[1)] | | Basic Human Needs Reserve[2)] (Class 0) | Ground Water Quality Reserve[3)] | |
|---|---|---|---|---|---|
| | Zwartkrans (77 samples) | Tweefontein (5 samples) | | Zwartkrans | Tweefontein |
| **Electrical Conductivity (mS/m)** | 65 | 39.7 | < 70 | 71.5 | 43.6 |
| **Na (mg/l)** | 32.5 | 1.4 | < 100 | 35.8 | 1.6 |
| **Mg (mg/l)** | 39.0 | 27.6 | < 70 | 31.9 | 30.4 |
| **Ca (mg/l)** | 48.8 | 43.0 | <80 | 53.7 | 47.3 |
| **Cl (mg/l)** | 39.6 | 1.6 | < 100 | 43.6 | 1.8 |
| **$SO_4$ (mg/l)** | 88.4 | 8.4 | < 200 | 97.3 | 9.2 |
| **$NO_3$ (mg/l)** | **27.9** | 1.6 | < 24 | 30.7 | 1.7 |
| **Fluoride (mg/l)** | 0.2 | 0.1 | <0.7 | 0.25 | 0.15 |

[1)] Based on data obtained from the geochemical investigation in this study (only groundwater samples). Values reported are the statistical median of each parameter.
[2)] SANS (2005) South African National Standard (241) Drinking Water (Edition. 6).
[3)] Where a difference in the water quality values for the ambient groundwater quality and basic human needs was found, the lesser or more protective value was selected for the groundwater quality Reserve. Where the ambient groundwater quality was selected as the groundwater quality Reserve, the value was scaled up by 10 per cent.

The degrading groundwater quality is clearly evident in the Zwartkrans compartment, although no serious health risks could be identified from the Table 5.4. Holland and Witthüser, (2007) identified samples downstream of the mine drainage area with ion concentrations exceeding the recommended drinking values for water.

## 5.6. Resource Quality Objectives

The integrity of the dolomite aquifer must be maintained and protective measures applied to ensure any further degradation, both in terms of quantity and quality. It is important therefore to establish a set of Resource Quality Objectives (RQO's) for the Zwartkrans compartment which impacts can be judged and interventions and mitigation applied if necessary. The following protective measures are proposed and could be applied to most karst aquifers:

*Risk Assessment*

A risk assessment that will cover ground stability, effect on the sustainability of the available groundwater resource, impact on groundwater quality and impacts on spring flow and dependant ecology. Recently tools have been developed such as the SAGDT (South African Groundwater Decision Tool) which utilise principles of Fuzzy Logic risk to define sustainability, impact on groundwater quality and surface water - groundwater interaction (DWAF, 2006).

*Hazard and vulnerability mapping*

The basic premise underlying the concept of aquifer vulnerability is the variation of groundwater recharge mechanisms, which provides a direct link to a reserve determination of the area. The European approach to vulnerability, hazard and risk mapping for karst aquifers (Zwahlen, 2003) provides a good starting point. Pollution vulnerability mapping will take into account such aspects as topography and slope, thickness of soil cover, depth to water table, permeability and/or transmissivity of the dolomite aquifer and existing groundwater quality. The degree of vulnerability of the karst aquifer will depend to a large extent on the intended land use. Aquifer vulnerability mapping is currently underway in the Cradle of Humankind by the University of Pretoria as part of a Water Research Commission project using the COP method.

*Protection zones*

On the basis of the vulnerability and hazard mapping undertaken, and in order to manage effectively any identified recharge areas and potential source of significant pollution that may be present or may occur in time (e.g. from sewage works waste water disposal sites, mine drainage areas, cattle feed lots), it may be necessary to establish protection zones in aquifer systems and potential impacts. Protection zones are likely to be required around public water supply boreholes, recharge areas and within a spring capture zone. The spatial extent of the zone will depend upon the status of the resource and intended use of the borehole or spring.

*Long-term monitoring*

Accurate and reliable monitoring systems are required in karst systems. The ASTM (1995) standard guide for design of groundwater monitoring systems in karst could be of great help to practitioners. The value of long-term isotope, chemical, flow and discharge data cannot be emphasized enough. An example of specific monitoring required could be:

- All groundwater users in excess of 1 L/s are required to monitor groundwater abstraction and groundwater levels on a weekly basis and chemistry on a quarterly

basis. Users of groundwater in excess of 5 L/s need to install data loggers and monitor groundwater levels on a 2 hr basis.

*Other general RQO's*

- To prevent and/or manage decreasing groundwater level trends.
- To prevent the deterioration of the groundwater quality.
- To prevent stress on groundwater dependent ecosystems and to maintain the groundwater component of baseflow.
- To manage groundwater optimally within the catchment taking into account:
    - Increasing groundwater use in the catchment.
    - Increasing disputes around groundwater use.
    - The increasing numbers of boreholes completed and/or failing.
    - The increasing number of potential groundwater pollution sources.
    - Increasing groundwater pollution from existing sources.

# 6. Conclusion and Recommendations

## 6.1. General

The dolomites of the Chuniespoort Group, which underlie the Cradle of Humankind World Heritage Site, are the only readily available water resource for many farms in the region. These dolomites are also a vital component of the water resources needed for the expanding demand of the urban complexes in Gauteng and Rustenburg; hence it is considered as one of the most important aquifers in South Africa (Barnard, 2000). The Cradle of Humankind requires a sustainable balance between utilisation and protection of the water resource, in order to protect its vast treasure chest of fossilized remains of past life forms, found in the numerous karst caves. Despite its importance, the ongoing exploitation of the karst aquifer and surrounding catchment have resulted in the deterioration of both the quality and quantity of the groundwater resource. It was therefore important to accurately characterise the karst system and investigate the current status of the aquifer. The approach required an explanation of the understanding of karst terrain in South African and international literature, as well as the various conceptual models and methodologies applied to determine karst functioning.

The hydrogeological investigation exposed the heterogeneity of the karst aquifer, created and organised by groundwater flow which represents both a quick allogenic and autogenic recharge mechanism as well as diffuse infiltration (epikarst zone). Both the borehole hydrographs as well as the isotope investigation indicated the duality of the karst system in terms of recharge, flow and storage. The bounding effect that the low permeability dykes have on the compartments were clearly illustrated on the groundwater contour map and spatial chemical distribution maps, although the extent of leakage through the lower permeability medium were not established. The geochemical description of the karst waters show that the application of multivariate statistics in collaboration with graphical displays and spatial distribution maps can provide useful assessment of controls over water composition and assist in the identification of anthropogenic processes. The best indicators for the present contamination on the available dataset are elevated electrical conductivity and increased concentrations of sulphate, chloride and nitrate. The greatest risk to the use of groundwater is related to the polluted mine drainage, with ion concentrations exceeding the recommended drinking values for water.

## 6.2. GRDM Assessment

Because of the complexity of karst medium, belief might be that each karst aquifer requires different methods of investigation. Fortunately karst terrains do present some common characteristics in their conduit organization and in groundwater flow conditions, which allow us to use common exploration and exploitation methods (Bakalowicz, 2005). This study could not comprehensively cover all the karst specific investigation methods proposed by Balalowicz (2005) due to the lack of site-specific data and costs of professional investigations. In spite of the potential shortcomings inherent from the hydrogeologic investigation, the need to gain experience to classify resources, determining Reserves and setting RQO's is vital to the emerging Integrated Water Resource Management (IWRM) paradigm.

The GRDM assessment undoubtedly indicated that Reserve determination and groundwater allocation in karst terrain requires a much more comprehensive understanding of the underlying groundwater system compared to homogenous aquifers. It is suggested that the level of confidence of GRDM assessments in karst will almost always be at low confidence level unless accurate inflows, outflows, baseflow and recharge rates are determined through thorough hydrogeological investigations. Nevertheless, applying Resource Directed Measures is a proactive and adaptable approach, which is of paramount importance to successful groundwater management over the long term.

## 6.3. Recommendations

Apart from the recommended RQO's, improved understanding and accuracy of the following factors will greatly enhance the significance of the GRDM assessments in this and other karst terrain. In return this will account for better decision making of the development of karst groundwater resources in the Cradle of Humankind.

- A comprehensive hydrocensus of the both the Zwartkrans and Tweefontein compartments must be conducted to determine all groundwater users in the area.
- Monitoring locations should be established and continuous groundwater level and groundwater quality monitoring should be conducted.
- The geology of the area must be updated to differentiate between dolomitic formations and include previously unmapped areas (currently underway).
- The role of bounding dykes, faults and formation contacts on the groundwater flow and extent of lateral leakage of compartments should be clearly understood.
- Isotope investigations which should include groundwater dating together with tracer tests have proven to be greatly successful in karst hydrogeological

investigations (Kranjc, 1997; Trcek, 2003) and a monitoring programme should be initiated to build up long term data.

- Monitoring of the natural drainage of both ground- and surface water of the total area through the installation of flow gauging stations.
- Capturing of abstraction rates from large scale irrigation points is vital to evaluate the role of groundwater fluctuations and changes.
- The monitoring done by DWAF should be relevant to the study area and the impacts involved. Boreholes should be identified to successfully explain the extent and source of contamination.

In this context it is important to recognise that not all human activities are equally significant nor detrimental to the environment. The challenge to custodians, managers, scientists and stakeholders are to identify the most sensitive areas and accurately predict the significance of changing land use or other impacts on these terrains.

# 7. References

American Society for Testing and Materials (ASTM). 1995. Standard Guide for Design of Ground-Water Monitoring Systems in Karst and Fractured-Rock Aquifers. ASTM Designation D5717-95. ASTM, West Conshohocken, PA.

International Association of Hydrogeologists (IAH) Karst Commission. (2004). Focus on Karst groundwater. Available from: http://www.karst-hydrogeology.de/iah-karst.html.

Bakalowicz, M. (2005). Karst groundwater: a challenge for new resources. *Hydrogeological Journal,* **13**, 148-160.

Barnard, H. (1997). Geohydrological investigation of the catchment of Maloney's eye. M.Sc Thesis (unpublished). University of the Free State, Bloemfontein, RSA.

Barnard, H.C. (2000) *An Explanation of the 1:500 000 General Hydrogeological Map*. Department of Water Affairs and Forestry, Pretoria.

Bäumle, R. (2003). Geohydraulic Characterization of Fractured Rock Flow Regimes. PhD Thesis (unpublished). Karlsruhe University, Germany.

Bredenkamp, D.B., Van der Westhuizen, C., Wiegmanns, F.E. and Kuhn C.M. (1986). Groundwater supply potential of dolomite compartments west of Krugersdorp. Technical Report Gh3440. Directorate Geohydrology. Department of Water Affairs, Pretoria.

Bredenkamp, D.B. (1995). Dolomitic Groundwater Resources of the Republic of South Africa. Technical Report Gh3857. Directorate Geohydrology. Department of Water Affairs, Pretoria.

Bredenkamp, D.B., Botha, L.J., Van Tonder, G.J. and Van Rensburg, H.J. (1995). Manual on quantitative estimation of groundwater recharge and aquifer storativity. Water Research Commission Report No. TT 73/95. WRC, Pretoria.

Bredenkamp, D.B., Vogel, J.C., Wiegmans, F.E. Xu, Y. and Janse Van Rensburg, H. (2007). Use of natural isotopes and groundwater quality for improved estimation of recharge and flow in dolomitic aquifers. Water Research Commission Report No. KV 177/07. WRC, Pretoria.

Brink, A.B.A., and Partridge, T.C. 1965. Transvaal karst: some considerations of development and morphology, with special reference to sinkholes and subsidences on the Far West Rand. *South African Geographical Journal*, **47**,11-34.

Bögli, A. (1986). *Karst hydrology and physical speleology*. Springer Verlag, Berlin.-283.

Bouwer, H and Rice, R.C. (1976). Slug test for determining hydraulic conductivity of unconfined aquifers with completely or partially penetrating wells. *Water Resources Research,* **12** (3), 423-428.

Boussinesq, J. (1904). Recherches théoriques sur l'écoulement des nappes d'eau infiltrées dans le sol et sur le débit des sources. [Theoretical research on the groundwater flow and on springs discharge]. *J Math Pure Appl*, 10, 5-78.

Butler, J.J., Garnett, E.J. and Healey, J.M. (2003). Analysis of slug tests in formations of high hydraulic conductivity. Ground Water, **41** (5), 620-630.

Cabezas, H. and Fath, B.D. (2002). Towards a theory of sustainable systems. *Fluid Phase Equilibra,* **194**, 3-14.

Clendennin, C.W. (1989). Tectonic influence on the evolution of the Early Proterozoic Transvaal Sea, Southern Africa. PhD Thesis (unpublished). Wits University, Johannesburg.

Colvin C., Cavé L and Saayman I. (2004). A Functional Approach to Setting Resource Quality Objectives for Groundwater. Water Research Commission Report No. 1235/1/2004. WRC, Pretoria.

Cook, P.G. (2003) *A Guide to Regional Groundwater Flow in Fractured Rock Aquifers.* CSIRO-Seaview Press, South Australia. ISBN 1740082338.-108 pp.

Cooper, H.H. Jr., Bredehoeft, J.D. and Papadopulos, I.S. (1967). Response of a finite diameter well to an instantaneous charge of water. *Water Resources Research*, **3** (1), 263-269.

Craig, H. (1961). Isotopic variation in meteoric water. *Science,* **133**, 1702-1703.

Courtnage, P.M., Gibson, R.L., Charlesworth, E.G. and Andreoli, M.A.G. (1995). Post-Transvaal deformation between the Johannesburg dome and the Bushveld Complex., Centennial Geocongress G.S.S.A Vol. 1 Ext. Abs. pp 287-290.

Cvijic, J. (1893). Das Karstphänomen. Versuch einer geographischen Morphologie. (Karst phenomena. Geographical morphology). Geogr. Abhandlungen von A. Penck, Vienna, V, **3**, 217-230.

De Kock, W.P. 1964. The geology and economic significance of the West Wits line. In Geology of some Ore Deposits in southern Africa. *Journal of Geological Society South Africa*, 323-386.

Dreybrodt, W. (1988). *Processes in karst systems. physics, chemistry and geology*. Springer series in physical environment. Springer Verlag, Berlin.-288 pp

Drew, D and Hötzl, H. (1999). *Karst hydrogeology and human activities: impacts, consequences and implications.* Balkema, The Netherlands.- 308pp.

DWAF (Department of Water Affairs and Forestry). (1999). Resource directed Measures for Protection of Water Resources, Volume 2: Integrated Manual Version 1.0. Pretoria.

DWAF (Department of Water Affairs and Forestry). (2006). A Guideline for the Assessment, Planning and Management of Groundwater Resources within Dolomitic Areas in South Africa, Volume 2. Pretoria.

Enslin, J.F. and Kriel, J.P. (1959). Some results obtained from a hydrological study of a dolomitic catchment area in the Transvaal, Union of South Africa. Report no. 1.2.6.A. Department of Water Affairs and Forestry. Pretoria.

Enslin, J.F. and Kriel, J.P. (1967). The assessment and possible use of the dolomitic groundwater resources of the Far West Rand, Transvaal. International Conf. Water Peace, Washington.

Enslin, J.F. (1971). Notas oor die dolomitise groundwater bronne in die waterbeplanningstreek Wes-Transvaal. Technical Report Gh1784. Directorate Hydrology. Department of Water Affairs, Pretoria.

EPA (Environmental Protection Agency). (2002a). A Lexicon of cave and Karst terminology with special reference to environmental Karst hydrology. EPA/600/R-02/003. Office of Research and Development, Washington D.C.

EPA (Environmental Protection Agency). (2002b). The QTRACER2 Program for Tracer-Breakthrough Curve Analysis for Tracer Tests in Karstic Aquifers and Other Hydrologic Systems EPA/600/R-98/156a and 156b. Office of Research and Development, Washington D.C.

EPA (Environmental Protection Agency). (2006). Technical support document for section 194.14/15 evaluation of karst at the WIPP site. Office of Radiation and Indoor Air Center for the Waste Isolation Pilot Plant, Washington D.C.

Eriksson, E. and Khunakasem, V. (1969). Chloride concentrations in groundwater, recharge rate and rate of deposition of chloride in the Israel coastal plain. *Journal of Hydrology*, 7, 178-197.

Eriksson, P.G. and Reczko, B.F.F. (1995). The sedimentary and tectonic setting of the Transvaal Supergroup floor rocks to the Bushveld Complex. *Journal of African Earth Sciences*, **21**, 487-504.

Fetter, C.W. (2001). *Applied Hydrogeology*. 4th edition. Presentice-Hall, New Jersey.

Fleisher, J.N.E. (1981). The Geohydrology of the dolomite aquifers of the Malmani sub-group in the south-western Transvaal, Republic of South Africa. Technical Report Gh3169. Directorate Geohydrology. Department of Water Affairs, Pretoria.

Ford, D.C., Williams, P.W. (1989). *Karst geomorphology and hydrology*. Unwin Hyman, London.-601pp.

Foster, M.B.J. (1984) Steenkoppies and Zwartkrans dolomite compartments – Preliminary geological report. Technical Report Gh3346. Directorate Geohydrology. Department of Water Affairs, Pretoria.

Galloway, J.N., Knap, A.H. and Church, T.M. (1983). The composition of Western Atlantic precipitation using shipboard collectors. *Journal of Geophysical Research*, **88**, 10859-10854.

Glynn, P.D and Plummer, L.N. (2005). Geochemistry and the understanding of ground-water systems. *Hydrogeology Journal*, **13**, 263-287.

Government Gazette. (1998). National Water Act. *Government Gazette 398*, No. 19182. Government Printer, Pretoria.

Güler, C., Thyne, G.D., McCray, J.E. and Turner, A.K. (2002) Evaluation of graphical and multivariate statistical methods classification of water chemistry data. *Hydrogeology Journal*, **10**, 455-474.

Gunn, J. (1986). Modeling of conduit flow dominated karst aquifers. In Günay, G. and Johnson, A.I. (eds), *Karst Water Resources*. IAHS, Publication, **161**, 587-596. Wallingford, UK.

Han, G. and Liu, C. (2004). Water geochemistry controlled by carbonate dissolution: a study of the river waters draining karst-dominated terrain, Guizhou Province, China. Chemical Geology, **204**, 1-21.

Healy, R.W. and Cook, P.G. (2002). Using groundwater levels to estimate recharge. *Hydrogeology Journal,* **10** (2), 91-109.

Heikkinen, P.M., Korkka-Niemi, K., Lathi, M., Salonen, V.P. (2002) Groundwater and surface water contamination in the area of the Hitura nickel mine, Western Finland. *Environmental Geology* , **42**, 313-329.

Heppner, C.S. Nimmo, J.R. Folmar, G.J. Gburek, W.J. and Risser, D.W. (2006). Multiple-methods investigation of recharge at a humid-region fractured rock site, Pennsylvania, USA. Hydrogeology Journal, DOI:10.1016/j.jhydrol.2004.12.014.

Hiscock, K.M. (2005). *Hydrogeology: Principles and Practices*. Blackwell Science, UK.-388pp.

Holland, M., Witthüser, K.T., Jamison, A.A., Van Niekerk, H.J. and Bredenkamp, D.B. (2005). Hydrology of the Cradle of Humankind World Heritage Site. Geology, Surface- and Groundwater. IUCN Karst Commision, Pretoria.

Holland, M. and Witthüser, K.T. (2007). Geochemical characterization of karst groundwater in the Cradle of Humankind World Heritage Site. *Environmental Geology*, Under Review.

Hovorka, S., Phu, T., Nicot, J.P. and Lindley, A. (2004). Refining the Conceptual Model for Flow in the Edwards Aquifer—Characterizing the Role of Fractures and Conduits in the Balcones Fault Zone Segment. Bureau of Economic Geology. University of Texas, Austin.

Hussein, M.T. (2004) Hydrochemical evaluation of groundwater in the Blue Nile Basin, eastern Sudan, using conventional and multivariate. *Hydrogeology Journal*, **12**, 144-158.

Hvorslev, M.J. (1951). Time Lag and Soil Permeability in Groundwater Observations: U.S. Army Corps of Engineers Waterways Experiment Station, Bulletin No. 36.-50pp.

IAEA (2004). Global Network of Isotpoes in Precipitation. The GNIP Database accessible at: http://isohis.iaea.org

Jamison, A.A. (2001). Status Quo Report. Cradle of Humankind State of Environment IECMP, Gauteng. Wits University.

Jamison, A.A., Van Niekerk, E.J. and Viljoen, M.J. (2004). Bedding-parallel, shear & sinistral wrench faulting influencing location and formation of caves in the Cradle of Humankind, Gauteng, South Africa. Ext. Abs Geocongress 2004. GSSA.

Jukić, D. and Denić-Jukić, V. (2004). A frequency domain approach to groundwater recharge estimation in karst. *Journal of Hydrology*, **289**, 95-110.

Katz, G.K., DeHan, R.S., Hirten, J.J. and Catches, J.S. (1997). Interactions between groundwater and surface water in the Suwannee River Basin, Florida. JAWRA, **33** (6), 1237-1254.

Kazemi, R. (2003). Reconnaissance of karst hydrology in the Lar catchment, Iran using RS and GIS. M.Sc Thesis (unpublished). International Institute for Geo-Information Science and Earth Observation, The Netherlands.

King, L.C. (1963). *The South African Scenery*. Oliver and Boyd. Edinburgh. U.K.-308pp.

Kinzelbach, W., Aeschbach, W., Alberich, C., Goni, I.B., Beyerle, U., Brunner P., Chiang, W.H., Rueedi J., and Zoellmann K. (2002). A Survey of Methods for Groundwater Recharge in Arid

and Semi-arid regions. Early Warning and Assessment Report Series, UNEP/DEWA/RS.02-2. United Nations Environment Programme, Nairobi, Kenya.

Kiraly, L. (2003). Karstification and Ggroundwater Flow. *Speleogenesis and Evolution of Karst Aquifers*, **1** (3), 2-26.

Kovács, A., Perrochet, P., Kiraly L and Jeannin, P. (2005). A quantitative method for the characterisation of karst aquifers based on spring hydrograph analysis. *Journal of Hydrology*, **303**, 152–164.

Kranjc, A. (ed) (1997). *Karst Hydrogeological Investigations in South-Western Slovenia*. Association of Tracer Hydrology. Karst Research Institute. Ljubljana, Slovenia.-388.

Krešić N. (1997). *Quantative solutions in hydrogeology and groundwater monitoring*. Lewis Publishers, Florida. 269-302pp.

Krige, (2006). Hydrological/Chemical aspects of the Tweelopiespruit, Rietspruit and Blaauwbankspruit, with specific reference to the impact water, decanting from the western basin mine void, has on the system. Africa Environmental Development Consultants.

Kuhn, C.M. (1986). Geohydrological investigation of the western and central Steenkoppies compartment. Technical Report Gh3446. Directorate Geohydrology. Department of Water Affairs, Pretoria.

Lambrakis, N., Antonakos, A. and Panagopoulos, G. (2004). The use of multicomponent statistical analysis in hydrogeological environmental research. *Water Research*, **38**, 1862-1872.

Mahlknecht, J., Schneider, J., Merkel, B., de Leon I.N. and Bernasconi, S. (2004). Groundwater recharge in a sedimentary basin in semi-arid Mexico. *Hydrogeology Journal,* **12**, 511-530.

Maillet, E. (1905). *Essais d'hydraulique souterraine et fluviale*. (Essays on groundwater and river hydraulics). Eyroles, Paris-218pp.

Marker, M.E. (1971). Karst landforms of the northeastern Transvaal. PhD Thesis (unpublished). Wits University, Johannesburg.

Marker, M.E. (1972) Karst landform analysis as evidence for climatic change in Transvaal. *South African Geographical Journal*, **54**, 152-162.

Marker M.E. (1980) A systems model for karst development with relevance for Southern Africa. *South African Geographical Journal.* **62**, 151-163.

Martini, J.E.J. and Kavalieris, I. (1976). The karst of the Transvaal (South Africa). *International Journal of Speleology*, **8**, 229-251.

Martini, J.E.J., Wipplinger, P.E., Moen, H.F.G. and Keyser, A. (2003). Contribution to the Speleology of Sterkfontein Cave, Gauteng Province, South Africa. *International Journal of Speleology*, **32**, 43-69.

Mathes, S.E. and Rasmussen, T.C. (2006). Combining multivariate statistical analysis with geographic information systems mapping: a tool for delineating groundwater contamination. *Hydrogeology Journal*, **14**, 1493-1507.

Mayer J (1999) Spatial and temporal variation of groundwater chemistry in Petitjohns cave, Northwest Georgia, USA. *Journal of Cave and Karst studies*, **61**(3), 131-138.

Mavurayi, A. (2005). Groundwater Resource Directed Measures from the Resource Directed Measures Perspective. Biennial Ground Water Conference. CSIR Conference Center Pretoria, South Africa.

McElwee, C.D. (2002). Improving the analysis of slug tests. *Journal of Hydrology*, **269**, 122-133.

McNeil, V.H., Malcolm, E.C. and Preda, M. (2005) Assessment of chemical water types and their spatial variation using multi-stage cluster analysis, Queensland, Australia. Journal of Hydrogeology, DOI:10.1016/j.jhydrol.2004.12.014.

Moon, S., Woo, N.C. and Lee, K.S (2004). Statistical analysis of hydrographs and water-table fluctuation to estimate groundwater recharge. *Journal of Hydrology*, **292**, 198-209.

Musy, A. (2001). *e-drologie*. Ecole Polytechnique Fédérale, Lausanne, Suisse.

Novel, J., Dimadi, A., Zervopoulou, A and Bakalowicz, M. (2006). The Aggitis karst system, Eastern Macedonia, Greece: Hydrologic functioning and development of the karst structure. *Journal of Hydrology*, **334**, 477-492.

Obbes, A.M. (2001). The structure, stratigrgaphy and sedimentology of the Black Reef-Malmani-Rooihoogte succession of the Transvaal Supergroup southwest of Pretoria. Bulletin 127, Council for Geoscience, South Africa.

Pannatier, E.G., Broers, H.P., Venema, P. and Van Beusekom, G. (2000). A new process-based hydro-geochemical classification of groundwater. Netherlands institute for applied science.

Parsons, R and Wentzel, J. (2007). Setting Resource Directed Measures (RDM) for groundwater: A pilot study. Water Research Commission Report No. TT 299/07. WRC, Pretoria.

Partridge, T.C. and Maud R.R (1987). Geomorphic evolution of southern Africa since the Mesozoic. *South African Journal of Geology,* **90**(2), 179-208.

Pearson, A.V. and Hartley, H.O. (1970). Biometrica tables for statisticians, Vol 1. Cambridge University. Cambridge, England.

Perrin, J. (2003). A conceptual model of flow and transport in a karst aquifer based on spatial and temporal variations of natural tracers. PhD Thesis (unpublished). University of Lausanne, Switzerland.

Perrin, J., Jeanin, P., and Zwahlen (2003). Epikarst storage in a karst aquifer: a conceptual model based on isotopic data, Milandre test site, Switzerland. Journal of Hydrology, **279**, 106-124.

Pinault, J.L., Bakalowicz, M., Plagnes, V., Aquilina, L. (2001) Inverse modeling of the hydrological and the hydrochemical behavior of hydrosystems: characterization of karst system functioning. *Water Resource Research*, **37**, 2191-2204.

Polivka, J. (1987a). Geohydroglogical investigation of the Schoonspruit compartment in the dolomitic area of Ventersdorp. Technical Report Gh3524. Directorate Geohydrology. Department of Water Affairs, Pretoria.

Polivka, J. (1987b). Geohydroglogical investigation of the Groot-Marico compartment in the dolomitic area north-east of Lichtenburg. Technical Report Gh3590. Directorate Geohydrology. Department of Water Affairs, Pretoria.

Powers, J.G. and Shevenell, L. (2000). Transmissivity Estimates from Well Hydrographs in Karst and Fractured Aquifers. *Ground Water*, **38** (3), 361-369.

Raj, P. (2004). Classification and interpretation of piezometer well hydrographs in parts of southeastern peninsular India. *Environmental Geology*, **46**, 808-819.

Reimann, C., Filzmoser, P. and Garrett, R.G. (2005). Background and threshold: critical comparison of methods of determination. *Science of the Total Environment*, **346**, 1-16.

Romanov, D. (2003). Evolution of karst aquifers in natural and man made environments: A modeling approach. PhD Thesis (unpublished). Bremen University, Germany.

Rorabaugh, M.I, (1964). Changes in bank storage: Publication. No.63, IASH, Gentbrugge, 432-441.

Rutledge, A.T. (2006). Basic Concepts for the linear model of groundwater level recession. Groundwater, **44** (3), 483-487.

SACS (South African Committee for Stratigraphy). (1980). Stratigraphy of South Africa. Part 1 (Compiler L.E. Kent). Lithostratigraphy of the Republic of South Africa, South West Africa / Namibia, and the Republics of Bophuthatswana, Transkei and Venda: *Handbook of the Geological Survey of South Africa*, 8, 690pp.

SANS (South African National Standard) (241). (2005). Drinking Water (Edition. 6). South Africa, Pretoria.

Samani, N. (2001). Response of karst aquifers to rainfall and evaporation, Maharlu basin, Iran. *Journal of Cave and Karst Studies*, 33-40.

Scanlon B.R., Healy R.W. and Cook P.G. (2002). Choosing appropriate techniques for quantifying groundwater recharge. *Hydrogeology Journal*, **10**, 18-39.

Scanlon, B.R., Mace, R.E., Barrett, M.E., Smith, B.D. (2003) Can we simulate regional groundwater flow in a karst system using equivalent porous media models? Case study, Barton Springs Edwards aquifer, USA. Journal of Hydrology, **276**, 137-158.

Shaban, A., Khawlie, M. and Abdallah, C. (2004). Use of remote sensing and GIS to determine recharge potential zones: the case of Occidental Lebanon. *Hydrogeology Journal*, **14**, 433-443.

Shapiro, A.M., Hsieh, P.A. (1998). How good are estimates of transmissivity from slug tests in fractured rock? *Ground Water*, **36** (1), 37-48.

Shevenell, L. (1996). Analysis of well hydrographs in a karst aquifer: estimates of specific yields and continuum transmissivities: *Journal of Hydrology*, **174**, 331-355.

Singh, K.P., Malik, A., Mohan, D. and Sinha, S. (2004). Multivariate statistical techniques for the evaluation of spatial and temporal variations in water quality of the Gomti River (India) – a case study. *Water Research,* **38**, 3980-3992.

Sukhija, B.S., Reddy, D.V. Nagabhushanam, P., Bhattacharya, K.S., Jani, R.A. and Kumar, D. (2006). Characterisation of recharge processes and groundwater flow mechanisms in weathered-fractured granites of Hyderabad (India) using isotopes. *Hydrogeology Journal*, **14**, 663-674.

Subyani, A. and Sen, Z. (2006). Refined chloride mass-balance method and its application in Saudi Arabia. *Hydrological. Processes,* **20**, 4373-4380.

Sweeting, M.M. (1973). Karst landforms and limestone, *South African Geographical Journal*, **55**, 81-88.

Thyne, G., Güler, C., Poeter, E. (2004). Sequential analysis of hydrochemical data for watershed characterization. *Ground Water*, **42**, 1-12.

Toran, L., Herman, E.K., and White, W.B. (2007). Comparison of flowpaths to a well and spring in a Karst Aquifer. *Ground Water,* **1** , 1-7.

Trček, B. (2003). Epikarst zone and the karst aquifer behaviour: a case study of the Hubelj catchment , Slovenia. Geološki zavod Sloveije.

Truswell, J.F. (1977). *The Geological Evolution of South Africa*. Purnell & Sons, Cape Town.

Van Biljon, M. (2006). Geo-hydrogeological review of the potential impact on the Sterkfontein dolomite during increased surface water run-off. Rison Groundwater Consulting, Krugersdorp.

Van Der Kamp, G. (1976). Determining aquifer transmissivity by means of well response tests: the underdamped case. *Water Resources Research*, **12** (1), 71-77.

Van Tonder, G and Xu, Y. (2001). A guide for the estimation of groundwater recharge in South Africa. The Institute for Groundwater Studies, Bloemfontein.

Van Tonder, G. and Vermeulen, P.D. (2005). The applicability of slug tests in fractured-rock formations. *Water SA*, **31** (2), 157-159.

Vegter, J.R. and Foster, M.B.J. (1990). The hydrogeology of dolomitic formations in the southern and western Transvaal. Internal report. Department of Water Affairs, Pretoria.

Verhagen, B, Smith, T.H., McGeorge, P.E., Dziembowski, I. (1979). Tritium profiles in Kalahari sands as a measure of rainwater recharge. Isotope Hydrology 1979 IAEA, Vienna, 733-749.

Wang, Y., Ma, T., and Luo, Z. (2001). Geostatistical and geochemical analysis of surface water leakage into groundwater on a regional scale: a case study in the Liulin karst system, northwestern China. *Journal of Hydrogeology*, **246**, 223-234.

Weaver, J.M.C., Talma, A.S. and Cavé, L.C. (1999). Geochemistry and Isotopes for Resource Evaluation in the Fractured Rock Aquifers of the Table Mountain Group. Water Research Commission Report No 481/1/99, WRC, Pretoria.

White, W.B. (2002). Karst Hydrology: recent developments and open questions. *Engineering Geology*, **65**, 85-105.

Wilkins, C.B., Eriksson, P.G. and Van Schalkwyk, A. (1987). Two generations of karst fill sedimentary rocks within Chuniespoort Group dolomites south of Pretoria. *South African Journal of. Geology*. **90**, 155-167.

Williams, T.M. and Smith, B. (2000). Hydrochemical characterization of acute acid mine drainage at Iron Duke Mine, Mazowe, Zimbabwe. *Environmental Geology*, **39**, 272-278.

Wood, W.W. and Sanford, W.E., (1995). Chemical and isotopic methods for quantifying ground water recharge in a regional, semi-arid environment. *Ground Water*, **33**, 458-468.

Wright K.A. and Xu Y. 2000: A Water Balance approach to the sustainable management of groundwater in South Africa *Water SA,* **26** (2), 167-170.

Veltman, S. (2003). A methodology for groundwater management in dolomitic terrains with the Schoonspruit Compartment as pilot area. M.Sc Thesis , Department of Geohydrology,

University of the Free State, South Africa.

Xu, Y. and Van Tonder, G. (2000). Recharge excel spreadsheet. The Institute of Groundwater Studies. Bloemfontein.

Xu, Y. and Van Tonder, G. (2001). Estimation of recharge using a revised CRD method. *Water SA*, **27** (3), 341-343.

Xu, Y., Titus, R., Holness, S.D., Zhang, J. and van Tonder, G.J., 2002. A hydrogeomorphological approach to quantification of groundwater discharge to streams in South Africa. Water SA, **28** (4), 375-380.

Xu, Y. and Beekman, H.E. (Eds) (2003). *Groundwater Recharge Estimation in Southern Africa*. UNESCO IHP Series No. 64. UNESCO, Cape Town.

Xu, Y., Colvin, C., Van Tonder, G.J., Hughes, S., le Maitre, D., Zhang J., Mafanya, T. and Braune, E. (2003). Towards the resource directed measures: Groundwater component. Water Research Commission Report No. 1090-2/1/03. WRC, Pretoria.

Zwahlen F. (Ed). (2003). Vulnerability and risk mapping for the protection of carbonate (karst) aquifers, final report COST Action 620, European Commission, Directorate-General for Research. EUR 20912: Luxemburg.

# Appendix A

# Monitoring Boreholes

**Table 1.** Monitoring boreholes.

| Borehole ID | LONGITUDE | LATITUDE | Z COLLAR | Date Last Measured | Water Level (mbs) | Water Level (mamsl) |
|---|---|---|---|---|---|---|
| KBH-1 | 27.78170 | -25.98120 | 1410.00 | 2006/07/30 | 8.30 | 1401.70 |
| RBT-B1 | 27.78163 | -25.98671 | 1414.50 | 2006/07/30 | 12.26 | 1402.24 |
| RBW-B1 | 27.77510 | -25.98622 | 1419.00 | 2006/07/30 | 15.83 | 1403.17 |
| HW-1 | 27.77689 | -25.99381 | 1414.50 | 2006/07/30 | 8.00 | 1406.40 |
| R-B1 | 27.78068 | -25.98803 | 1421.00 | 2006/07/30 | 11.65 | 1409.35 |
| DR-P15 | 27.74526 | -25.99809 | 1474.00 | 2006/07/30 | 59.00 | 1414.94 |
| DPL-1 | 27.75241 | -26.00381 | 1433.00 | 2006/01/25 | 15.00 | 1417.71 |
| GBH | 27.75823 | -26.00326 | 1441.50 | 2005/12/09 | 23.00 | 1418.14 |
| SWBH-1 | 27.75707 | -26.00528 | 1447.50 | 2006/07/30 | 28.00 | 1419.51 |
| SBH-1 | 27.76386 | -25.99973 | 1442.00 | 2006/07/30 | 22.26 | 1419.74 |
| M-B1 | 27.73614 | -26.01049 | 1451.00 | 2006/07/30 | 15.07 | 1435.93 |
| SF-1 | 27.73571 | -26.01339 | 1453.50 | 2006/07/30 | 17.00 | 1436.50 |
| OA-1 | 27.72378 | -26.02427 | 1463.00 | 2005/12/09 | 26.00 | 1436.64 |
| G36325 | 27.68233 | -26.03444 | 1511.68 | 2006/01/25 | 74.00 | 1437.84 |
| G37791 | 27.68428 | -26.03254 | 1508.00 | 2005/12/09 | 70.00 | 1438.10 |
| M-B2 | 27.73849 | -26.00889 | 1446.00 | 2006/07/30 | 7.53 | 1438.47 |
| G36324 | 27.69753 | -26.03134 | 1516.82 | 2005/12/09 | 78.00 | 1438.50 |
| G37789 | 27.68756 | -26.02875 | 1502.00 | 2005/12/09 | 63.00 | 1438.80 |
| G37794 | 27.71136 | -26.01740 | 1464.00 | 2006/07/30 | 25.06 | 1438.95 |
| G36323 | 27.71527 | -26.02441 | 1475.15 | 2006/07/30 | 36.13 | 1439.03 |
| G36320 | 27.70823 | -26.01632 | 1468.19 | 2006/01/25 | 29.00 | 1439.07 |
| SW-1 | 27.71866 | -26.02633 | 1457.00 | 2005/12/09 | 18.00 | 1439.18 |
| NRB-1 | 27.73468 | -26.03637 | 1509.00 | 2006/08/11 | 70.00 | 1439.30 |
| ZW-1 | 27.70695 | -26.01686 | 1469.00 | 2006/07/30 | 29.64 | 1439.36 |
| G33786 | 27.70513 | -26.02766 | 1496.00 | 2006/07/30 | 56.00 | 1440.29 |
| HV-1 | 27.80547 | -25.94572 | 1455.50 | 2005/12/09 | 15.00 | 1440.46 |
| G37792 | 27.68227 | -26.03161 | 1508.00 | 2005/12/09 | 67.00 | 1440.80 |
| B-1 | 27.79926 | -25.95528 | 1475.00 | 2006/07/30 | 34.16 | 1440.84 |
| Boland-B1 | 27.73458 | -26.00261 | 1463.00 | 2006/07/30 | 22.15 | 1440.85 |
| G-B1 | 27.71722 | -26.03273 | 1462.00 | 2006/07/30 | 20.36 | 1441.64 |
| G36326 | 27.70936 | -26.03707 | 1492.22 | 2006/01/25 | 51.00 | 1441.72 |
| RT-2 | 27.72103 | -26.03256 | 1471.00 | 2007/02/13 | 28.00 | 1443.00 |
| VW-1 | 27.80139 | -25.95635 | 1457.00 | 2006/07/30 | 13.14 | 1443.86 |
| SF-2 | 27.70807 | -26.03763 | 1498.50 | 2006/07/30 | 54.50 | 1444.00 |
| RT-1 | 27.71886 | -26.03466 | 1470.00 | 2007/02/01 | 25.00 | 1445.00 |
| G36327 | 27.71563 | -26.03614 | 1467.47 | 2006/01/25 | 21.00 | 1446.72 |
| G36331 | 27.70893 | -26.04762 | 1488.25 | 2006/07/30 | 27.28 | 1460.97 |
| PS-1 | 27.71234 | -26.04756 | 1475.32 | 2007/03/08 | 12.32 | 1463.00 |
| G36334 | 27.69966 | -26.05844 | 1493.01 | 2007/02/08 | 26.00 | 1467.01 |
| K-1 | 27.69672 | -26.06333 | 1505.10 | 2007/02/13 | 35.10 | 1470.00 |
| G36328 | 27.67872 | -26.04625 | 1543.61 | 2006/01/25 | 67.00 | 1476.61 |
| G36335 | 27.66656 | -26.06526 | 1543.59 | 2006/01/25 | 61.00 | 1482.44 |
| DR-GF2 | 27.74445 | -25.96622 | 1511.00 | 2006/07/30 | 26.93 | 1484.07 |
| DR-GF1 | 27.74241 | -25.97584 | 1497.00 | 2006/07/30 | 11.00 | 1485.95 |
| DL-1 | 27.67536 | -26.07119 | 1565.00 | 2007/02/08 | 62.00 | 1503.00 |
| RS-1 | 27.66973 | -26.07808 | 1576.03 | 2007/02/01 | 73.03 | 1503.00 |
| AR-1 | 27.66978 | -26.08091 | 1579.26 | 2007/02/01 | 76.26 | 1503.00 |

| Borehole ID | LONGITUDE | LATITUDE | Z COLLAR | Date Last Measured | Water Level (mbs) | Water Level (mamsl) |
|---|---|---|---|---|---|---|
| CE-1 | 27.67491 | -26.08664 | 1596.65 | 2007/02/06 | 76.65 | 1520.00 |
| G36356 | 27.66521 | -26.09470 | 1596.56 | 2006/07/30 | 58.00 | 1538.36 |
| WN-1 | 27.69800 | -26.09717 | 1601.00 | 2007/01/31 | 60.00 | 1541.00 |
| MF-1 | 27.69169 | -26.07945 | 1592.95 | 2007/02/08 | 43.95 | 1549.00 |
| G36337 | 27.68628 | -26.07922 | 1594.49 | 2006/01/25 | 45.00 | 1549.33 |
| D-1 | 27.70167 | -26.08814 | 1592.96 | 2007/01/31 | 30.96 | 1562.00 |
| BN-1 | 27.69403 | -26.08978 | 1613.20 | 2007/01/31 | 44.20 | 1569.00 |
| LF-1 | 27.69742 | -26.10120 | 1610.54 | 2007/02/21 | 39.54 | 1571.00 |
| JN-1 | 27.69461 | -26.09089 | 1617.22 | 2007/01/31 | 46.22 | 1571.00 |
| BV-1 | 27.70011 | -26.10383 | 1625.09 | 2007/02/01 | 53.09 | 1572.00 |
| G36338 | 27.69634 | -26.08914 | 1614.92 | 2007/02/01 | 42.00 | 1572.92 |
| AC-1 | 27.70178 | -26.09650 | 1607.00 | 2007/02/08 | 27.00 | 1580.00 |
| PE | 27.68703 | -26.11906 | 1663.00 | 2007/02/21 | 14.00 | 1649.00 |
| AJ-1 | 27.72903 | -26.10955 | 1672.50 | 2007/03/08 | 18.50 | 1654.00 |
| AJ-2 | 27.72903 | -26.10955 | 1672.50 | 2007/03/08 | 18.50 | 1654.00 |
| BE-1 | 27.68750 | -26.12181 | 1657.32 | 2007/02/21 | 2.32 | 1655.00 |
| CES-1 | 27.68750 | -26.12191 | 1658.00 | 2007/02/21 | 2.00 | 1656.00 |
| RG-3 | 27.72066 | -26.10992 | 1665.50 | 2007/02/07 | 7.19 | 1658.31 |
| RG-1 | 27.72470 | -26.11217 | 1666.00 | 2007/02/07 | 6.00 | 1660.00 |
| RG-2 | 27.72627 | -26.11539 | 1678.00 | 2007/02/07 | 10.00 | 1668.00 |
| SH-8 | 27.72006 | -26.13545 | 1713.46 | 2007/02/01 | 41.46 | 1672.00 |

# Appendix B

# Hydrograph Analysis

## Nouklip Hydrograph Analysis

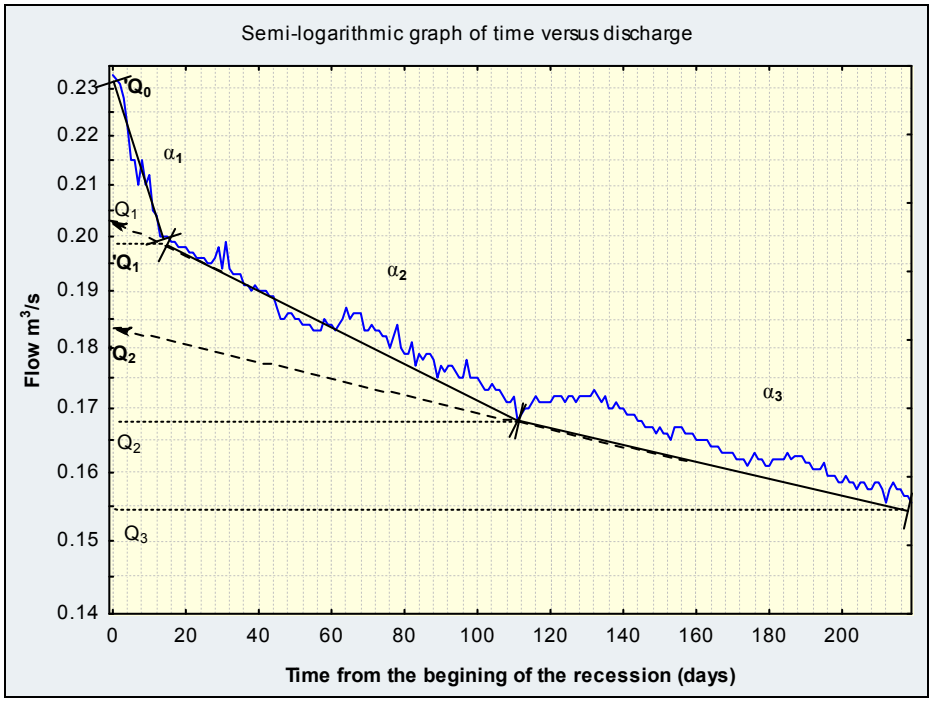


**Figure 1.** Response curve of the discharge over time for the 2005 hydrological year for the Nouklip gauging station according to the Maillet equation.

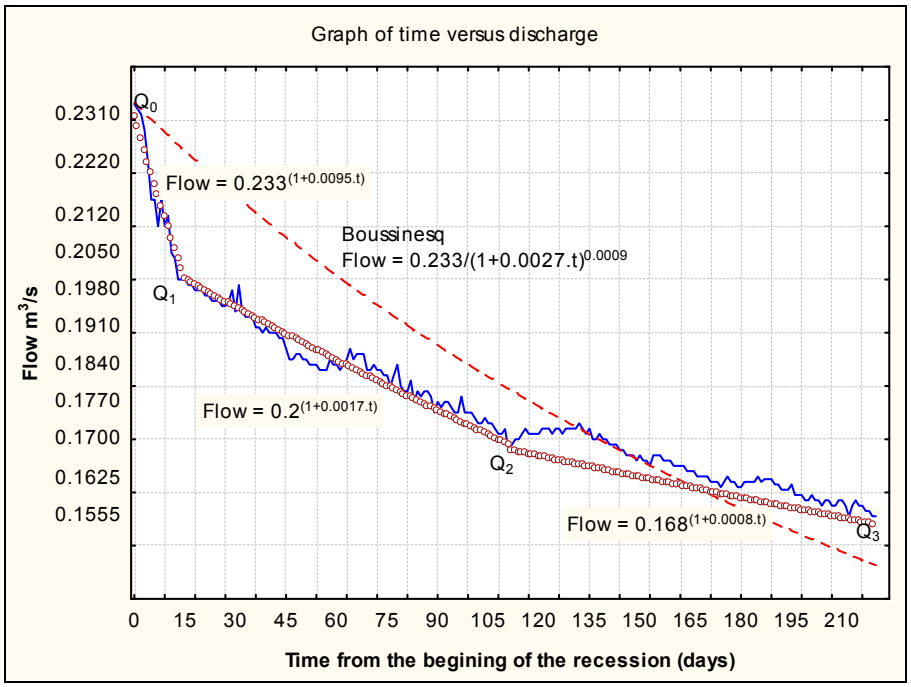


**Figure 2.** Response curve of the hyperbolic function of Boussinesq and the Maillet equation for 2005.

## Borehole Hydrograph Analysis

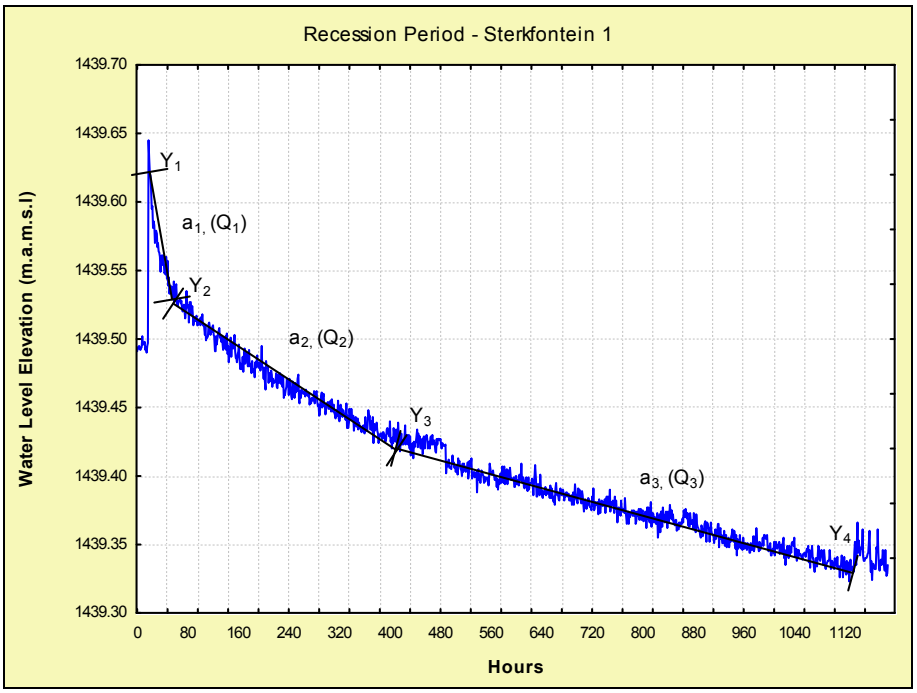


**Figure 3.** Recession curve Sterkfontein 1.

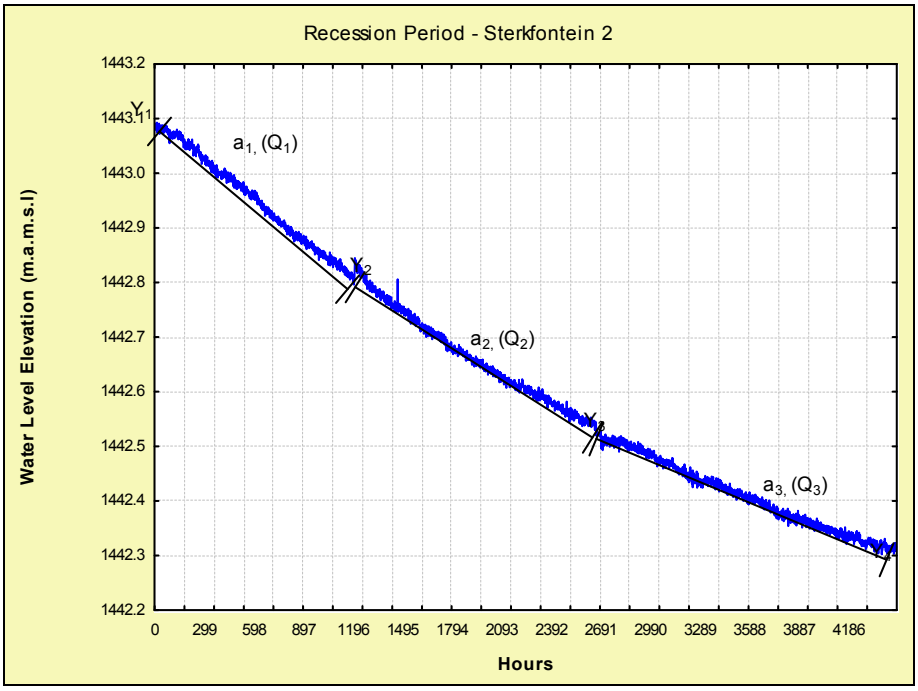


**Figure 4.** Recession curve Sterkfontein 2.

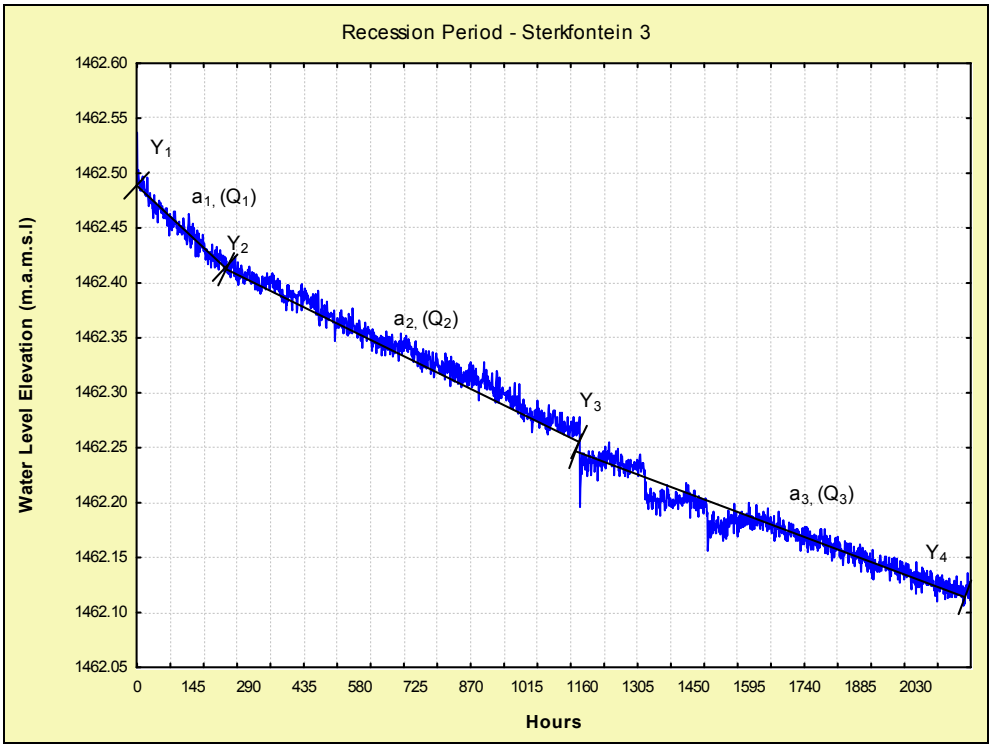


**Figure 5.** Recession curve Sterkfontein 3.

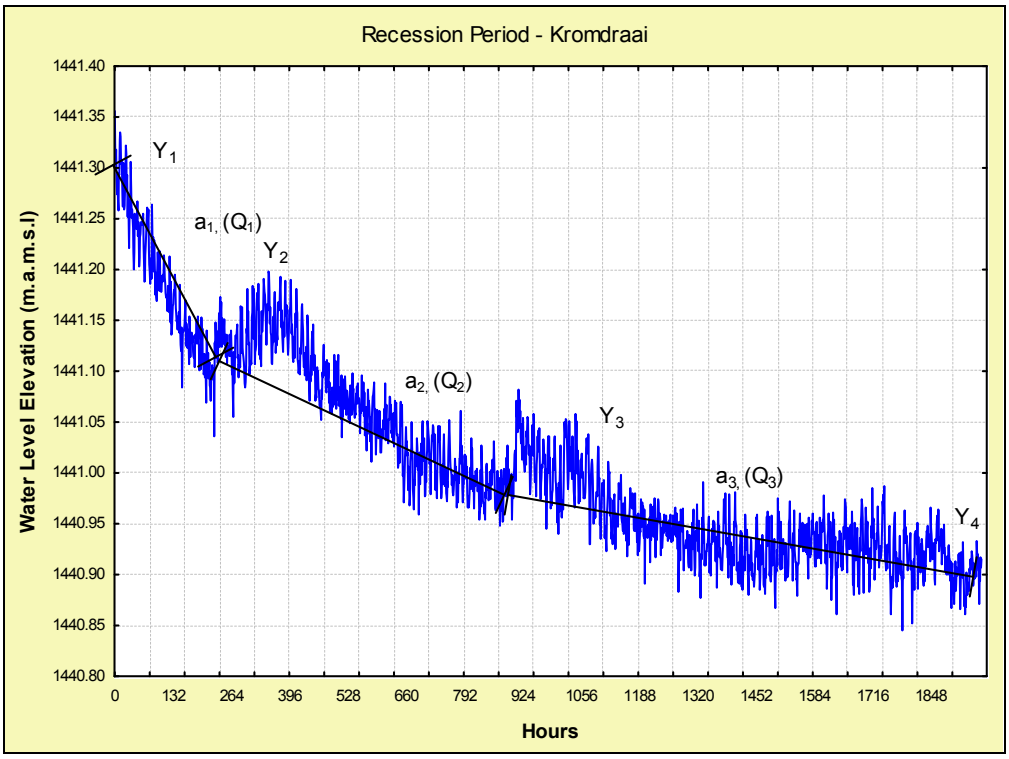


**Figure 6.** Recession curve Kromdraai.

# Appendix C

# Slug Test Analysis

## Slug Test Analysis

Kromdraai BH-1

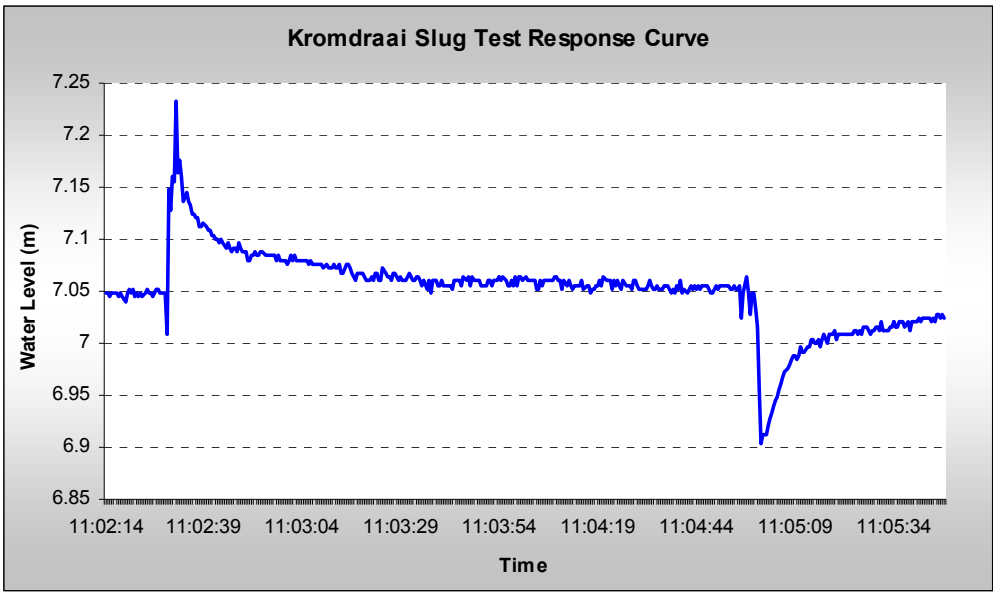


**Figure 1.** Response curve of the water level over time for Kromdraai borehole.

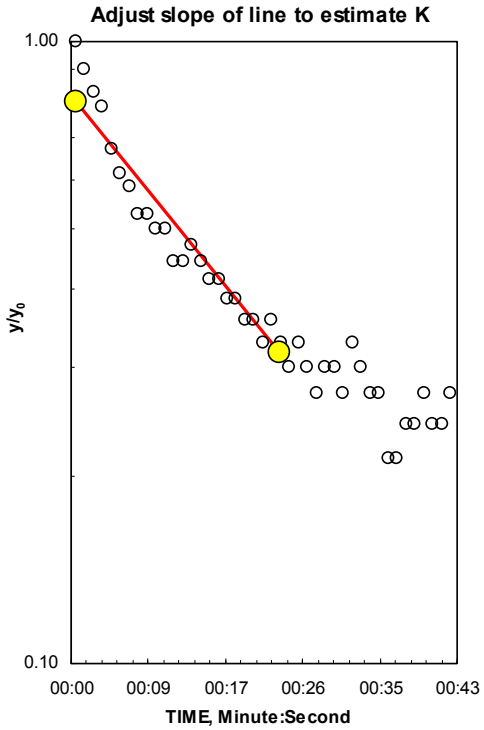


**Figure 2.** Bouwer and Rice (1976) – Graph (K = 0.89m/day).

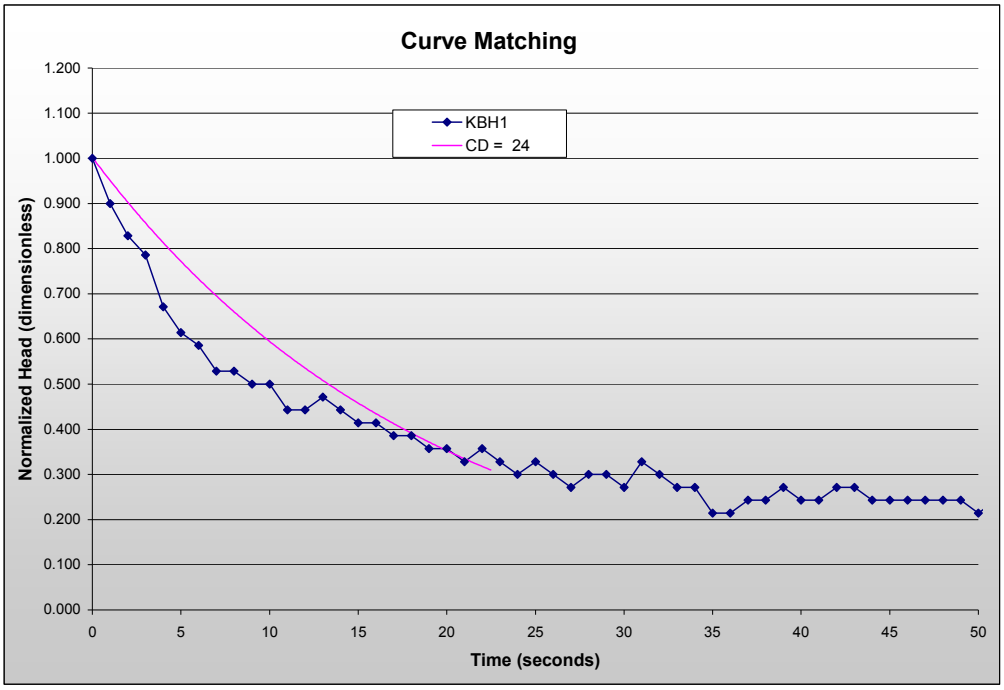


**Figure 3.** Butler et al. (2003) – Graph (K = 1.08m/day).

Boland BH-1

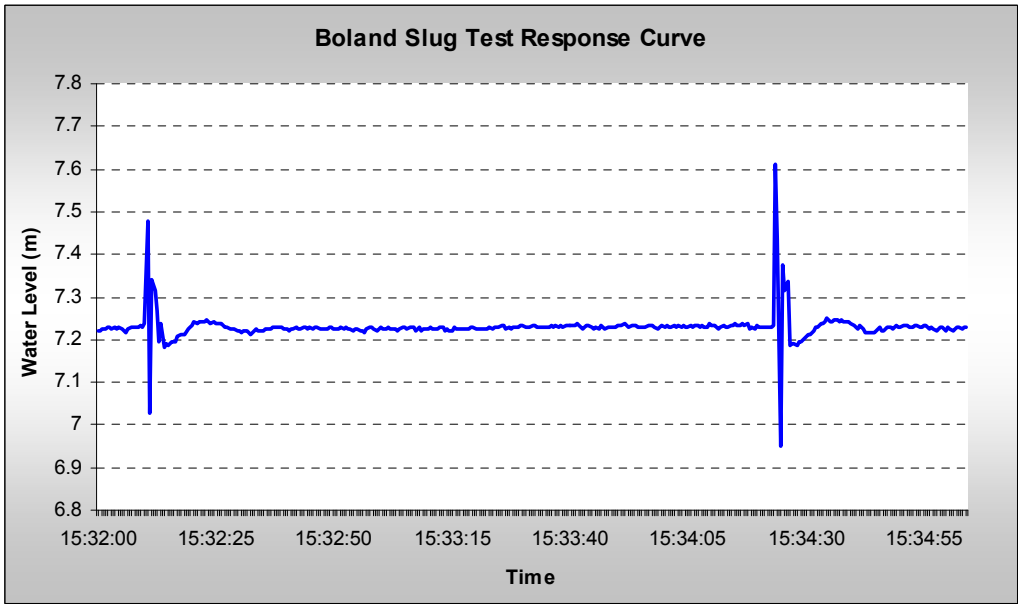


**Figure 4.** Oscillating response curve of the water level over time for Boland borehole.

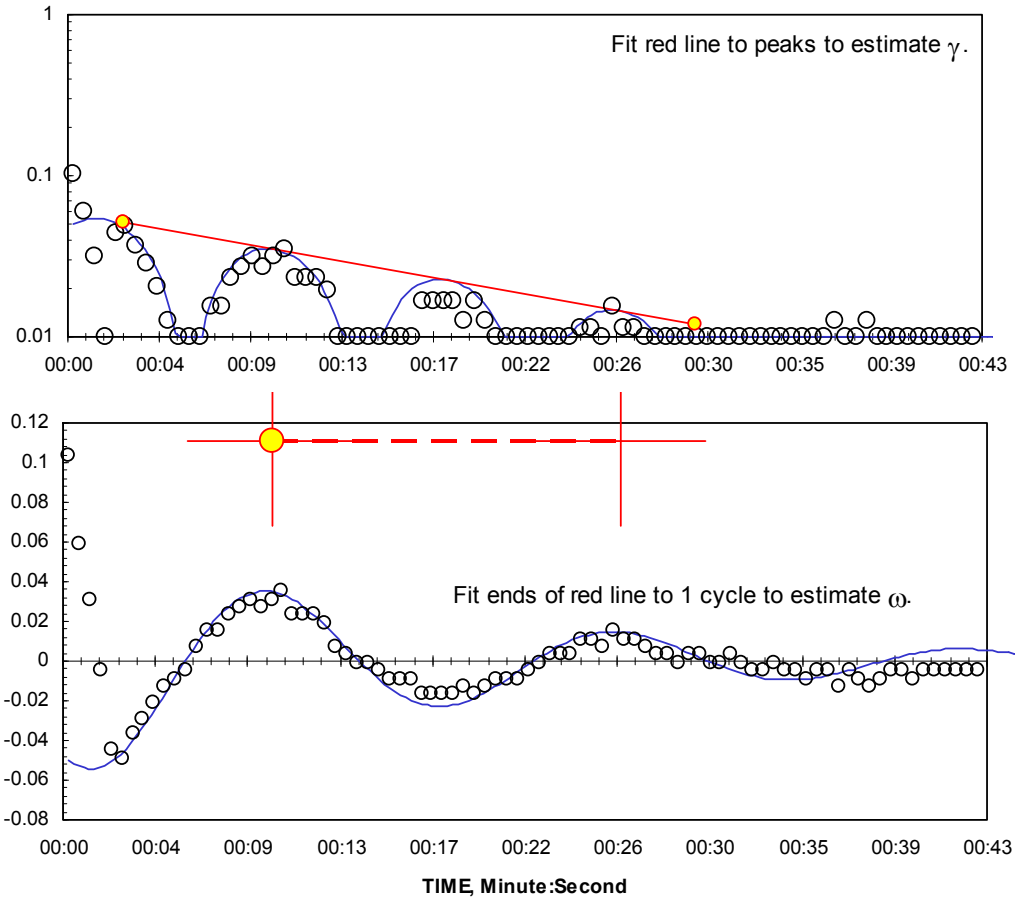


**Figure 5.** Van der Kamp (1976) – Graph (K = 19 m/day).

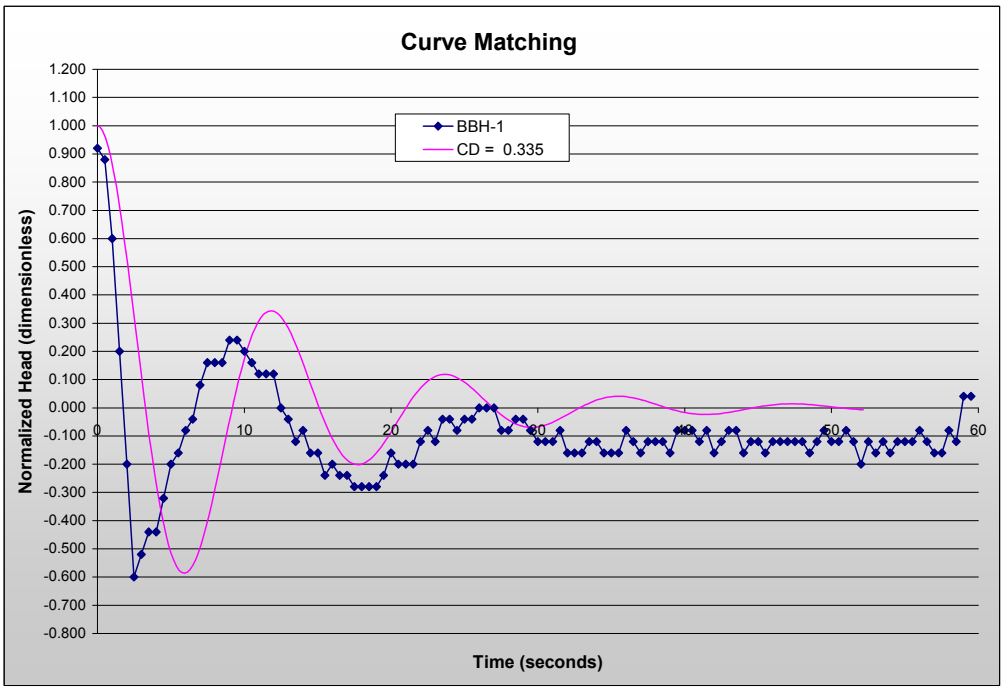


**Figure 6.** Butler et al. (2003) – Graph (K = 26.54 m/day).
Sterkfontein BH-2

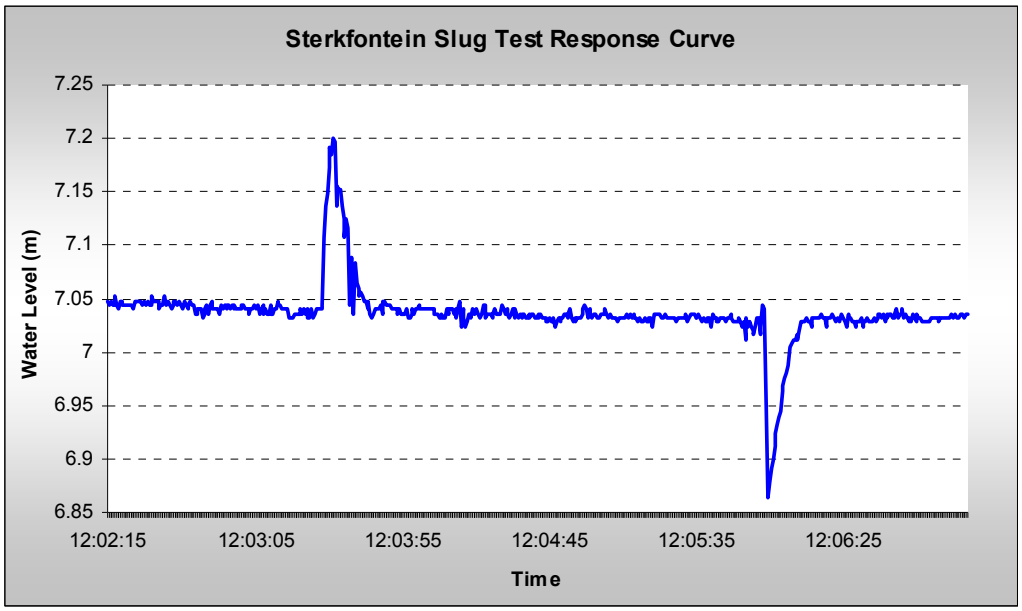


**Figure 7.** Response curve of the water level over time for Sterkfontein borehole.

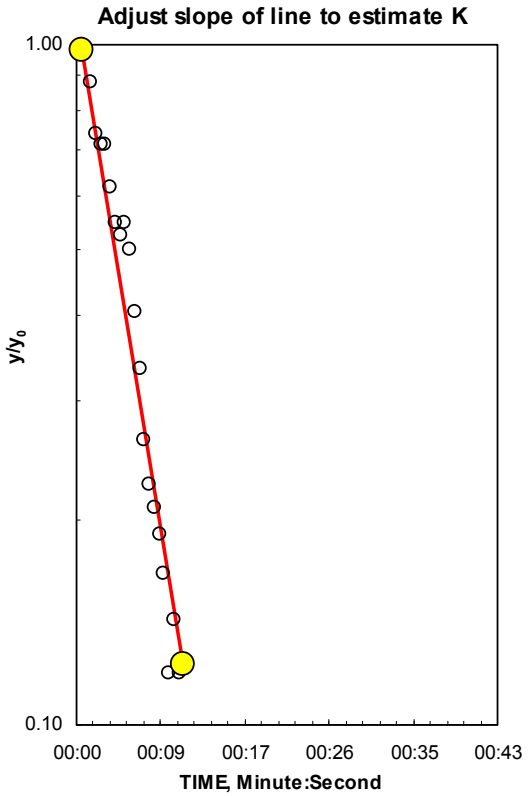


**Figure 8.** Bouwer and Rice (1976) – Graph (K = 4.3/day).

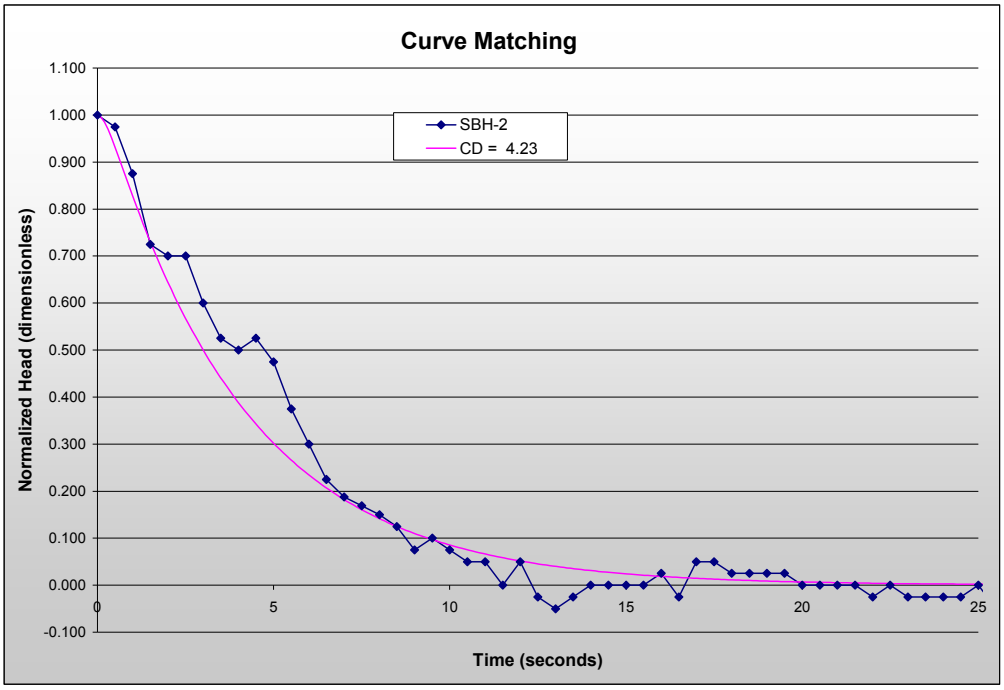


**Figure 9.** Butler et al. (2003) – Graph (K = 6.72 m/day). Slug Inserted.

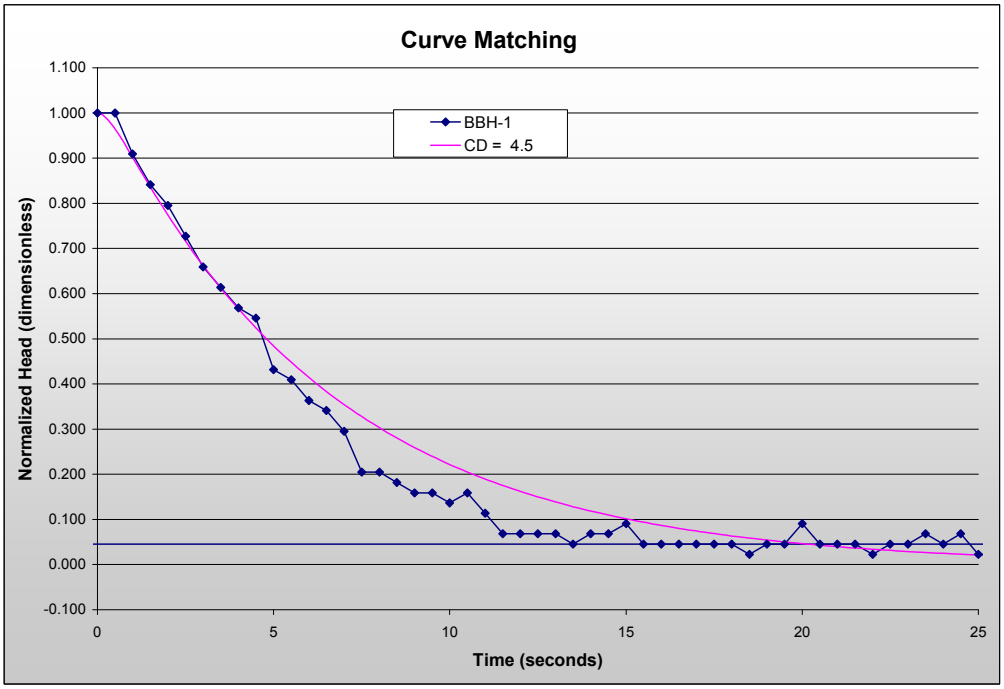


**Figure 10.** Bulter et al. (2003) – Graph (K = 4.19 m/day). Slug Ejected.

Van Wyk BH-3

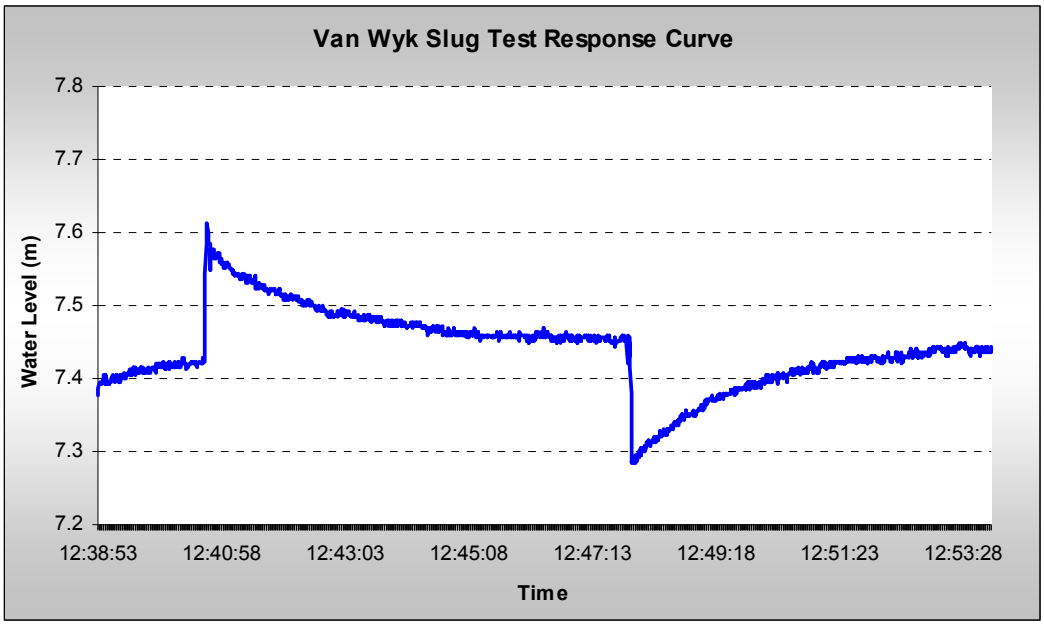


**Figure 11.** Response curve of the water level over time for Van Wyk borehole.

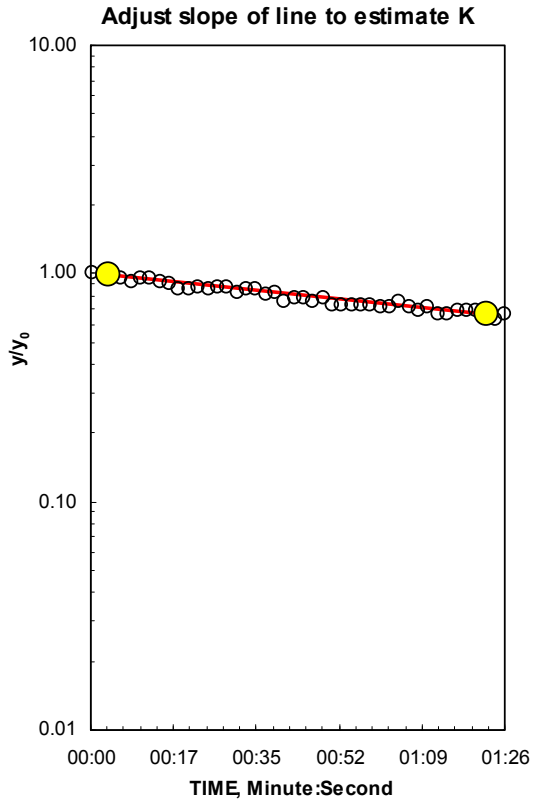


**Figure 12.** Bouwer and Rice (1976) – Graph (K = 0.26 m/day).

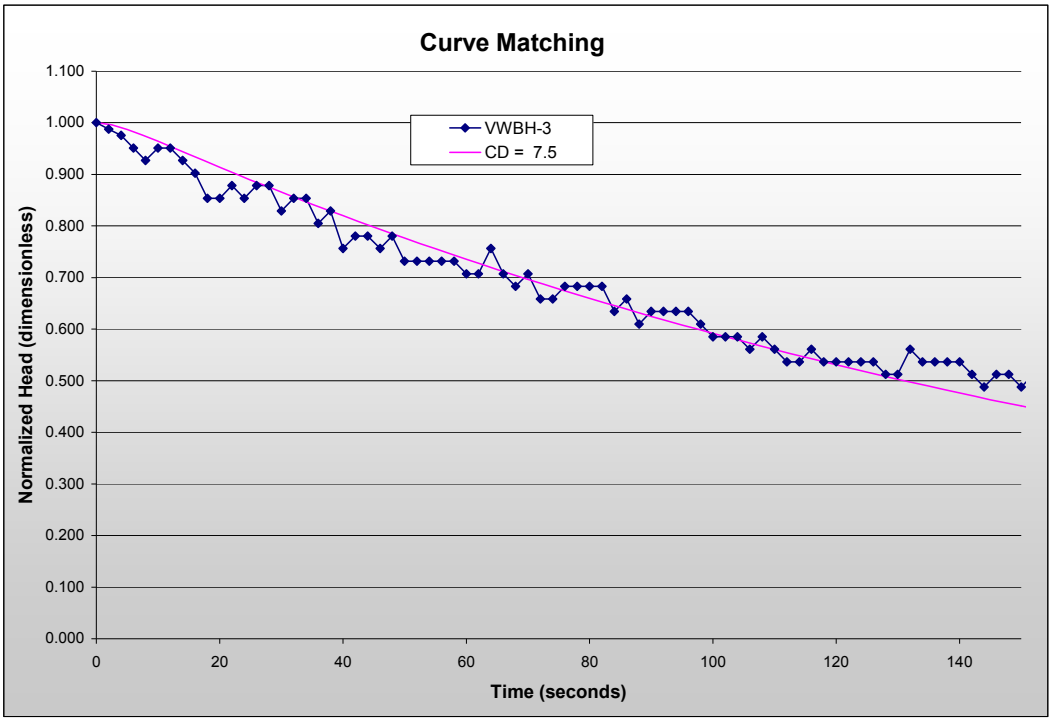


**Figure 13.** Butler et al. (2003) – Graph (K = 0.21 m/day).

# Appendix D

# Cluster Analysis

# Cluster Analysis

Dendrogram using Ward Method

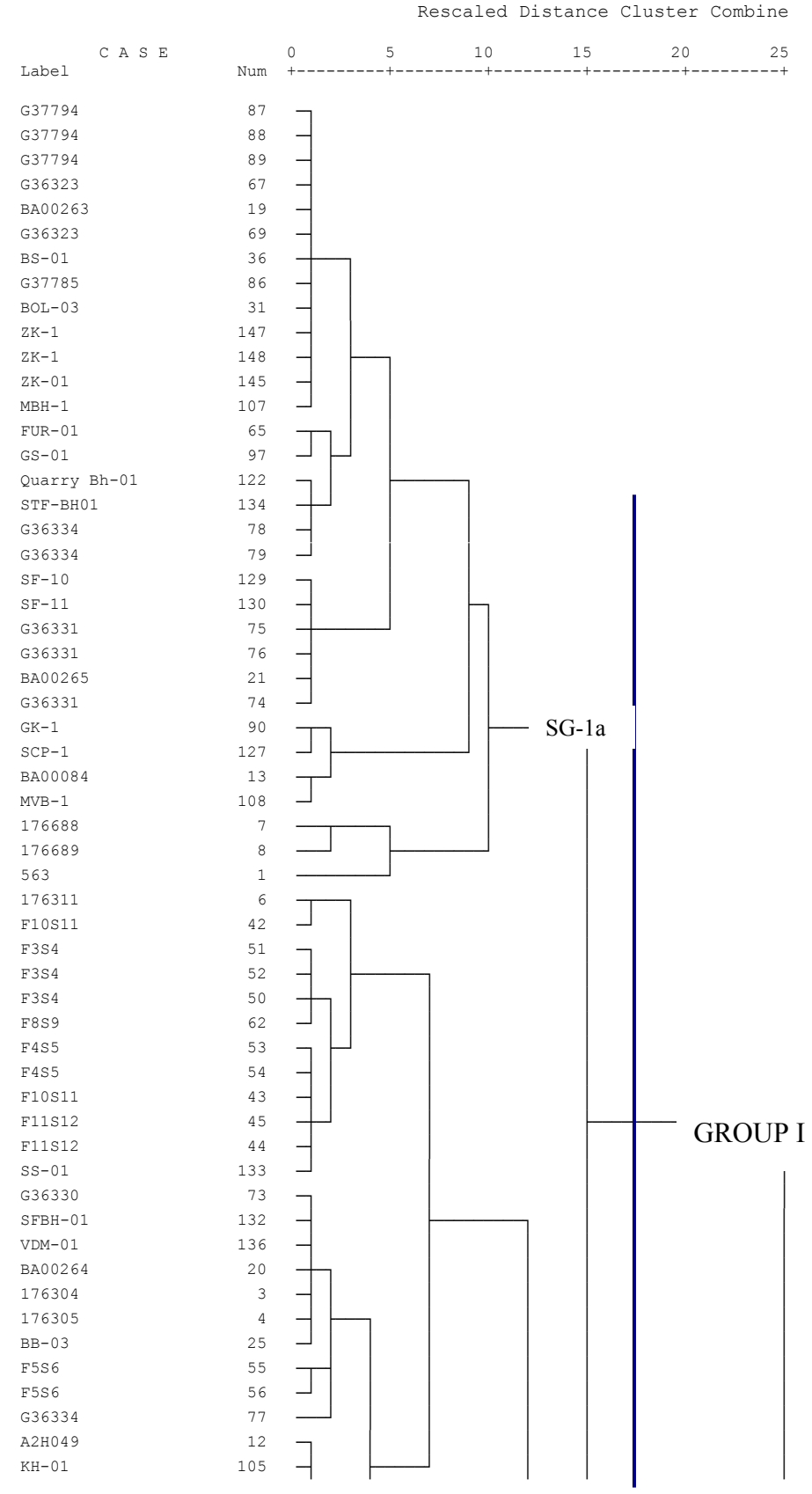

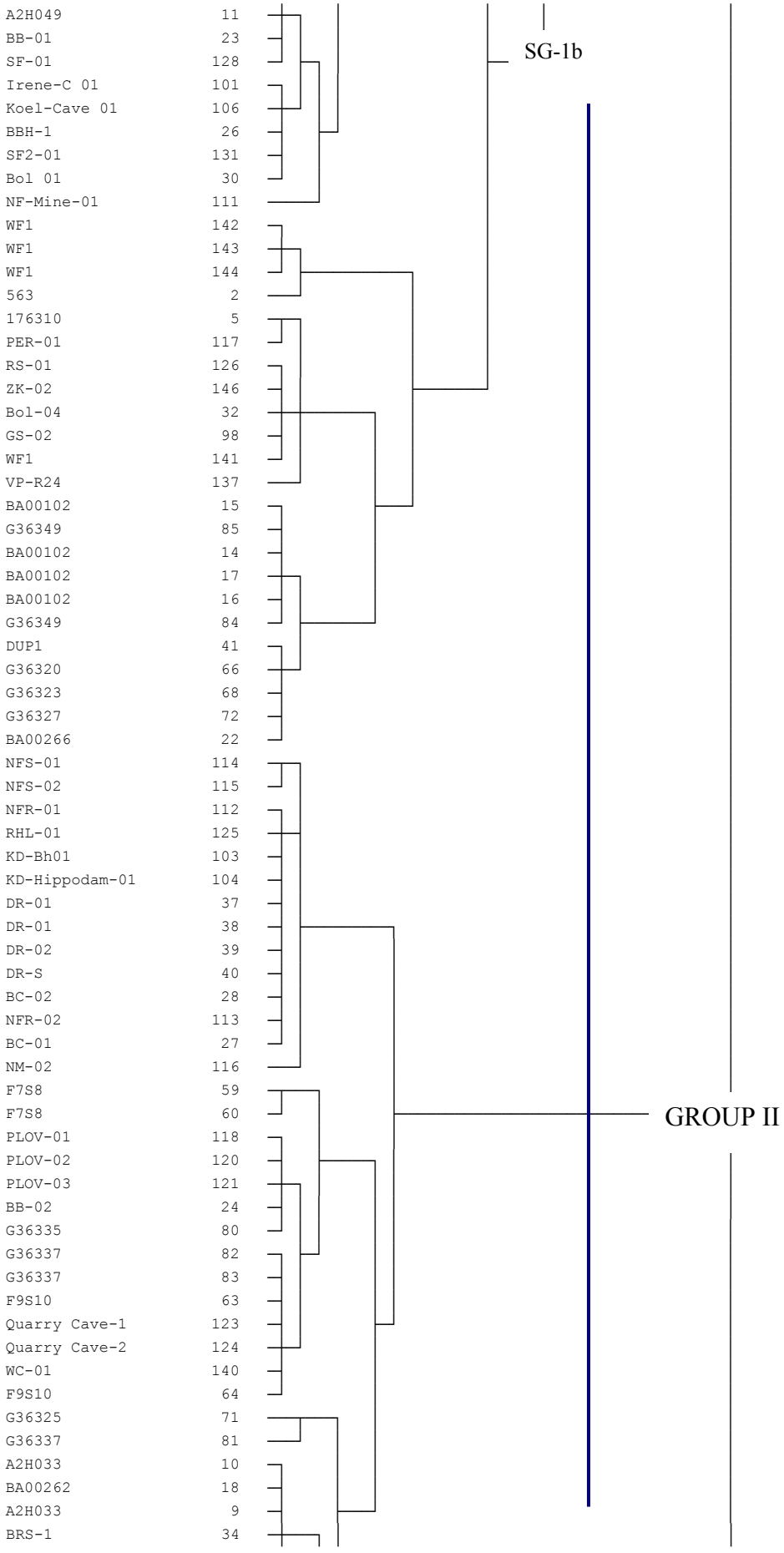
A2H049 11
BB-01 23
SF-01 128
Irene-C 01 101
Koel-Cave 01 106
BBH-1 26
SF2-01 131
Bol 01 30
NF-Mine-01 111
WF1 142
WF1 143
WF1 144
563 2
176310 5
PER-01 117
RS-01 126
ZK-02 146
Bol-04 32
GS-02 98
WF1 141
VP-R24 137
BA00102 15
G36349 85
BA00102 14
BA00102 17
BA00102 16
G36349 84
DUP1 41
G36320 66
G36323 68
G36327 72
BA00266 22
NFS-01 114
NFS-02 115
NFR-01 112
RHL-01 125
KD-Bh01 103
KD-Hippodam-01 104
DR-01 37
DR-01 38
DR-02 39
DR-S 40
BC-02 28
NFR-02 113
BC-01 27
NM-02 116
F7S8 59
F7S8 60
PLOV-01 118
PLOV-02 120
PLOV-03 121
BB-02 24
G36335 80
G36337 82
G36337 83
F9S10 63
Quarry Cave-1 123
Quarry Cave-2 124
WC-01 140
F9S10 64
G36325 71
G36337 81
A2H033 10
BA00262 18
A2H033 9
BRS-1 34
SG-1b
GROUP II

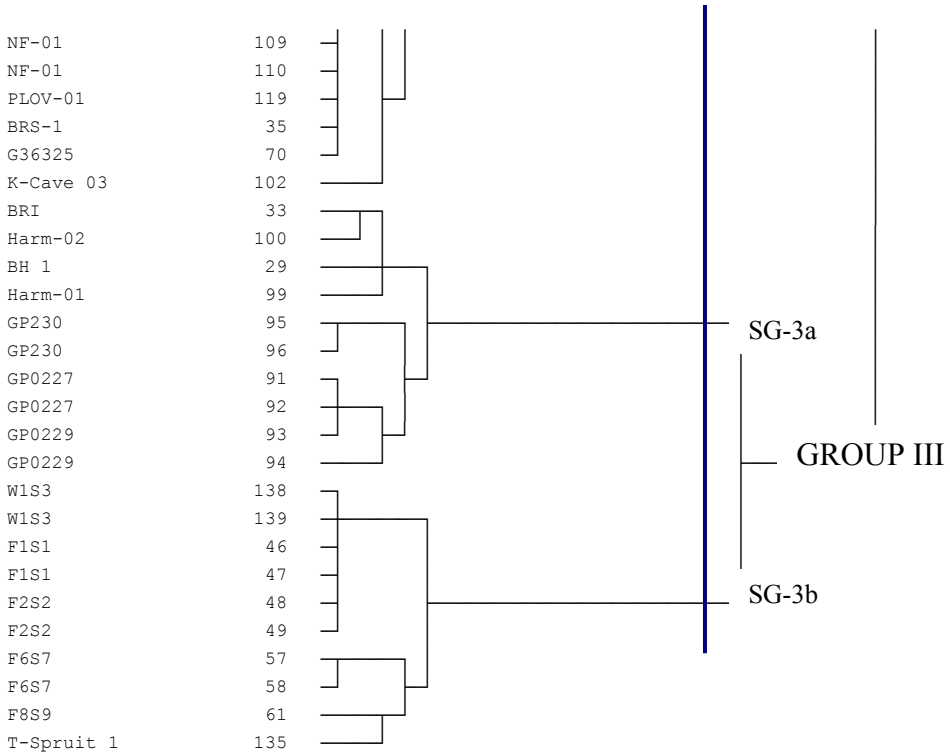


**Figure 1.** Resulting dendrogram from Hierarchal Cluster Analysis.